Seismic Hazard in the Taupo - Reporoa Region.

A thesis
submitted in partial fulfilment
of the requirements for the degree
of
Master of Science (Technology) in Earth Sciences
at the
University of Waikato
by Adrian Pyne.

1995

Department of Earth Sciences
University of Waikato
Private Bag 3105, Hamilton, New Zealand
Fax (+64-07) 856-0115, Telephone (+64-07) 838-4024

Abstract

New Zealand lies astride a convergent plate margin, as a result it experiences hundreds of earthquakes a year. This study was commissioned in response to Environment Waikato's contingency planning for such natural disasters.

The Taupo - Reporoa region was identified in a report to Environment Waikato (Waikato Regional Council) as needing to be studied, in order to quantify the level of earthquake hazard. This region lies in the centre of the Taupo Volcanic Zone, and has, over thousands of years built up considerable thicknesses of unconsolidated mainly volcanogenic materials. It is recognised that towns and cities that are sited on these materials are at risk from amplification of seismic waves and will experience greater damage, than if they were on hard rock.

Soils were analysed by the following geotechnical tests: hand penetrometer, Bush penetrometer, shear vane, the standard compression test, and dynamic cyclical loading. Samples were also taken for soil moisture and bulk density. The results from these tests have been used to evaluate the region for seismic hazard, and to semi-quantitatively correlate with reports and claims of damage from earthquakes. A number of parameters were able to be derived from the field tests and the cyclic loading which were used in the final analysis.

The results showed that some soils were substantially weaker than others, which correlated with historical accounts of damage. A seismic microzoning map was constructed on the basis of the difference in soil strengths.

Acknowledgements

I would like to thank Dr Peter Hodder and Dr Vicki Moon, for their time and their patience. Also, a special thanks to Steve Bergin for his help in the lab and the field, and who wisely demonstrated to me that time versus time is a perfectly linear relationship!

Also I would like to thank Michael Bent and Peter Cochrane from Environment Waikato who helped sponsor and supervise my work. Their enthuasium is how I initially became interested in this thesis topic.

Also a thanks to my fiancée Kim, her parents Neil and Karrene, and other friends who have put up with me, and who have helped to motivate me.

I also wish to thank Landcare for allowing me to use unpublished soil descriptions.

Lastly, thanks to Frank Bailey, the university draughtsperson, for helping to construct and draw up an excellent soils map for the whole study area, as well as giving lots of useful advice.

Table of Contents

List of Figures

List of Tables

Chapter One

Chapter One

Introduction

1.1 Introduction and Review

"The longer it's been since the last one, the sooner it'll be till the next one."

Byerly's Law (seismologist)

New Zealand is situated along the convergent boundary of the Indo-Australian and Pacific plates. As a consequence, New Zealand experiences hundreds of earthquakes each year (figure 1.1). In the past, government agencies such as the Geophysics Division of DSIR (now IGNS) have monitored and collected data from earthquakes. Their catalogues date back to 1840, but the location and size of earthquakes are not well defined until 1940 when seismological instruments began to provide greater accuracy.

The historic database of earthquakes in New Zealand is far too short to predict the frequency of future large quakes and where they are likely to occur. On this basis, it is not possible to accurately estimate the hazard to people, homes, hospitals, and schools. Few specific studies have been undertaken on regions which experience frequent tremors such as the Bay of Plenty and Fiordland, however Smith *et al.* (1986) have defined regional earthquake hazard for New Zealand from inferences of seismology and geology. However some specific studies have been undertaken in areas where there are large concentrations of population in this area, and these are mentioned later.

Fig 1.1 Earthquake Activity in New Zealand (IGNS 1994 calender)

1.2 Aims and Objectives

The aims of this thesis are to provide Environment Waikato with a report and map of the Taupo - Reporoa region which shows, on the basis of soil types, areas which are susceptible to damage from significantly large earthquakes.

Work is being undertaken by IGNS with respect to the study of faulting through this region, so the thesis is a complimentary study based on microzoning from soil properties. Hodder and Graham (1993) state that for the 1987 Edgecumbe earthquake, "predictions were sufficiently in accord with observations to suggest that soil properties that reflect geotechnical properties of the upper parts of the regolith, particularly those that measure the shear strength, shear wave velocity and viscous damping of the material, may be useful for earthquake microzoning purposes in areas where there is a considerable thickness of unconsolidated materials above the bedrock."

The study area is underlain by lake sediments, rhyolite and ignimbrites on basement rock. Above these, lie hundreds of metres of tephras and pyroclastic flows from eruptions from Taupo and associated vents. These materials are certainly unconsolidated, due mainly to their young age, and are found to be sufficiently deep enough to justify this approach.

The objectives of the thesis are:

1) To use a number of different geotechnical tests on soils found within a particular region to determine their strength and behaviour during ground shaking.
2) To confirm the relationship between various soil tests, and the amount of damage that actually occurs during an earthquake to buildings and structures.
3) To provide Environment Waikato with an assessment of seismic hazard for this particular region, for planning for Civil Defence.

The most seismically active part of the region within the Waikato Regional Council's boundaries is the Central Volcanic Region, which includes in it, the area being studied (figure 1.2).

Since 1840, in the greater Waikato region (defined by the boundaries of the Waikato Regional Council) there have been approximately 300 shallow earthquakes of magnitude 4 and greater (on Modified Mercalli Scale). Figure 1.3 shows those earthquakes which have occurred near to the study area. The largest known event was near Lake Taupo in 1895 and was of Magnitude 6.5. The Taupo area again in 1922

experienced a large earthquake of M 6.0 followed closely by a large swarm of quakes over several months. Again, swarms occurred in 1964 - 65 and as recently as 1983 (Berryman, 1993).

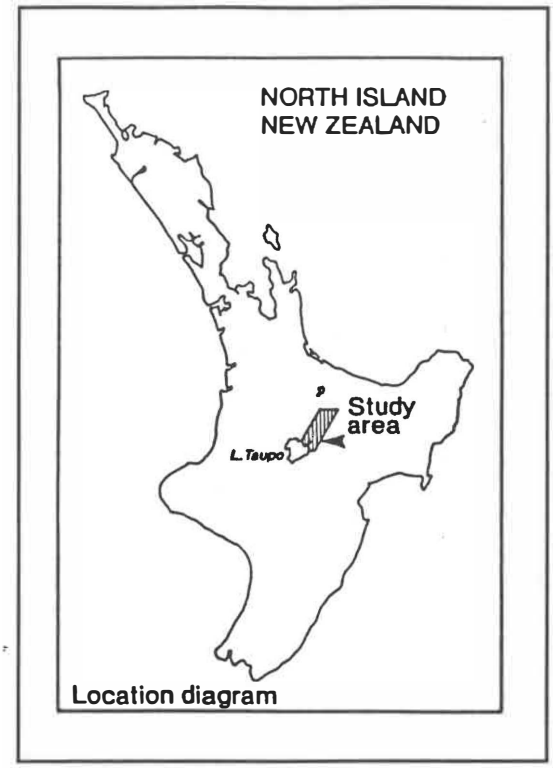

Fig 1.2 Study area in the Taupo - Reporoa region

The major active faults occur in the Taupo Volcanic Zone. This zone is defined by recently active vents, and multiple calderas which overlap each other. A NNE oriented group of normal faults run from Mt Ruapehu to the coast. These faults are assumed to be associated with volcanism (studies have yet to be undertaken to prove this), and in the Reporoa area faults have been recently discovered. Only the upper two kilometres of crust have been explored by electrical resistivity and gravity mapping. IGNS (Institute of Geological and Nuclear Sciences) estimates that the crust is only 15 - 17 kilometres thick, also nothing is known about how much strain is taken up by this crust or by caldera formations (Houghton, *et al.,* 1986).

The thesis examines an area identified by Berryman (1993), as needing further investigation. He also states that there may be a number of active faults in this region that need quantifying in order to establish the maximum sized earthquake likely to affect the towns and cities in the area. He found that there were three geographical areas within the Regional Council's boundaries that needed further investigation in terms of earthquake hazard.

One of the these, was the area in the Taupo Volcanic Zone which stretched from Taupo, NNE to just south of Waiotapu, including the Reporoa Basin (where faults have been recently recognised). The thesis was initiated as a result of the Waikato Regional Council's (Environment Waikato) need for contingency planning for Civil Defence emergencies and disasters.

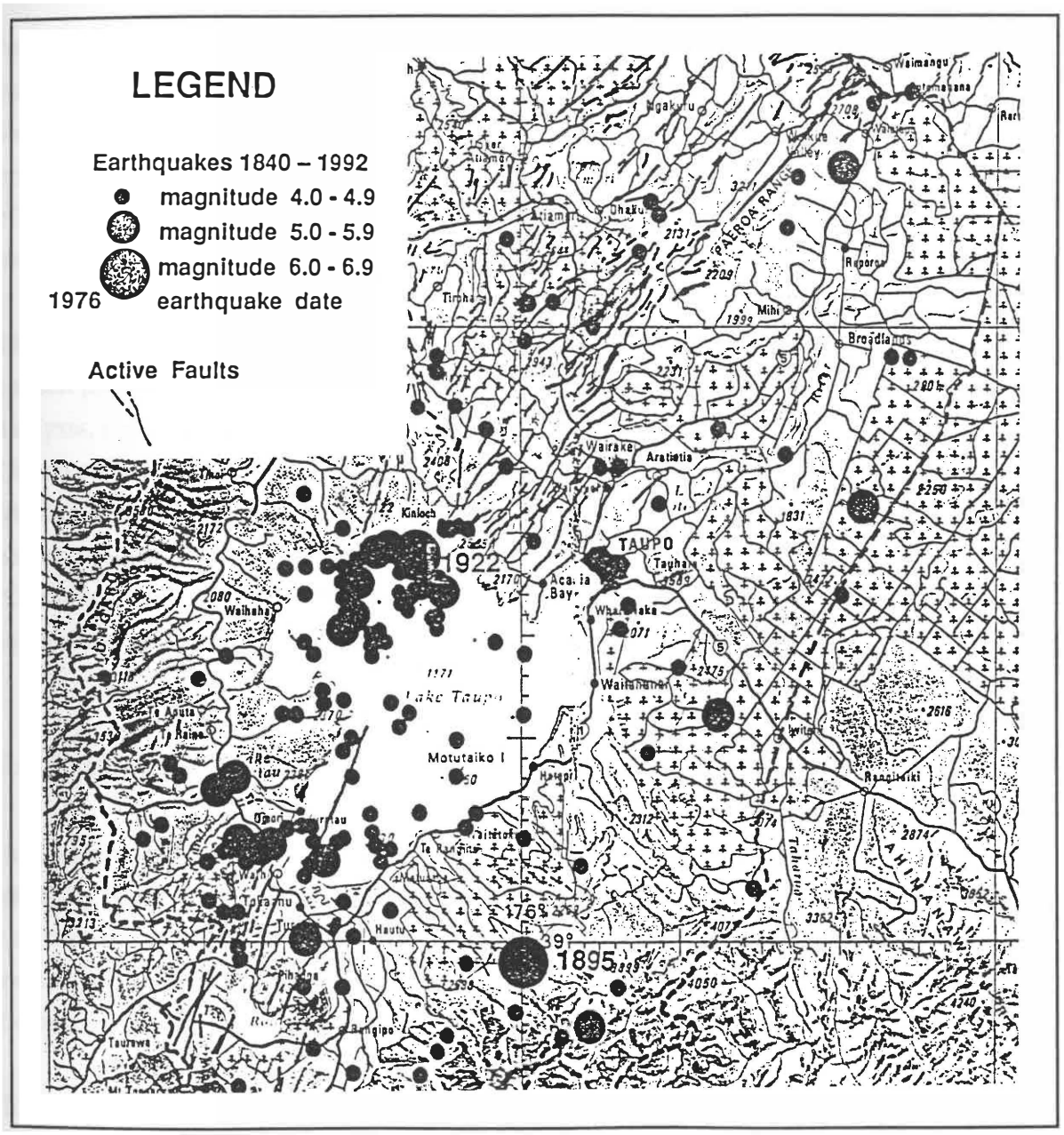

Fig 1.3 Shallow Earthquakes and Active Faults in the Taupo - Reporoa Region (Berryman 1993)

There are in the study area a number of buildings and structures which could be at risk. These include parts of State Highways 1 and 5, schools, Taupo airport, Taupo town and other small townships as well as access to a number of important utilities.

1.3 Methods

An initial survey of 43 sites in the Taupo - Reporoa region was undertaken along the valley floor from Taupo township to the north end of the Reporoa valley, a tract of land some 45 kilometres in length. The soils studied were mainly from the valley floor however a few sites were examined on the lower slopes of the Paeroa Range, at the edge of the Kaingaroa Plateau, and on a eroded plateau just west of Taupo. The initial investigations used only the shear vane, hand penetrometer, and bush penetrometer.

The actual sampling program consisted of investigating nine sites in detail for the chosen parameters of soil strength. These were soil moisture, bulk density, particle size analysis, shear vane, hand penetrometer, bush penetrometer, and two tests on the Geomechanics GDS triaxial testing system; the Standard compression test, and Cyclic loading of soil cores. These parameters were chosen because they had been previously shown to have a reasonable correlation with the amount of damage to buildings (Graham, 1993). Three more sites had incomplete data on them which was also useful in the final analysis.

1.4 Previous Work

A moderate earthquake which caused widespread minor damage, was the subject of a study by IGNS (formerly DSIR) in Wellington in 1968. Grant-Taylor (1974) proposed that microzoning on the basis of regolith properties could be quantified. The correlations between damage relative to drainage, structure and parent material, could be transferred to other sites of interest.

Examining the geotechnical properties of soils and relating them to earthquake damage in a quantitative sense is a fresh approach, using a basic knowledge of soils and engineering. Investigating only the topmost metre of sediments, can obviously only be applied to buildings (mainly single or double storey dwellings) on shallow foundations. It assumes that if material in close proximity to foundations fails significantly during ground shaking, this will cause building damage.

The thesis aims to earthquake microzone the Taupo - Reporoa region on a similar basis to Graham (1993). It also looks at other factors such as liquefaction and resonance. in order to better predict damage. Graham's approach was to compare geotechnical parameters to actual damage from the 1987 Edgecumbe earthquake in the Bay of Plenty. The results that were obtained confirmed that there was a reasonable correlation for the bush penetrometer, hand penetrometer, and shear vane, as well as dynamic shear modulus and shear wave velocity (calculated from the cyclic loading tests), with damage to structures. Graham calculated a damage parameter against which the above geotechnical tests could be plotted. Damage data from a Civil Defence survey was compiled and was calculated from the following equation:

Damage parameter = log (no. of structures damaged / 1000 structures)

Some of the same geotechnical parameters were used in an assessment of 'Seismic Risk to Underground Services in Hamilton City' (Hodder and Moon, 1994). This used just the shear vane and hand penetrometer as basic indicators of strength, together with soil moisture and bulk density. Other parameters such as Attenuation, Amplitude Enhancement and Seismic Rigidity were inferred from the shear strength readings averaged over the entire one metre profile. The sediments in Hamilton basin were divided into four units, on the basis of their origin, and then were characterised by the geotechnical properties. The hazard assessment showed that there were large differences in the soil units to susceptibility to ground motion, liquefaction, and landsliding.

Other work in seismic hazard studies includes: 1) Grant-Taylor *et al.* (1970) Pauatahanui area which has a similar approach to the Wellington study. 2) Elder *et al.* (1991) Christchurch and McCahon *et al.* (1993) Dunedin which model hazard from seismicity (earthquake occurrence probability), attenuation (energy loss and wave modification through basement rock), and site response (prediction of changes to earthquake waves as they travel up through the unconsolidated materials overlying bedrock).

1.5 Background to the Study

Local variations in near surface geology and soil conditions can produce marked differences in the effect of a given earthquake at different places in the same general area (Grant-Taylor *et al.*, 1970). In general, when a earthquake occurs, the seismic waves approach from below through the basement rock. As they pass through layers of

less dense and weaker material, the velocity of the waves decrease which causes an increase in amplification.

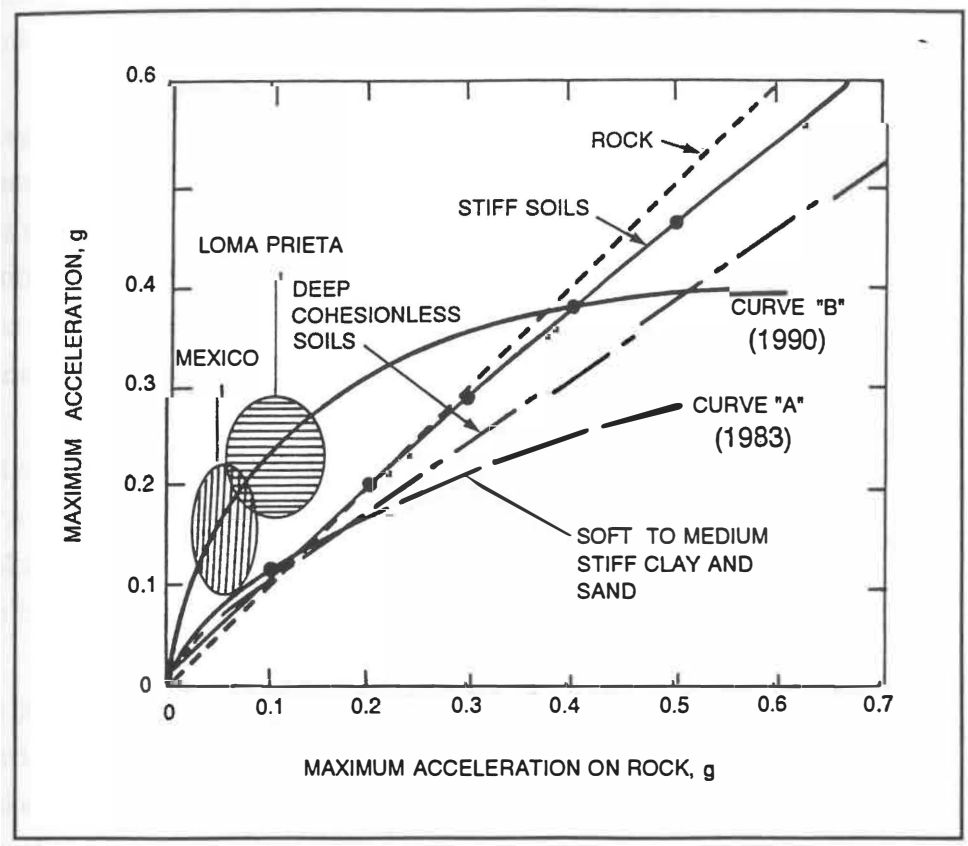

Figure 1.4 Engineering predictions of amplification on soft ground. The two curves correspond to predictions by the same author (Idriss, 1990), (A) before, and (B) after the Mexico and Loma Prieta earthquakes. From Finn (1991).

Grant-Taylor *et al.* (1974) states "for such near surface material to produce this effect, it must be at least ten metres deep... basins with depths of the order of 10 m of sediment would need to be 100 m or more across, before they would considerably increase amplification."

Figure 1.4 shows how the effects of increased accelerations in soft ground have been underestimated in the past, and have since been revised (curve B) from recent data. "Soft ground is now generally acknowledged to amplify strong motion at all amplitudes up to a level of about 0.4g. At higher accelerations a deamplification is still expected" (Lomnitz, 1994). Amplitudes of up to 1.5g have been recorded near faults. Low resonant frequencies and low shear wave velocities are common in soft ground.

Hodder *et al.* (1993) also states "high values of viscous damping could have deleterious consequences for the foundation of buildings; on the other hand, high values for shear modulus imply a greater proportion of energy is transmitted into any structure built on the soil."

The region being studied, as a whole is underlain by thick predominantly unconsolidated volcanogenic materials. However, some areas are more upstanding than others due to uplift and down-faulting as described in Chapter two (though the materials are still thick - at least 1100 metres, above ignimbrites). Topographic relief in the study area is more a function of these features than of any material's ability to withstand erosion, with the exception of rhyolitic cones.

Most of this relief occurs in the southwest corner of the study area where S.H.1 passes over a number of faults just northwest of Taupo, such as the Kaiapo, Whangamata and Whakaipo Faults. All of these have moved during earthquakes this century, as well as there being some ground cracking along smaller faults.

This present thesis therefore, takes the approach that in areas of deep unconsolidated materials, the near-surface geology (soils and shallow regolith) is largely responsible for the damage caused by earthquakes. It attempts to determine the most suitable geotechnical methods by examining historical earthquake damage to the region.

This approach should be useful to Civil Defence in helping to plan pro-actively for seismic hazards. One of the reasons for this study relates to the Resource Management Act, which requires Regional Councils to "collect and distribute information on natural hazards, and to develop policies and objectives related to hazard mitigation" (Berryman, 1993).

Chapter Two

Chapter Two

Geological Background, Initial Site Investigation & Seismicity

2.1 Geomorphology and Structure

Berryman (1993) describes the Taupo Volcanic Zone as "an active NNE-trending belt of normal faults defining a graben structure within which the central North Island volcanoes have formed (see figure 2.1) There is a close structural association of faulting and volcanism. Active faults occur in close proximity to Turangi and Taupo at either end of Lake Taupo, and the zone of faults about 25 km wide extends to the NNE to Rotorua." He also notes "Recently discovered active faults in the Reporoa area require further study."

The edges of Taupo - Reporoa region are marked by Patetere in the west and the Kaingaroa Plains in the east which are some 550 to 600 m above sea level at their highest, though they are downwarped towards the edges of the graben. The floor of this graben is very uneven as it has been broken up by faults that have been tilted or warped, and by extrusions of lava. The Paeroa range borders the western edge of the study area and is an uplifted north east trending range. At one time or another, lake beds have covered most of the low ground in the region.

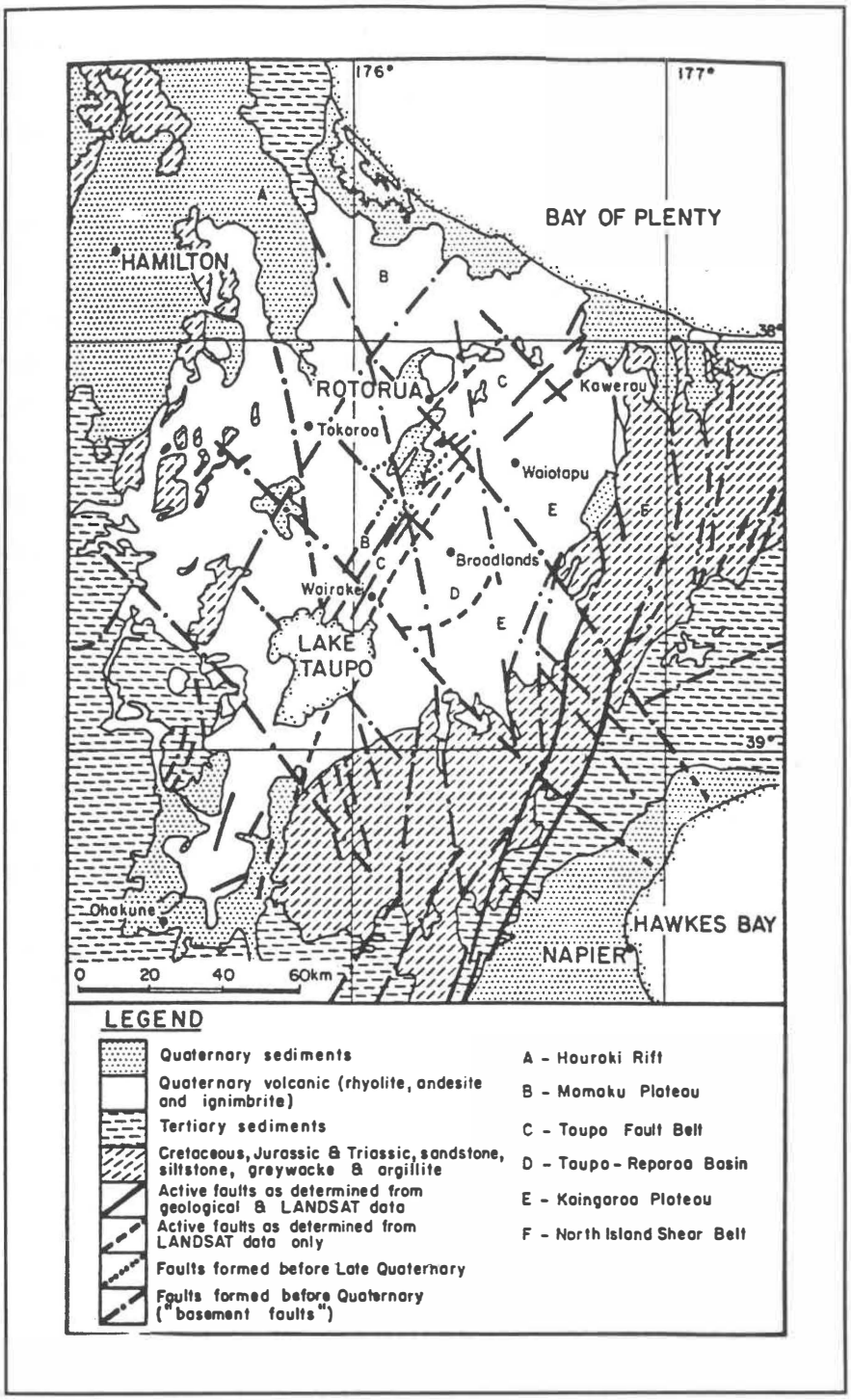

Figure 2.1 Structural sketch map of the TVZ showing lineaments visible on Landast photos (from Wan Tianfeng and Hendenquist, 1981)

In and around the study area are a number of volcanoes, most are rhyolitic which form domes, but some, notably Mt. Tauhara (dacite) are cone shaped. These volcanoes, along with the thick blankets of pumice that have regularly showered the region, have been the main factors in shaping the land. The volcanic rocks are mostly rhyolitic and occur in three different forms: (1) Incoherent pumice breccia and tuff, the Waitahanui

Series, (2) Lava domes or sheets which may join in places, eg. the sheet north of Lake Taupo, and (3) widespread ignimbrite sheets that were erupted around the same time and so can be considered as one (variable) sheet.

The Kaingaroa Plateau (Plains) forms the eastern boundary of the study area and blends gradually into the lowlands that extend to the edge of Lake Taupo. It was formed largely from ignimbrite sheets, but had it's surface built up significantly by large pumice type eruptions. Along the line of cliffs already mentioned, is the fault-scarp at which the Taupo-Rotorua graben was downthrown. This 150 m high fault forming the plateau's western edge, continues both northwards towards Waiotapu, and southwards towards Waitahanui River, although is obscured in part by Tauhara volcano. At one time the northern part of the scarp formed the edge of a much larger Lake Taupo. There are lake benches at its base, and opposite Reporoa a good example is found 30 m above the basin floor with a 10 m high straight wave-cut cliff paralleling it. In the south, the plateau's edge terminates in the north east corner of Lake Taupo (Tapuaeharuru Bay), and along an old lake basin which the Waikato River occupies.

The Paeroa Range is a 300m high fault scarp formed along a continuation of the fault on which Tarawera erupted in 1886. It is 21 km long and has a south east dipping backslope. The highest point occurs roughly midway along the range. It is a block of an ignimbrite sheet that was originally deposited horizontally. On the eastern side the back-slope is gentle, although well eroded. At the southern end it has been moderately eroded to produce a broad area of knobbly small hills extending to the Waikato River. A few of these hills such as Pukepapataringa and Te Waro rise above the general elevation of the range. The northern end of the range is truncated and fractured by a small northwest system of faults near the village of Waiotapu.

Just to the west of Tapuaeharuru Bay is the edge of an extensive area of rhyolite, that has been split into north east trending blocks due to faulting. The rhyolite is thought to be underlain by the same ignimbrite that outcrops some 19 km further north. Lake Taupo, which forms the southern boundary of the study area, has formed in a giant caldera complex. Much of the ejected material from the lake now mantles the surrounding topography as the Taupo Pumice Formation. The most recent eruptive material (from an ultra-plinian eruption) has been dated at 186 A.D., based on atmospheric effects in the Northern Hemisphere at that time (Wilson *et al.*, 1981).

In the Reporoa valley there are some well preserved terraces which were cut by the last Pleistocene lake that once filled the valley. The broadest of these is found on the eastern side at the base of the Kaingaroa fault scarp. It starts near Mangaharakeke

Stream and extends south for 6.5 kilometres with an average width of just under 800 metres. On the western side, terraces are best observed just south of Waiotapu village at the north end of the valley and then again approximately 10 kilometres south down State Highway 5. On the side of Mt Kairuru are minor lake terraces at 362 and 371 metres high, and again at 375 and 396 metres are some, being either wave or river cut. Grange (1937, p45) speculates that the top of Kairuru, 463 metres high, has been river-truncated to produce a relatively flat surface. He also states that "Observations in the Waiotapu (Reporoa) basin are far too few to allow reasonable correlation of the terraces with those about Taupo, though the benches near the 1300 ft (396 metres) contour are probably related. Wave-cut or wave-built terraces below the level of Taupo suggest the existence of a lake or chain of lakes now entirely drained."

In summary, the main features of the region (including the study area) are:
1) A large graben was formed oriented NNE, well defined in the east, but irregularly bounded in the west.
2) The overall orientation of faults is NNE parallel to the structural axis of New Zealand.
3) All the faults are assumed to be normal tension faults, also there are very few transverse faults.
4) The Taupo-Reporoa basin was in recent times covered by a lake(s).

2.2 Nature of the Soil Forming Tephras and Pyroclastic Flows

The entire study area has been covered with volcanic tephras and pyroclastic flows numerous times in the last 10,000 years. In places the thickness of unconsolidated ash and pumice exceeds 24 m (Healy *et al.*,. 1964). Under this lie unwelded pumiceous ignimbrites (Froggatt, 1981) and lake sediments. The most recent member of this group, the Taupo Ignimbrite (corresponding to Upper Taupo Pumice and Rhyolite Block members of Healy *et al.*, 1964) covers an approximately circular area of 80 km centred on Lake Taupo. "Thicknesses range up to 100 m or more, the deposits always being thickest in the valleys and thinning rapidly up slopes and ridges" (Froggatt, 1981) as shown in figure 2.2. Walker *et al.* (1980) notes that the ignimbrite climbed 1500m above its source vent elevation at 45 km distance.

The soils in the study area have, for the most part, developed on a group called the Taupo Pumice Formation. Within this there are 8 members ranging in age from 200 B.C. to 1000 A.D. The Type Section for this formation used to be the Terraces Pumice Pit (U18:823-723) on State Highway 5 (Healy *et al.,* 1964), but each member now has

it's own Type Section. Further away from the vent, it is less likely it is that all the members of the formation will be present, and the average particle size of the erupted material may decrease. Taken from Froggatt (1981), is a condensed description of four youngest (which comprise most of the volume of the formation) of the eight members.

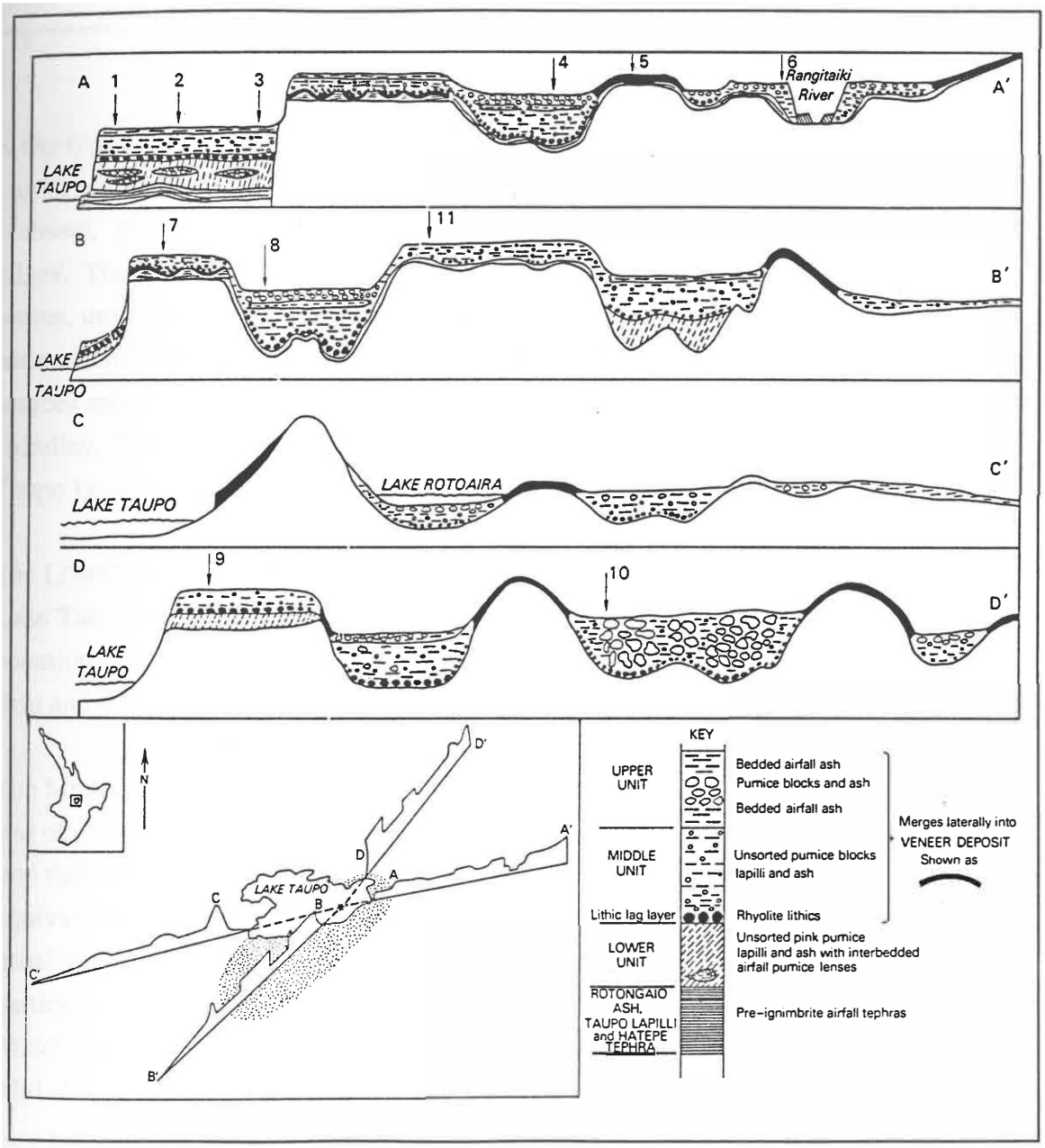

Figure 2.2 Schematic cross-sections (not to scale) through Taupo Pumice Formation to show the relationship and distribution of each unit and facies of Taupo ignimbrite as shown in the key. Stippled area on location map indicates the approximate extent of the Lower unit. (Froggatt, 1981) Profile D - D' corresponds reasonably well with the long axis of the study area.

Description:

From oldest to youngest they are: Lower unit, Lithic lag layer, Middle unit, Upper unit, which comprise the:

Taupo Ignimbrite

In the type area, it consists of all the primary pyroclastic deposits overlying the Taupo Lapilli or those deposits occupying an equivalent stratigrphic position where the lapilli is absent. As stated earlier, it is thickest in the valleys and thinnest on slopes and ridges. The ignimbrite shows no systematic variation of thickness with distance from source, unlike most other pyroclastic deposits. This deposits exhibits a remarkably wide variation in nature, which has led many people to postulate several different sources and extensive redeposition by mudflow and fluvial means (Grange, 1937; Grindley, 1960; Healey *et al.* 1964). Three pyroclastic flow units are recognised in Taupo Ignimbrite. The relationship of these is shown in figure 2.2.

The LOWER UNIT is restricted in occurence to a sector from northeast to southeast of Lake Taupo and consists of typically pink to red-brown unsorted pumce lapilli with occasional interbedded layers of better sorted coarse lapilli. The unit generally is very firm and stands in vertical sections.

The MIDDLE UNIT forms the main body of the ignimbrite and is remarkably widespread and of a highly variable character. Despit it's variable nature, the unit can be grouped into three broad 'lithofacies', but each is distinctive and they form lateral stratigraphic equivalents.. The facies grade laterally and sometimes vertically into each other, usually over a short distance. Each is considered to have been formed as a result of a particular flow characteristic of the pyroclastic flow. North and west of Lake Taupo, Middle unit appears to be predominant over the other units, but east of Lake Taupo the Middle and Upper units predominate.

The UPPER UNIT is a usually discontinous sequence of interbedded flow and airfall material, some of which has subsequently been removed by erosion or obscured by soil formation. Thickness is typically 0.3 - 0.4 m , but ranges up to 5 m or more. Two notable features are the extensive distribution of chalazoidites (accretionary lapilli) in fine ash airfall beds and the occurence of large pumice blocks up to 0.4 m diameter in unsorted units only 1 m thick. This unit corresponds to the coarse blocks often seen in the top of the ignimbrite, especially on Kaingaroa Plateau.

Within these units there are three facies types: the 'valley facies' (VF), 'fines-depleted facies' (FDF) and ignimbrite veneer facies (IVF). VF is the typical unwelded, unsorted mixture of pumice ash, lapilli, and blocks found in valleys over a wide area of the central North Island. At the reference section at Waitahanui River it is over 50 m thick. The full thickness of VF is seldom exposed, and the deposit is thickest in valleys and thins rapidly upslope to grade into IVF. VF is the predominant facies of the Taupo Ignimbrite and it is estimated as >60% of the total volume. This facies was formed by the pyroclastic flows 'ponding' in valley floors and depressions, thus producing a flat near horizontal upper surface.

FDF are found within the Valley facies as pods of coarse, well rounded and highly porous pumice blocks lacking the usual fine ash matrix and they are clast supported. These pods grade both laterall and vertically into VF. They occur within about 40 km of the source and are generally found in the thickest central part of the ignimbrite valley ponds. They vary from about 1 m to more than 10 m in lateral extent, and occasional discontinuous series of pockets extend up to 2 km across within the larger ponds.

IVF is formed where the Taupo Ignimbrite deposits become thinner and apparently more fine grained upslope, merging laterally into a compact ignimbrite facies that conformably mantles the higher topography with a thin 'veener' of ignimbrite. It is areally the most extensive facies of Taupo Ignimbrite see (figure 2.3) and forms about 50% or more of the total area, but only 30% of the total volume. It is easily identified by a position on higher topography above valley ponds and by a compact fine ash nature with no pumice lapilli (except discontinuous lenses of lapilli within 20 km of the source).

Most soils in the Taupo-Reporoa region (Map One in pocket) being formed on the Taupo Pumice Formation, are very young in age. The thickness of the "A" horizon was often only a few centimetres, and would average five centimetres. The "A" and "B" horizons combined, which are loosely defined to contain organic matter and moderate to light weathering, were found to extend to no more than 20 centimetres depth in all the sites, except those in peat.

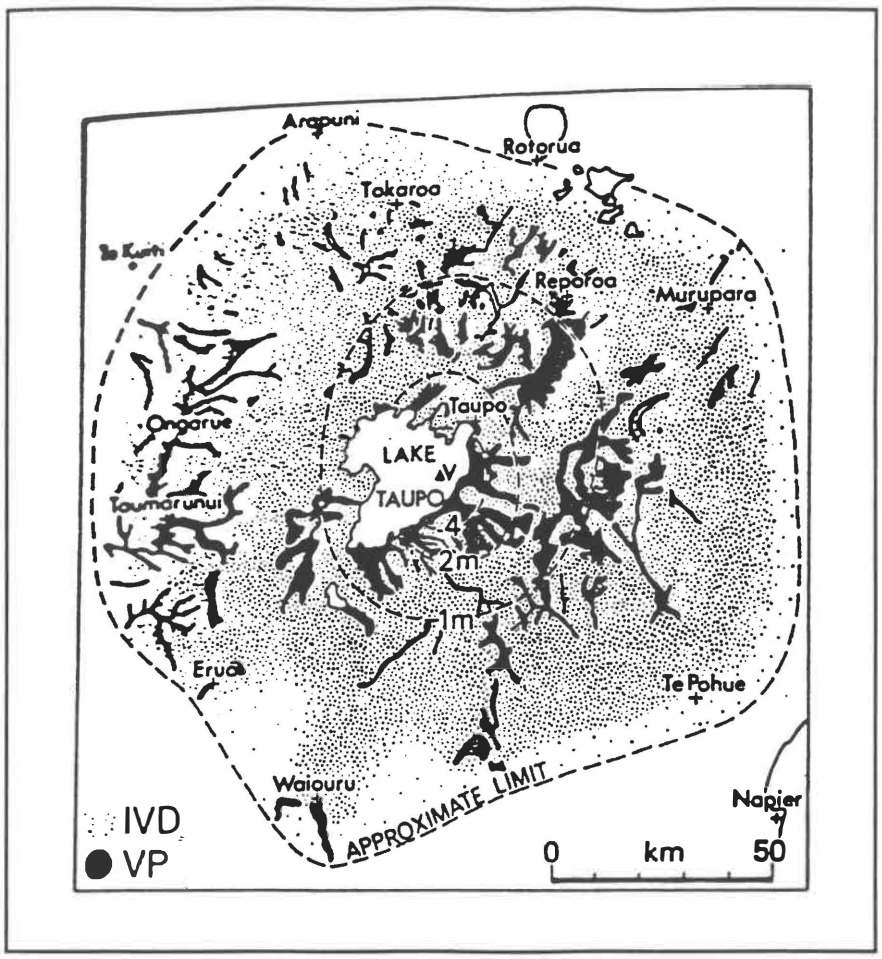

Figure 2.3 Map of the Taupo Ignimbrite distinguishing semi-schematically between IVF (stippled) and VF (solid black). The dashed are the approximate average thickness of IVF, and V is the vent position. (Walker *et al.*, 1981)

The "C" horizon was always found to be largely unweathered tephra or pyroclastic flow material (except peat sites). From Pullar *et al.* (1973) it was found that the Taupo Pumice Formation comprises the top layer of erupted material in the study area, and so essentially most soils (except the peat or alluvial soils) are formed at the same time and from similar parent material (for further information refer to Appendix I)

Soils which have formed on peat comprise about 5 - 10% of the study area. The depth of the peat is only a metre in some sites nearer slopes, but does exceed two metres in others (evidence from profiles in drains.). They are mainly found in the north end of the Reporoa basin and are relatively young and as there is very little volcanic detritus found in them, it can be safely assumed that they post-date the most recent Taupo eruptions.

2.3 Site Investigations

Sites were chosen on the basis of accessibility, and then on there being a reasonable distance to the soils' boundaries. An effort was also made to have a good spread of sites through the region, although this was difficult as many areas of soils were not large enough to be sure of locating a site accurately within them. There is some doubt about the accuracy of the soil maps when dealing with some of the smaller pockets of different soils.

Soils that have had or have forestry on them have been avoided as the profile is destroyed by this sort of activity. Also, areas immediately next to earthworks (within a few metres), such as roadworks or drain digging, have been avoided in order to sample the conditions of the soil in their predominant "natural state". This was so the results would more accurately reflect the dominant conditions in the soil.

To a certain extent, it is acknowledged that almost all the soils in this region have undergone some degree of disturbance, whether it be from agriculture, earthworks, or drainage. Some soils in the area of study were not considered for one or a combination of reasons, but are included on the soil map. These reasons include: slope is too steep, too small an area of coverage, inadequate depth of parent material above basement rock, or accessability to a site would have been difficult.

Soils were chosen on the valley floor and lower slopes, as the approach of soil strength assessment to seismic hazard is suitable for materials of some thickness, where the soil properties measured reflect the upper parts of the regolith (Hodder, 1993). Soils on the steeper slopes in the area of study, are also not considered in the assessment of hazard as they contain only a very small number of buildings and infrastructure. However an effort was made to choose the initial sites as being as representative as possible of the soils as a whole.

In total 43 initial sites were tested for the parameters of shear vane, Bush penetrometer, and hand penetrometer down each of the Horizons A, B, and C, as defined in Chapter 3 in the discussion of soil moisture. The sites were examined in summer so there is some seasonal variation between these results, and those obtained from the final sites later in the year. The final sites, those that were chosen (from the initial 43 sites) for a more comprehensive investigation, were then re-tested for shear vane, Bush penetrometer, and hand penetrometer. They were also sampled for soil moisture, bulk density, and cores were taken for use in GDS triaxial testing.

The sites are listed below in numerical order, not all the numbers are there as not every single site chosen was visited. Listed below, is a grid reference, road reference, and soil type. Distances along roads are approximate. For a description of the soils, please see Appendix I.

No.	Grid Ref.	Road Reference	Soil
1	809-703 I	junction of Settlers Rd and Wharepapa Rd	34
2	805-704 I	Wharepapa Rd, 500m from junction	33
3	809-700 I	200m south of Settlers and Loop Rd junction, paddock opposite milk shed	31a
5	795-684 I	Reporoa Rd, approx. 1km from Reporoa town centre	12a
6	780-688 I	junction of Reporoa Rd and S.H.5	10b
7	780-694 I	500m north of site 6, at dairy factory	11+10a
8	791-718 I	junction of Wharepapa Rd and S.H.5	11+10a
9	787-721 I	500m along Handcock Rd (unnamed on map), next left down S.H.5 after Wharepapa Rd	12+32
10	777-725 I	1.3 km down Handcock Rd	32a
11	805-739 I	junction of Settlers Rd and S.H.5	2a
12	806-741 I	junction of Campbell Rd and S.H.5	31
13	845-702 I	Alamein Rd, 800m from Forest Rd junction (near milking shed)	2a
14	816-659 I	in vicinity of Kopuhurihuri Stm, east paddock	12
15	803-679 I	Reporoa: small section opposite Takeaways	10
16	832-741 I	Rotorohe Rd and Forest Rd junction (50m south of)	2
17	745-619 I	Mihi: 100m down Mangamingi Rd from junction with Tutukau Rd	10b+10a
18	789-657 I	Homestead Rd bridge	31b
19	976-953	100m north of junction of Ohaaki Rd and S.H.5	Wn
20	984-936	at junction, 2km from turnoff from S.H.5	Wng
21	007-937	Broadlands: at junction in village	Mok+Ma
22	002-907	Broadlands Rd junction - entrance to Taupo Lucerne	Wng
23	987-869	Broadlands Rd, 500m from eastern side of forest	Hn
25	037-930	Earle Rd, 200m back from junction	Wh
26	026-874	vehicle track off Western Boundary Rd	Tpls
27	848-782	junction of Broadlands Rd and View Rd	Ai
28	795-845	1.3km along View Rd from junction with Broadlands Rd	Tpd
29	846-815	View Rd, at left bend 1km from Aratiatia Rd	Tp
30	861-778	McKenzies Rd bend	Yp

31	833-766	junction of Centennial Dr and Broadlands Rd	Ai
32	817-756	junction of Broadlands Rd and refuse tip road	Tpe
33	813-777	junction of Rakanui Rd and Aratiatia Rd	Tp
34	750-???	Acacia Bay Rd, 200m north of camp ground	Hn
36	807-730	junction of Crown Rd and S.H.5	Tpe
37	825-832	800m along Aratiatia Rd off S.H.5	OiH
38	823-785	1.5 km along Aratiatia Rd from junction with Rakanui Rd	Tpd
39	745-824	junction of Te Mihi-Poipipi Rd and Oruanui Rd	Ypg
41	874-688	S.H.5	Tpe
42	813-831	S.H.5 near Wairakei Village	Ai
43	802-859	junction of Palmer Mill Rd with small track	Oi
44	824-853	400m along Palmer Mill Rd from junction with S.H.5	Yp
45	027-056	1.6 km along Settlers Rd from junction with Wharepapa Rd	33
46	978-914	200m along Ohaaki Rd from junction with road that crosses a bridge	Wn
47	042-027	100m along Otto Rd from junction with Longview Rd	12a+12

Sites are found on Map One (in pocket), however due to the scaling process used, some sites may be located on soil boundaries whereas in the real situation they are definitely within the boundaries of the soil being examined.

2.4 Seismicity

Swarms of quakes occurred in or near the study area (figure 2.5) in 1895, 1922, 1964, and 1983 (Grindley *et al.,* 1986) In 1922, the biggest swarm caused 3 - 4 m of regional subsidence within the Taupo Fault Belt. The 1895 shock was not investigated in terms of obtaining instrumental data, and in the 1964 - 65 swarms no deformation data were recorded. Earthquake swarms in 1983 produced < 0.1 m fault movement on an existing scarp, and the events as a whole were able to be monitored from earth deformations before and during the swarms. The Whakaipo and Kaiapo Faults which are mentioned below are found in the southwest corner of the study area.

1895

Seismicity occurred continually over a period of 3 - 6 weeks, with a mud volcano eruption, landslides and subsidence in the area north and to the east of Taupo. Fissures

opened between Tauhara and Manganamu and the road south out of Taupo was damaged. The magnitude is estimated to be 6.0 to 6.9

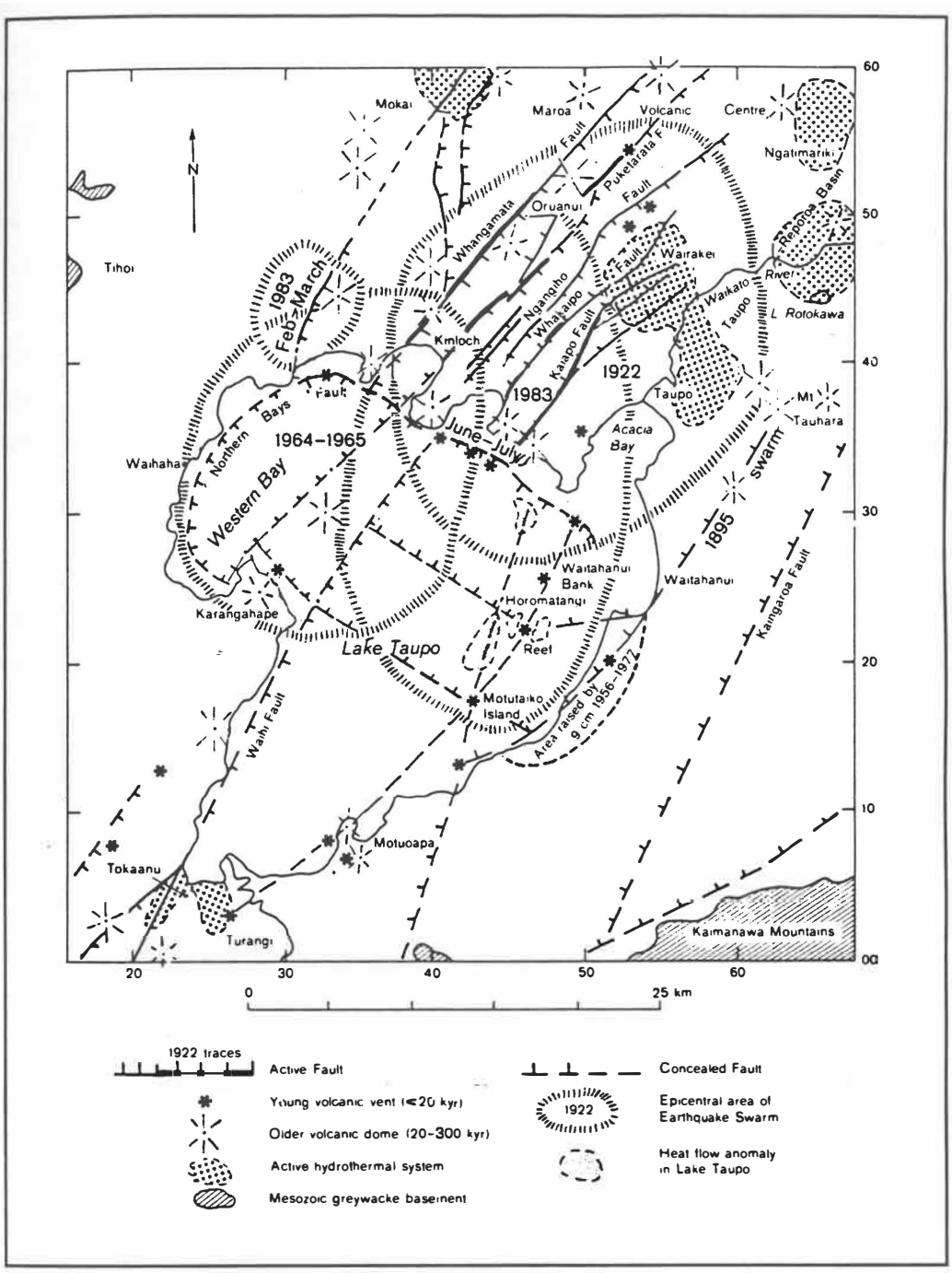

Figure 2.4 Epicentral areas for earthquake swarms (Grindley *et al.*, 1986)

1922

Seismicity occurred over a long period of eight months, and the largest quake which occurred in June, was estimated to be of magnitude 6 - 7.5 (Eiby, 1968). In June and July there were up to 100 events a day that could be felt. There were landslides and

fissuring in the Wairakei geothermal area on the Kaiapo Fault, as well as changes in geothermal activity. Subsidence occurred on the northwest shore of Lake Taupo; most of which occurred after the main period of seismicity. The area between the Whangamata and Whakaipo Faults dropped between 2.3 to 3.7 m. This subsidence was preceded by the ground cracking along pre-existing fault scarps, possibly from the largest shock in June.

1964 - 65

Seismicity started in December 1964 at 100 - 150 events per day centred in Western Bay but these also extended to north of the lake, and over time moved southeast into the northern Lake Taupo. Seismicity in early January 1965 occupied a narrow belt across the lake from Waihaha to Horomatangi Reef. The largest event was magnitude 4.6. An area on the east shore of the lake rose 100 mm between levelling survey in 1956 and 1977 which is thought to be related to this earthquake swarm.

1983

Before 1983, a network of lake level gauges and tilt level sites was set up around Lake Taupo, which helped provide a good record of deformation and tilt from the swarms. The first swarm in January to March was matched with a uplift of 43 mm centred on Kinloch and Moturoa northwest of the lake. The largest event in this swarm was magnitude 3.75, and focal depths were 4 - 8 km. A second swarm occurred in June and July, with a largest event of magnitude 4.3, and focal depths of less than 1 km. There was slight normal faulting over 1.2 km of the Kaiapo Fault soon afterwards.

More recently there have been:

1995

An earthquake centred in the NW corner of Lake Taupo on 27 January 1995 of approximate magnitude 5.5, and another earthquake of magnitude 5.9 on 23 March 1995.

Chapter Three

Chapter Three

Field and Laboratory - programme and methods

3.1 Introduction

In the field, samples of loose soil were taken from each of the three horizons A, B, and C. For the purposes of this study they are defined on the basis of weathering of the profile. The uppermost horizon A, is what would normally be defined as topsoil and at most sites was from a few centimetres to ten centimetres thick. The B horizon is the middle unit of soil that is still weathered but contains little organic content and is often quite different in colour and texture from the A horizon. The C horizon was defined to be the largely unweathered parent material. In this region the soil is young and so the top of the C horizon is commonly at 15 - 30 centimetres depth. The exception to this is, of course, peat soils.

As stated in Chapter two, sites were tested in the field with the shear vane, Bush penetrometer, and hand penetrometer. The lab tests that were carried out were soil moisture, bulk density, and two tests on the GDS Triaxial Testing System: the standard compression test and the cyclic loading test. Each of these tests will now be considered in turn.

3.2 Soil Moisture

The soil samples were taped up in plastic bags for transport to the laboratory where they were immediately tested for the moisture content. Ten small sub-samples were taken out of each bag and dried out in tin foil dishes in a conventional oven at 105^{o}C. The sub-samples after drying, were weighed and reweighed until they obtained a constant

weight. This is reached when the changes between repeat weighings are less than 0.1% of the original sample weight. Ten samples were found to be enough to give a standard error of < 3 % of the mean value. This procedure for drying and weighing the soils was that of Vickers (1978), known as thermogravimetric determination for which advantages and disadvantages of this method are summarised by Smith *et al.* (1991).

A number of points to be noted are: the samples were chosen to be representative of the soil, the length of time between placing the soil in the dishes and then being weighed and placed in the oven was minimised to avoid premature loss of moisture. Also, a desiccator was always used to allow samples time to cool down before weighing without regaining moisture from the air. Vickers (1978) states "the sample must be sufficiently large to give adequate weighing", however as ten samples not just one, were always analysed for moisture content, the results should be precise.

3.3 Bulk Density

Three bulk density samples were taken at each of the three horizons using small coring rings. They have a diameter of 60 mm and a length of 50 mm. Where the soil did not perfectly fit the rings, birdseed was added to determine the amount of soil missing. The samples were wrapped in plastic film in a plastic bag, and taped to prevent drying out. They were analysed in the laboratory within several days. The three readings from each horizon were sufficient to give a standard error of < 6 % of the mean value.

The wet bulk density of a soil is the mass including any water per unit volume, and the dry bulk density is the oven dry soil per unit volume of moist soil. These two parameters are simply related by the equation involving soil moisture content.

$$\rho_S = 100 \times \rho / (100 + W)$$

Where ρ_S is the dry bulk density, ρ is the wet bulk density, and W is the soil water content expressed as a percentage.

The coring method is widely used, and in this case the three rings were hammered gently into the ground at each of the three horizons. Baver *et al.* (1972) however, have suggested that insertion by hammering may cause shattering, so as much care as possible was taken. The rings were pressed into the ground only as far as the top of the ring or just before, depending on the flatness of the surface, so as to avoid compressing the sample. The most obvious source of error in this method is the disturbance of the

core due to compression, (although it is likely there is some lateral movement no matter how careful you are). Coarse sands and gravels are not sampled satisfactorily by this method, but give an approximate bulk density value.

To make the rings easier to insert, the following hints were followed as suggested by Smith *et al.* (1991), which was to use a cylinder wall that was as thin as possible but still stiff enough not to bend, and to lightly lubricate the inside (and outside) of the coring rings.

3.4 Particle Size Analysis

Depending on the sample, sieving and / or a sedimentation procedure was used. Samples were available for most of the final sites. Wet sieving was used for all samples with gravel and sand - sized particles, and for fractions or samples smaller than this the pipette method was used. The procedure is found in Lewis *et al.* (1994). Only five sites contained a large enough mud (silt and clay) fraction for a sedimentation procedure to be carried out.

3.5 Shear Vane

Shear Vane tests were carried out in the field with an inspection vane borer. Although the vane (figure 3.1) is designed to be used to measure the *in situ* undrained shear strength in clays, it has been found to be quite adequate for use in coarser soils which are not too compacted (Dunn *et al.*, 1980). The measuring part of the vane is a spiral spring. When the handle is turned, the spring begins to load up and the upper and lower parts of the vane move opposite to each other, giving an angular displacement, until a point at which the blades shear in the soil. This is measured by a rotating ring on the handle that has a graduated scale.

There are three sizes of blades supplied: standard size - 20 X 40 mm, small - 16 X 32 mm (readings to be multiplied by 2), and large - 1" X 2" (readings to be multiplied by 0.5). This makes it possible to measure harder or softer soils more accurately, although observations in the field suggest that the three different blades used in the same soil may give slightly varying results. The maximum shear strength that may be measured is 20 t/m^2 and this requires a force of 40-50 kilograms to insert the vane into the soil. As the readings were always taken in a soil profile, no extension rods were needed.

The part of the shear vane are: (1) - handle, (2) - spiral spring, (3) - rotating ring, (4) - lower half of vane into which the shaft (5) and vane (6) attach onto. The dimensions are in millimetres.

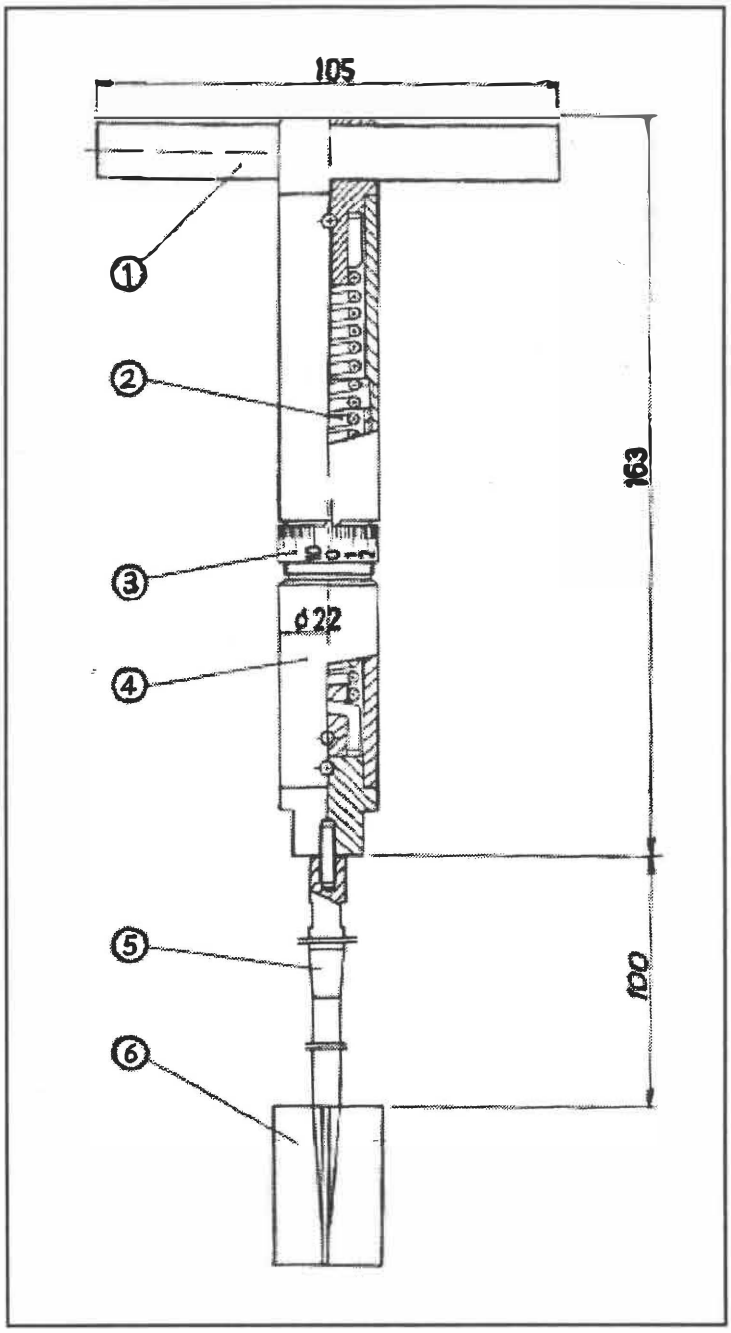

Fig. 3.1. The Shear Vane (from instruction leaflet)

The expression for shear strength, taken from Dunn *et al.* (1980) is

for Rod diameter 1/2 in.

$$S = T / (p D^2 (H / 2 + D / 6)$$

where

S = shear strength
T = maximum torque
H = height of vane
D = diameter of vane

Remoulded shear strength was not examined, as some of the soil material was either too crumbly or coarse.

For the final sites, shear vane readings were taken across each of the horizons. Twenty readings were taken at each horizon, and then an average, standard deviation, and standard error were calculated. As most soils were fairly variable even over small distances, it was necessary to have this many readings for an accurate result. Moon (1990) notes that to achieve an acceptable standard error "Usually five to ten repeats are adequate as a rule of thumb, but this depends very much on the nature of the experiment". Shear vane readings were also taken at each of the 43 initial sites, but with only ten readings at each horizon. Some sites did not have readings for their C horizon, as the soil was too strong to be penetrated by the shear vane or the horizon was comprised of loose pumice of variable size (which is like putting the shear vane in a bowl of marbles and trying to get a reading).

Selby (1993) states that "Shear vanes may be used successfully only in fine-grained soils without roots, clasts, or strongly developed structures. Soil strength is strongly controlled by moisture, so soil samples should be taken for moisture content, or all measurements should be made at a nearly uniform moisture content such as field capacity (the state at which the soil has drained freely under gravity, but retained water in the micropores)." The initial results were obtained under dry summer conditions when the soil moisture was at field capacity. The results from final sites were obtained along with samples for moisture content as they were sampled throughout the year.

The errors that arise in this method are from soil displacement (and hence the structure being weakened) as the vane blades are inserted, movement of the vane from side to side as it penetrates stiffer soils under heavy pressure, root resistance in the upper soil profile, and variation in the rate of rotation. Also, as the grain size increases, the reliability of the test decreases.

3.6 Hand Penetrometer

The hand (pocket) penetrometer (figure 3.2.) was also used for twenty readings down the three horizons for all of the final sites. Readings were also taken at all of the initial 43 sites with ten readings down each of the horizons.

This penetrometer is similar to the Soiltest pocket penetrometer, which was redesigned in 1970 (Sanglerat, 1972). Soiltest has analysed data from several thousand unconfined compressive strength tests on silty clays and clayey soils and compared them with penetrometer readings. Its conclusions were that there was a close relationship between penetrometer readings and soil type consistency, consistency in this case defining the coherence or hardness of the soil.

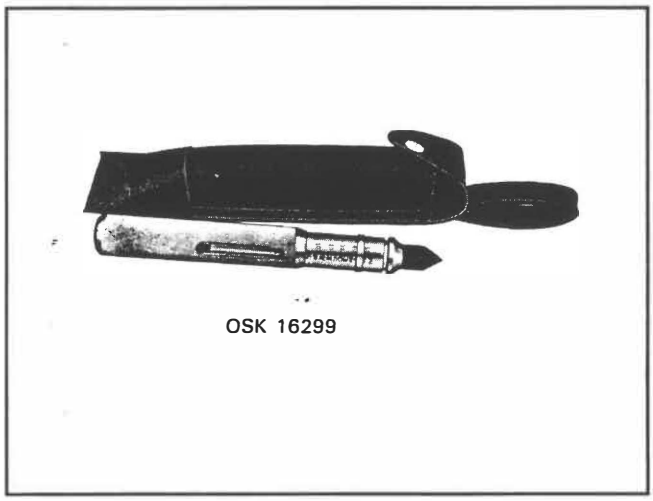

Fig. 3.2. The hand penetrometer

The penetrometer has a number of graduated scales along the shaft, with a sliding ring that moves along it. Before the reading was taken, the ring was moved to the zero mark, as pressure was applied the ring moved along the shaft to the maximum value of pressure that was exerted. All readings were recorded in kilograms of force then later converted to kilopascals.

Twenty readings were also recorded for each horizon in the final sites as opposed to ten in the initial sites, this was again done as some of the soils were quite variable.

3.7 Bush Penetrometer

Forty readings were taken at almost all the final sites within a ten metre radius around the pit from which the other measurements and samples were obtained. The penetrometer is able to take 15 readings down a soil profile at three centimetre intervals. This gives a total depth of 45 centimetres, which is comparable to the depth of most building foundations in the region.

Sanglerat (1972) states "A minimum of five readings at each depth is recommended in order to obtain a good estimate of the probable mean value. Initially ten readings were made at each of the sites, and then the values across each depth were averaged, and a standard deviation and standard error were calculated. In the final sites results, forty readings were made in almost every case with the exception of the first few, where only twenty readings were taken. It is considered that although forty readings seems excessive, the soils in the study area were in most cases sufficiently variable to warrant this.

As most of the soils are relatively young and unweathered, the A and B horizons are thin, and together make up only the top five - twenty centimetres on average. As a general rule the C horizon dominates the profile in which foundations are sitting in and on. Consequently, only the lower readings for the penetrometer are used in analysis of the sites. The readings on the digital display give a measure of resistance of the soil to the force applied on the rod, and are converted to the appropriate units of kilopascals.

The Bush penetrometer was developed in Scotland by soil scientists who wanted a lightweight unit suitable for use in soft or weak soils. It has an effective range of 45 centimetres (although extension rods can be used if necessary) and is operated by one person applying their body weight as the downwards driving force. It also has the capacity to download the data from each penetration to a portable computer.

Sanglerat (1972) states that the use of such light duty penetrometers "is primarily intended for fine grained soils. It can however be used in loose, dry sand, but firm sand is beyond the range of the instrument. The presence of stones does not preclude its use, provided measurements are rejected when it obvious that the cone has come into contact with a stone. It is not suitable for use in stony or gravelly soils." Most of the soils in the study area were suitable in these respects, as they are young and unconsolidated, although some had limited penetration.

No references were available that discussed the problems and errors in using the Bush penetrometer, but from field experience a few observations have been made.

- In soils that obtained a large number of cobble-sized materials quite a few penetrations had to be discarded before the quota was reached. It is possible that this may lead to a biased profile of what the soil is really like.
- The effective reach of the penetrometer may be insufficient in some of the soils as readings still may have been obtained below its range, showing that some soils were still soft at depth, compared with others.
- A larger penetrometer (eg. trailer mounted) that could achieve greater penetration through stiffer soils and to a greater depth would have been more useful, although far more time consuming.
- It was not always possible to penetrate the ground vertically as the base has to sit flat on the surface. (eg. on slopes).

3.8 GDS Triaxial Testing System

3.8.1 Sampling

The cores were collected in 400 mm long by 98 mm (internal) diameter thin-walled stainless steel sampling tubes with a tapered cutting edge, which are referred to as 'drive samplers'. The main advantages of using these samplers is that they are simple to use, and cause a minimum of disturbance in the soil. They were considered appropriate for the range of soils in the study area which included: fine sand and silt (cohesive and slightly cohesive soils); soft peat (very soft soil); very dense sand and silty and sandy soils which acquired cohesion through partial drying (compact or stiff soil). There were a few coarse gravelly and stony soils and it was difficult to sample these without disturbance of the soil. Freezing is the only effective method for obtaining undisturbed samples but it is very expensive.

A trench was dug: approximately 2:0 m long by 0.6 m wide, and 0.3 to 0.4 m deep. At the A and B horizons, samples were taken for soil moisture and bulk density, and in the top of the C horizon down the centre of the pit, samples were also taken. Along each side the samplers were driven into the ground as in figure 3.3 below. After the cores were excavated, readings for the hand penetrometer and then the shear vane were taken at either end of the pit (to avoid compaction from the vehicle), and Bush penetrometer readings were usually then taken.

Fig. 3.3 The 'slow jacking' arrangement for obtaining cores for the triaxial testing system.

The drive samplers were forced into the ground by 'slow jacking', but if this did not supply sufficient force then 'hammering' was used. Slow jacking is found to produce plastic deformation and changes in volume, as well as increased wall friction and adhesion and the entrance into the sampler of excess soil. However, "fairly satisfactory samples of not too soft cohesive soils may be obtained with soil jacking, provided thin wall samplers are used" (Hvorslev, 1962), although it should also be noted "distortions and shear failures may occur after a relatively short penetration". The exception to this was when the peat was sampled: this was accomplished by 'fast pushing' which gives superior results (Hvorslev, 1962).

In comparison hammering, almost stops entrance of excess soil at the beginning of the penetration, but it often produces shorter and somewhat distorted samples from cohesive soils. In cohesionless soils it disturbs the sample and may cause volume

changes and so is not recommended for soft or loose soils. Hvorslev (1962) states that hammering is quite suitable for forcing samplers into hard or dense and coarse soils.

The samplers are dug out and the ends, if necessary, were packed with newspaper and extra soil to ensure the core remained undisturbed during transport. The ends were either covered over with circular filter paper and covered with plastic film and taped up, or plastic caps were used. Finally the cores were placed individually in strong plastic bags, and taped up to help ensure air-tight storage.

3.8.2 Setting up the System

The samples were extruded using a hydraulic ram, and then cut to 200 mm length. Head (1984, Vol. 2) notes that for a maximum particle size of 20 mm, a sample size of 100 mm diameter and 200 mm length should be used. Almost all the sites satisfied this condition, but a few samples were found with slightly larger particle sizes. If the base or top of the sample was not sufficiently flat enough due to material falling out, it was gently repacked with the soil trimmings until a good surface was obtained (this is acceptable practice- Hvorslev (1962)). The most effective way of obtaining a square end was to use a palette knife with a blade width of greater than 100 mm. The samples were placed on the base pedestal in the hydraulic cell of the triaxial machine such as in figure 3.4, and filter paper was used on both sides of the copper plates on either end, to allow the water to flow through the sample more quickly.

The rubber membrane that is placed over the sample was checked thoroughly for holes: even the smallest pinhole will prevent the difference between cell pressure and back pressure being maintained. The membrane was secured with two rubber "O" rings on each end. All connections on the machine were checked for tightness and if there was any doubt about leakage, thread tape was used to ensure a good seal.

After the cell was filled with de-aerated distilled water the pore pressure controller was zeroed, so that it could be used to measure the amount of pressure when saturating the sample. For both the consolidated undrained test and the cyclic loading test, the samples were saturated with CO_2 and then with water (Fredrickson, 1988). This was achieved by connecting the CO_2 hose to the pore pressure tap. The CO_2 was fed through the system at no more than ten kPa (as most *in situ* confining pressures for the samples were in the range of 5 - 10 kPa) to minimise disturbance to the sample.

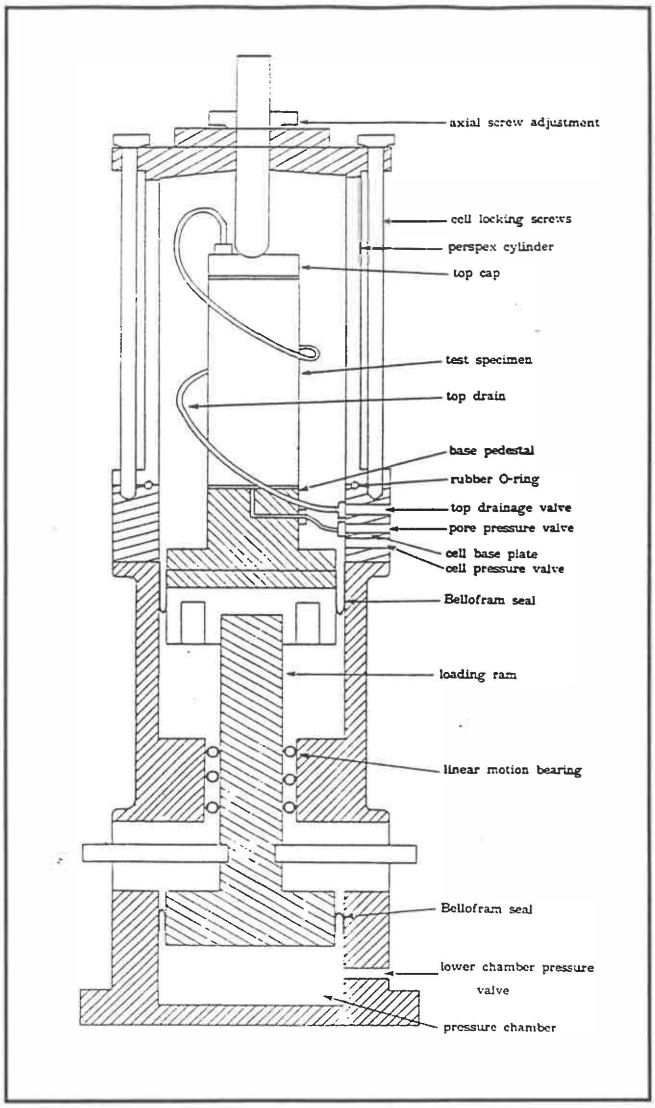

Fig. 3.4 Schematic cross section of triaxial cell (not to scale) (after Fredrickson 1988)

The hose from the "top" valve was disconnected at the controller end (back pressure) and put in a plastic measuring cylinder with water in it to be able to see the air being pushed through. The presence of CO_2 can be tested for, by holding a match in the end of the cylinder to see if it will be extinguished. This usually took from 5 - 45 minutes to complete, depending on the porosity of the sample.

The next stage of the saturation was to feed de-aerated distilled water through the sample in the same manner as the CO_2. Sometimes pressures higher than 10 kPa were required for the water to saturate the sample as the water would not pass through the sample easily. This saturation could take anywhere from ten minutes to several hours. Saturation was complete when no more 'air' was seen bubbling into the cylinder and coming out of the top hose on the sample inside the cell. However, the water was allowed to run for a short while longer to ensure saturation. This method of saturating

is preferred over the back pressure method, although it took longer, it was more reliable, and efficient (Fredrickson, 1988).

All the hoses were then reconnected to the appropriate fittings, and the valve on the top of the cell was opened to allow any excess pore pressure to dissipate. The cell could be "topped" up with water if necessary, by slightly emptying the cell pressure controller. The valve on top, was then closed off again and all the controllers were zeroed off. The sample was then ready to be tested for saturation using the "B check". The hydraulic cell is connected to three digital controllers which are linked to a computer which has a plotter and a printer attached as in figure 3.5.

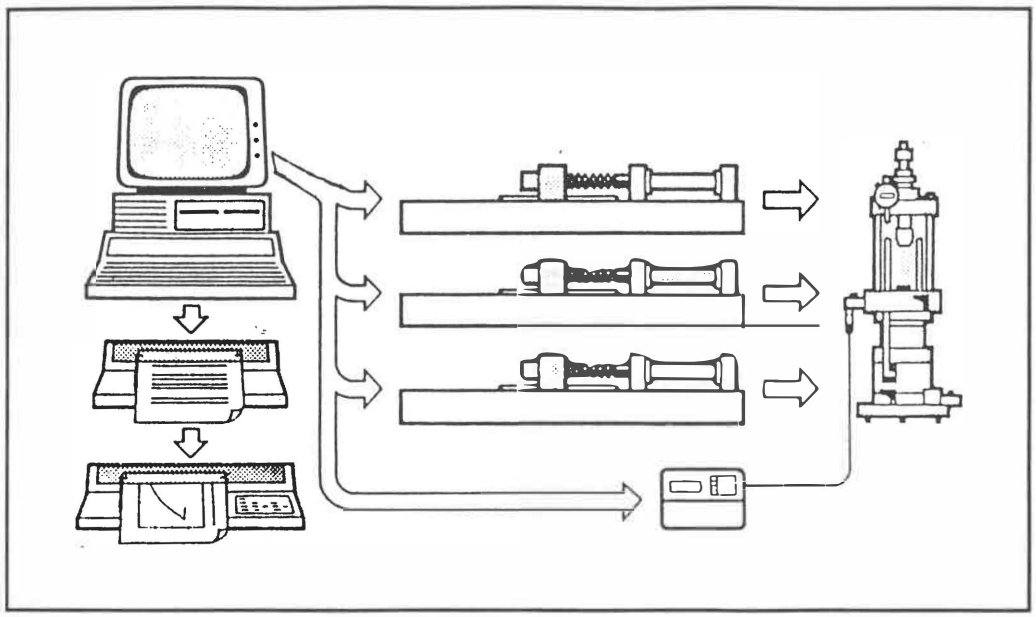

Fig. 3.5 Schematic layout of the GDS triaxial testing system (after Menzies, 1987)

The program "GDSTTS" was then loaded and run, and for all samples the diameter was set at 98 mm and the length 198 mm. The back pressure was always set at 500 kPa and the cell pressure was set at the back pressure plus the confining pressure. The confining pressure was varied over a number of tests, starting with 10, 20, and 40 kPa for the first three and then the results were plotted using Mohr circles. After this, intermediate confining pressures were used to fill in the gaps if necessary to help obtain a better fit for the curve predicted by the Mohr circles. Although confining pressure in the ground ranged from 5 - 10 kPa, the smallest pressure difference that could be reliably used was 10 kPa.

Once the cell and back pressures are reached, and the pore pressure has stabilised (usually slightly higher than the cell pressure), the sample was ready for the B check. A cell pressure change of 10 kPa was used and the check was run for 20 minutes. The B

check was found to be somewhat unreliable, as repeating the check on the same sample gave varying results. However, the check was usually run up to three times, with alternating negative and positive pressure changes of 10 kPa so as not to increase the confining pressure beyond the limit of the pressure for which it is being tested for. If the result was within ± 0.05 of 1.00, the sample is considered to be saturated.

The next stage of the pre-testing routine was to consolidate the sample under the appropriate confining pressure. The back and cell pressures are set at the same pressures as at the start. The maximum volume reduction was set at 200000 mm^3, and the minimum volume gain at 0 (as none of the samples contained enough clay, which might swell). The consolidation took only 5 - 10 minutes for a sandy soil, but 3 - 4 hours for a peaty soil. When it took a long time to complete, the back pressure controller was first disconnected and a third of its volume emptied and then reconnected before the consolidation stage was run. This was so that the controller would not reach its limit and terminate the consolidation prematurely. Consolidation is complete when the volume stops changing (as viewed by the curve 'flattening out' on the screen); the process was then stopped and the results saved. The computer then calculated the new dimensions for the sample.

Before the test (consolidated undrained or cyclic loading) began, a friction check was carried out. The minimum required displacement used was 0.1 mm but in most cases 0.5 mm was used, although increasing the displacement appeared to increase the calculated friction even when the triaxial apparatus had just been cleaned and had its bearings replaced. Any lower value gave unreliable results. The sample was then ready to be used for one of the tests.

3.8.3 Consolidated undrained test

This test is simply described by Bishop *et al.* (1962) as "a compression test in which the soil specimen is first consolidated under an all-round pressure in the triaxial cell before failure is brought about by increasing the major principal stresses, σ_1."

The " standard" triaxial compression test procedure is clearly explained in Head (1984, Vol. 2). The computer controlled method used in this study was taken from Fredrickson (1988), although a number of small errors were found in the explanation of the test.

When pore water pressure is to be measured, strain rates also depend on the permeability of the soil and whether or not side drains are used. Clay soils with side drains may take 3 - 6 hours to complete. As some of the samples were quite fine grained, a slightly slower rate for all samples was opted for; 15 mm/hr (100 mm sample). The strain was the same for all sites tested, to be consistent in the experimental procedure.

3.8.4 Cyclic Loading

The cyclic loading test was run as described in the GDS Users Handbook Part II (1988). It subjects the sample to cyclic axial stress in one of three waveforms. When considering the nature of earthquakes, the most appropriate waveform is a sine wave (Eiby, 1989) and for this reason it was used. The amplitude of the wave was set at 100 kPa, and the period of each cycle was 3 minutes. The Hewlett Packard computer had only the ability to store 15 cycles of loading and unloading, which is unfortunate as an average strong motion earthquake lasts for 50 - 60 cycles (Seed, 1960). Parton *et al.* (1971) used the third hysteresis loop from their tests to derive their parameters for earthquake response.

Cyclic loading of samples in the laboratory is primarily used to model the behaviour of normally consolidated soil, in which foundations lie which are subjected to repeated loading. Earthquakes may be expected to produce similar stresses on the soils under building foundations though these are admittedly somewhat more rapid (Parton *et al.*, 1971).

3.8.5 Analysis of results

The analysis is performed on a program called 'GDSFBP', where there is the option of tabulating or plotting the data. A graph of deviator stress versus percent axial strain was plotted in order to visually determine the point of 'failure'.

The strength of the rubber membrane is not taken into account as there is no appreciable difference when 98 mm (4 inch) diameter samples are used. Bishop *et al.* (1962) states that "for 4-in. diameter samples a rubber membrane 0.01 in. in thickness is often used and the value of M (extension modulus) determined experimentally is about 2.0 lb/in.....The correction is clearly very small and is usually neglected."

Types of failure in specimens is shown in figure 3.6. The determination of the failure point is found more easily in brittle failure (marked by a definite change in slope of the deviator stress), than in plastic (barrel) failure which the slope of the deviator stress reaches a maximum value and levels out.

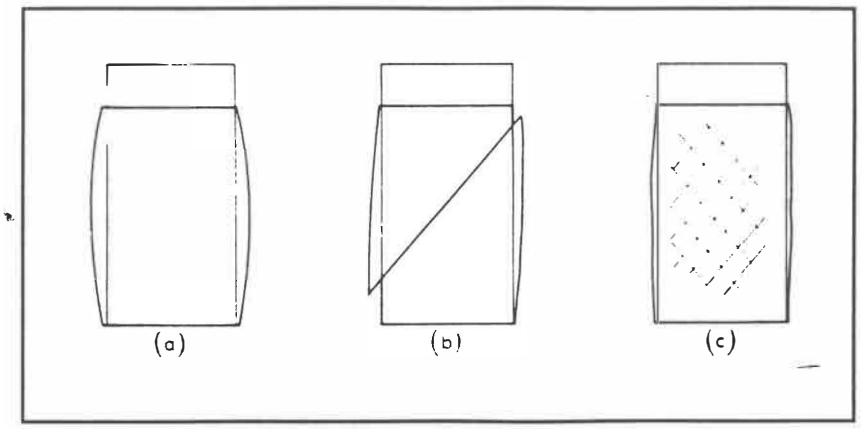

Figure 3.6 Types of failure in compression test specimens: (a) plastic failure (barrelling), (b) brittle failure (shear plane), (c) intermediate type (Head 1984 Vol. 2)

By knowing the deviator stress at the point of failure, which is a function of σ_1 - effective axial stress, and σ_3 - effective radial stress, a circle may be drawn on a Mohr Coloumb diagram. For each soil five (sometimes only four) results were obtained and were plotted to give the cohesion (c_u) and the angle of shearing resistance ø. The results are represented in the equation:

$$\tau_f = c_u + \sigma_n \tan \phi_u$$

Where τ_f is the shear stress acting on the failure plane at failure;
c_u is the cohesion intercept - for an undrained test;
σ_n is the normal stress acting on the failure plane at failure;
ϕ_u is the component of shear strength of a soil which is due to friction between the particles (Head, 1984, Vol. 2)

Head (1984, Vol. 2) notes, for most practical purposes this relationship holds true and it is the most widely accepted criterion of failure. He also states that for cohesionless soils, c_u will be zero, and they obtain their shear strength entirely from intergranular friction (tan ø), and for cohesive soils the opposite is true. In Chapter Four of this study typical values for soil are found.

For cyclic loading tests the following variables were tabulated: time, percent axial strain, axial stress, effective axial stress, effective radial stress, and average radial strain. Only the time, axial stress, and percent axial strain are needed in order to construct hysteresis loops. The loop was taken from the tenth cycle of each test where the sample was near 'steady state conditions'. In Chapter Four a figure shows how the loop was constructed.

From Parton *et al.* (1971) the equations for Dynamic Modulus of Elasticity (Ed) and Equivalent Viscous Damping Factor (D) were derived. Ed is measured as the slope of the line joining the opposite peaks of the loop, and D is found from:

$$D = A / (4\pi W)$$

Where A = the total area of the hysteresis loop,
and W = stored strain energy, or work area, defined by the area between a straight line from the origin to one loop peak and the deformation axis.

Poisson's Ratio is a measure "of stretching or compression along the longitudinal axis of a specimen accompanied by transverse thinning or thickening" (Selby, 1993), and so is given as:

$$\text{Poisson's Ratio } (\mu) = (\text{change in diameter} / \text{original diameter}) / (\text{change in length} / \text{original length})$$
$$= e_d / e_{ax}$$

It is generally assumed that the stronger the material the lower the value of μ, but near ultimate strength, this is not necessarily true, so most values of Poisson's ratio are taken at, or below 50% ultimate strength.

From these parameters, derived parameters can be obtained. For example,

Dynamic Shear Modulus (Gd) is defined by:

$$Gd = Ed / 2 (1 + \mu)$$

and, Shear Wave Velocity, is calculated from:

$$V_S^2 = Gd / \rho$$

Where ρ is the bulk density.

V_S gives an indication of the propagation of shear earthquake waves through the soil and it is assumed that the greater the velocity, the more rigid the medium.

Values and parameters derived from cyclic loading are thought to be the most useful of all the tests, in determining the behaviour of soils during earthquakes. The test though, is time consuming and owing to equipment limitations, only a small number of soils could realistically be sampled in the time available.

3.9 Summary

Soil moisture and bulk density were taken (from the final sites) in order to help establish the variation in field conditions, and what effect this may have on field readings from the shear vane, Bush penetrometer and hand penetrometer. These three field tests were done in both initial and final sites to examine the reproducibility of results. The standard compression test was run, in order to evaluate the strength of the soils under uniform controlled conditions, and see how weak the soils may be when saturated. Dynamic cyclic loading was performed on samples to model the likely seismic response in terms of shear wave velocity and the viscous damping.

Chapter Four

Chapter Four

Results and analysis of both initial and final sites

4.1 Background

The results for both initial and final sites were examined in a number of ways. The soils were analysed for various parameters to see whether particular soil properties discriminated between soils types. Secondly, for two soils there was the chance to see if different sites on the same soils showed any correlation of soil properties. It was also possible to try to group the sites on the basis of the major soil-forming units (tephras and pyroclastic flows). This gave the groups: Atiamuri, Taupo, Oruanui, Whenuaroa, Hinemaiaia, and Wharepaina. Reporoa & Mokai soils in the region were placed together in a group. In the field they were found to be similar despite the soil description given (Appendix I) which makes them seem quite different from each other. The amount of time involved in sampling just one site and processing the results meant that it was not possible to cover many sites in the final analysis.

In the Taupo - Reporoa region the major soil groups were formed from Taupo Pumice, re-sorted Taupo Pumice, alluvium, or in peat swamps. There were a few other soils in the region that were not covered as their areal extent was limited, or the topography unsuitable to be included in the study. Note: full soil names are found in Appendix I.

Where there are equations of regression analysis, the R (not R^2) coefficient is categorised in the following way: 0.25 - moderately weak; 0.50 - moderately correlated; 0.75 - strongly correlated; 1.00 - perfect. All errors shown are standard errors unless otherwise stated. 'Initial sites' refers to the first survey of sites that used only hand penetrometer, bush penetrometer, and shear vane; 'final sites' refers to sites chosen from

the initial survey for further investigation. The final sites were chosen, in order of importance, on the basis of the site:

- being considered representative of the soil type (from initial values)
- helping give a spread of sites in the region
- obtaining a spread of soil types (as well as a double up on two sites to check variability)
- accessibility (permission from landowners)

4.2 Moisture Content

All sites in the area were initially sampled in summer, and as detailed in the methods chapter, the soils were at field capacity, and so no moisture content samples were taken. In the final sites, moisture content was analysed to be used as: 1) an indicator of soil strength, 2) to examine the effect of moisture on variation in other parameters, and 3) so dry density could be calculated.

Values from the A horizon in some samples contained a significant portion of roots mainly from grasses, (which do not burn off at 105°C), and so this may influence results. Determination of moisture is summarised in table 4.1, reported as a percentage of the dry sample weight.

Table 4.1. Average soil moisture final values for final sites

Horizon / Site No.	5 (Wh)	6 (Wn)	8 (Hn+Wng)	11 (Tpd)
A	56.0±1.6	67.1±1.2	61.3±0.9	37.0±0.5
B	48.3±1.7	70.2±0.6	44.7±1.3	23.8±0.2
C	32.4±0.5	55.7±0.3	81.7±2.4	29.0±0.2
	12 (31)	**23 (Hn)**	**30 (Yp)**	**31 (Ai)**
A	63.0±0.3	30.8±2.2	9.8±0.6	50.2±3.1
B	39.5±0.5	25.8±0.3	7.7±0.1	39.6±0.4
C	18.5±0.4	41.6±1.0	19.5±0.2	36.0±0.2
	38 (Tpd)	**43 (Oi)**	**44 (Yp)**	**45 (33)**
A	23.1±1.1	24.5±1.0	47.6±1.5	145.7±3.7
B	13.8±0.2	12.1±0.5	28.6±1.1	270.3±4.4
C	21.1±0.2	30.0±2.2	17.1±0.2	485.0±7.3

The mean soil moisture content for the C horizon for all the final sites combined, was 35% (excluding peat), and the sites were sampled from autumn through to spring. Normally soil moisture is only quoted to two significant figures, but as the error was often so small, results are often quoted to an additional significant figure. Soil moisture was measured in all three horizons. No feature was found in soil moisture that differentiates between soil types or groups except for peat, which had high values from being poorly drained, and the water table being only 0.2 m below the surface of the ground.

Sites 5, 12, and 45 are also described as poorly drained, and show reasonably high soil moisture values especially 45 (peat), which support this. Site 6, which is excessively drained, was sampled during rainfall so higher values may have been obtained than would be expected. Site 23 is imperfectly drained but the soil moisture doesn't indicate this, the remaining sites are well drained and have correspondingly lower values.

4.3 Bulk and Dry Density

Both average bulk and dry density values were obtained for the final sites. The results are summarised in the two tables 4.2 and 4.3 below, and are reported in kg m^{-3}:

Table 4.2. Average bulk (wet) density for final sites (kg m^{-3})

Horizon/Site No.	5 (Wh)	6 (Wn)	8 (Hn+Wng)	11 (Tpd)
A	1022±31	1014±61	1157±45	1024±8
B	1099±15	889±65	1181±22	862±6
C	1095±14	992±59	861±45	956±47
	12 (31)	**23 (Hn)**	**30 (Yp)**	**31 (Ai)**
A	998±21	779±64	829±54	no result
B	862±119	897±48	959±25	1197±23
C	1086±66	1039±13	1138±28	1339±5
	38 (Tpd)	**43 (Oi)**	**44 (Yp)**	**45 (33)**
A	776±35	798±33	1065±41	1084±23
B	812±2	1064±48	1311±30	965±9
C	1074±34	795±28	1305±24	1050±13

Table 4.3. Average dry density for final sites (kg m^{-3})

Horizon / Site No.	5 (Wh)	6 (Wn)	8 (Hn+Wng)	11 (Tpd)
A	655	607	717	747
B	741	522	816	696
C	827	637	474	741
	12 (31)	**23 (Hn)**	**30 (Yp)**	**31 (Ai)**
A	612	595	755	no result
B	618	713	891	857
C	917	734	953	985
	38 (Tpd)	**43 (Oi)**	**44 (Yp)**	**45 (33)**
A	630	641	721	443
B	713	949	1019	261
C	887	611	1114	179

The values for all sites except peat are either below or well below those reported as typical by Head (1984) for dry uniform sand (loose), well graded sand or for soft clay. This tends to suggest that the material is very loose and unconsolidated. However, the wet and dry density values obtained for peat were close to those reported as being typical. Bulk density is, of course, affected by soil moisture, the greater the moisture content the higher the bulk density values. The larger the standard error, the greater the variability of the soil.

Bulk density is used in calculating a number of parameters from other tests. While the density may vary seasonally, the samples were obtained during wetter ground conditions than in summer which gives larger values , which when used in other calculations tends to slightly over-predict the strength in soil.

As a general rule, those sites with higher bulk densities have higher dry densities, this is shown later in the chapter. Some soils will have naturally occurring higher or lower soil moisture values than others at the same point in time due to factors such as textural differences, rainfall variation, topography and exposure to sunlight. In some cases, parameters calculated from both bulk and dry densities are given as some correlations show that one or the other is more appropriate to be used.

4.4 Shear Vane

In a few soils, the C horizon, which is the parent material, was layered with different grades of tephra and / or pyroclastic flows eg. ash, and fine pumice. Where the C horizon was comprised of more than one layer, readings were taken at varying depths within the horizon to give a more representative result.

In the A horizon, the results are influenced by root development, which is mainly grasses. The B horizon at all sites (except peat) had few roots or none at all. Readings were taken in the A and B horizons to help ascertain the reproducibility of all of the tests in the field. Table 4.4 shows the average values obtained for the final sites along with corresponding values previously obtained in the initial work. Table 4.5 shows worst case values for final site readings only. The worst case values are derived from the lowest reading made at any one point in a given horizon. With the shear vane, each reading is made independently of any reading apparently lying above or below it in the data set.

Table 4.4. Average shear vane values (kPa) of final sites

Horizon / Site No.	5 (Wh)	6 (Wn)	8 (Hn+Wng)	11 (Tpd)
A	41±2	48±3	29±2	28±2
B	67±5	54±3	83±10	63±6
C	51±5	62±3	100±7	75±8
	12 (31)	**23 (Hn)**	**30 (Yp)**	
A	36±3	62±3	50±3	
B	61±4	91±5	71±3	
C	37±7	102±6	C too hard	
	38 (Tpd)	**43 (Oi)**	**44 (Yp)**	**45 (33)**
A	66±3	49±2	46±2	36±2
B	59±3	51±2	62±2	36±1
C	67±6	23±3	62±4	63±3
	C is a min avg			

Site 8 is quite variable as shown by large standard errors, while site 45 (peat) is relatively uniform. At site 30, the ground was simply too hard to insert the vane, and at

site 38 only a limited number of readings could be made along the horizon. In the table where it says 'C is a minimum average' this means that a higher average would have resulted if it was possible to obtain all 20 readings. This is compared with readings taken in summer where it was possible to get all the readings or none at all.

Relatively speaking, both sites with Tpd soils compare quite well in the lower two horizons, whereas the two Yp sites are somewhat different. The maximum single reading obtained from any horizon from any site was 180 kPa. With this method an average value of around 100 kPa, like sites 8 and 23, is close to the highest average value likely to occur. The worst case values (table 4.5) show that some soils are poorly consolidated, presumably in small pockets.

Table 4.5 Worst case Shear Vane values (kPa) from final sites

Horizon/ Site No.	5 (Wh)	6 (Wn)	8 (Hn+Wng)	11 (Tpd)
A	24	30	20	18
B	26	33	54	33
C	16	25	60	46
	12 (31)	**23 (Hn)**	**30 (Yp)**	**38 (Tpd)**
A	22	45	22	38
B	45	60	41	30
C	14	50	too hard	32
	43 (Oi)	**44 (Yp)**	**45 (33)**	
A	39	32	23	
B	34	45	20	
C	6	34	39	

Overall, when all the horizons' results were combined and the worst values (y axis) were plotted against the average values (x axis) for the final results this gave the equation of a best fit line:

$$y = -0.70 + 0.59x \quad R = 0.87$$

This shows there is a strong relationship between the average readings and the worst readings, as would be expected.

Reproducibility of the results for the shear vane was tested in the following way,: the initial results were plotted against the final results, with each site individually analysed (with horizons combined) which gave:

5 (Wh)	y = 45.02 + 0.16x R= 0.34
6 (Wn)	y = 46.56 + 0.24x R= 0.86
8 (Hn+Wng)	y = 31.27 + 0.54x R= 0.89
11 (Tpd)	y = 46.81 + 0.32x R= 0.26
12 (31)	y = 46.03 + -0.05x R= 0.12
23 (Hn)	y = -27.04 + 1.64x R= 0.99
30 (Yp)	not done
38 (Tpd)	y = 63.49 + 0.02x R= 0.10
43 (Oi)	y = 64.22 + -0.45x R= 0.96
44 (Yp)	y = 49.46 + 0.13x R= 0.79
45 (33)	y = 46.27 + -0.03x R= 0.02

The correlations will be inexact as there are data from three horizons only, and the best fit line does not pass through zero on the x and y axis (possibly this is due to variation in bulk density over time). The low correlation coefficient (R) for the two Tpd sites implies there is a large degree of variability within Tpd, and from the description of parent material in Chapter Two this might be expected. The initial results for site 30 were quite substantially lower for the top two horizons but as the C horizon was too hard in the final readings no correlation could be made. Only three sites (12, 38 and 45) showed no correlation between initial and final values. Results for the sites from initial work are in Appendix II.

All the sites had all horizons plotted against each other for the initial values (y axis) versus the final values (figure 4.1).

This linear regression is moderately weak; however, by examining the spread of the data points over the y axis (initial values) it was possible to see that they cover a wider range of values than do the points along the x axis. This suggests that conditions in the ground have changed between the initial and final study of the same sites. The most likely explanation for this is that increased soil moisture (as final sites were sampled in wetter conditions) has reduced the variability of the soil strength.

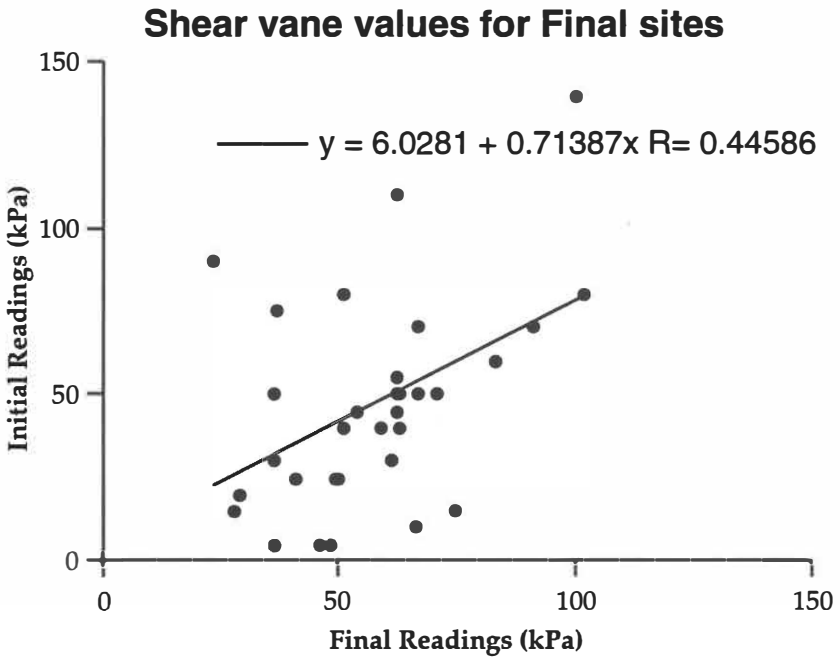

Figure 4.1 Correlation of shear vane values from initial and final readings

4.4.1 Other Parameters from the Shear Vane

For these same sites, proxies for amplitude enhancement, attenuation, and seismic rigidity were calculated from average values and worst case values in the final sites (see table 4.6), with just amplitude enhancement from the initial sites. Hodder *et al.* (1994) state that "the effects of earthquake waves may be enhanced or reduced by the local materials through which they are travelling. In particular, soft ground conditions serve to slow waves down, and as a result increase their amplitude."

Amplitude Enhancement (AEP) is described simply by the relationship:

$$AEP = f(\sigma^{-1})$$

where σ is the strength of the material.

The amplitude enhancement is calculated at 45 cm depth. The 45 cm depth was always located in parent material. It is also calculated for both average and worst case values at this depth, as well as dry and bulk density values (which helps to predict minimum values of 'strength' from dry values, along with typical field conditions from bulk values).

Attenuation is the ability of the soil to diminish the amount of energy from seismic waves which pass through it. From Hodder *et al.* (1994) the attenuation is derived. Knowing that the shear wave velocity (V_s) is equal to the $\tilde{A}(\sigma/\rho)$ and using σ as a proxy for the shear modulus (G) the attenuation may be derived:

$$\alpha = \rho^{0.5} / \sigma^{1.5}$$

where ρ is density (kg m^{-3}),
and σ is the strength of the soil (kPa).

Seismic rigidity (Hodder *et al.*, 1994) is usually defined as $J = \rho \times V_s$ (where V_s is the shear wave velocity) so it also can be derived as:

$$J = \sigma^{0.5} \times \rho^{0.5}$$

High amplitude enhancement and attenuation, and low seismic rigidity, characterise a weak soil. Hardin and Drnevich (1972) state the stress attenuation in the soil may be shown as:

$$D = D_{max} - \varepsilon / (\varepsilon + \gamma_r)$$

where ε is the shear stress,
and D is the damping ratio (also known as the damping factor).

This is defined (attenuation / damping factor) as the proportion of energy lost by internal dissipation to total wave energy (Lomnitz, 1994). From this the better known (to seismologists) quality factor Q may be calculated:

$$Q = 2\pi / D$$

From field observations, all values calculated from a 45 cm depth are representative of the parent material contained in the uppermost metre of the soil horizon. The reasons for choosing this depth are:

1) The soil development in the Taupo - Reporoa area is limited to the top 15 - 30 cm of the profile,
2) The readings obtained down through the profile generally increase owing to overburden pressure, so values from the 45 cm depth are usually weaker than values

from lower down the horizon and so should under-predict the strength of the soil, which is preferable,

3) The limit of the Bush penetrometer's range was 45 cm.

Table 4.6 Summary of proxies for attenuation, amplitude enhancement, and seismic rigidity calculated from bulk density and shear vane strength

Site / Soil	Amplitude Enhancement	Attenuation	Seismic Rigidity
	Average values		
5 (Wh)	0.01949	0.09006	237
6 (Wn)	0.01610	0.06436	248
8 (Hn+Wng)	0.00998	0.02925	294
11 (Tpd)	0.01330	0.04741	268
12 (31)	0.02725	0.14822	200
23 (Hn)	0.00981	0.03134	325
30 (Yp)	too hard	too hard	too hard
38 (Tpd)	0.01487	0.05940	269
43 (Oi)	0.04425	0.26243	134
44 (Yp)	0.01621	0.07454	284
45 (33)	0.01594	0.06519	257
Site / Soil	**Amplitude Enhancement**	**Attenuation**	**Seismic Rigidity**
	Worst case values		
5 (Wh)	0.06250	0.51704	132
6 (Wn)	0.04000	0.25197	157
8 (Hn+Wng)	0.01667	0.06314	227
11 (Tpd)	0.02174	0.09910	210
12 (31)	0.07143	0.62910	123
23 (Hn)	0.02000	0.09117	228
30 (Yp)	too hard	too hard	too hard
38 (Tpd)	0.03125	0.18104	185
43 (Oi)	0.16667	1.91848	69
44 (Yp)	0.02941	0.18222	211
45 (33)	0.02564	0.13304	202

The range of average values for attenuation and seismic rigidity is quite small, when the initial values for site 43 are compared with the final ones for amplitude enhancement, the initial value is greater. The values for peat tend to lie in the middle of the range implying that some of the soils are even weaker than peat. When values calculated from the dry density are examined (Appendix IV) it is obvious how much weaker peat is than other soils. A few soils change in strength relative to each other when comparing bulk density to dry density results. but on the whole they are spread evenly.

The parameters of the soils are calculated on the basis of bulk densities, because these values give an indication of the field conditions at the time of sampling. As the sampling was done throughout the year under a range of soil moisture and bulk density values it is difficult to be sure that typical field values are being compared, but most of the soils are well drained. It is also recognised, that different soils will always have different soil moisture contents at the same time of the season.

4.5 Hand Penetrometer

With the penetrometer, like the shear vane, readings were taken in both A and B horizons for reproducibility. Table 4.7 shows the average values obtained for the final sites along with corresponding values previously obtained in the initial work. The worst case values are derived from the lowest reading made at any one point in a given horizon. With the hand penetrometer, each reading is made independently of the reading above or below it in the data set.

The scale on the penetrometer was in kilograms of force. This needed to be converted into pressure (kPa) so that the readings were in the same units as the Bush penetrometer, the Shear vane, and the triaxial tests.

Table 4.7 Average Hand Penetrometer values (kPa)[1]

Horizon	5 (Wh)	6 (Wn)	8 (Hn+Wng)	11 (Tpd)	12 (31)
A	185±12	322±22	111±21	99±24	215±26
B	494±0	315±16	284±18	198±36	494±0
C	194±28	320±16	481±10	148±22	143±7
	B is min avg.		C is min avg.	B is min avg.	B is min avg.
23 (Hn)	**30 (Yp)**	**38 (Tpd)**	**43 (Oi)**	**44 (Yp)**	**45 (33)**
269±23	165±23	330±18	143±9	146±13	143±12
485±9	315±19	386±20	188±15	278±14	130±8
426±19	494±0	351±29	25±0	248±13	99±0
B & C are min avg.	C is min avg.		C is max avg.		

[1]The penetrometer has a conical point of 0.00575 m in radius and 0.011 mm along it's slant height. The formula to calculate the surface area is:

$A = {}^{1} r h (m^2)$

Knowing that 1 kgf = 9.81 N, and that 1 Pa = 1 N/m^2 then it is a simple case of dividing 9.81 by the area of the cone to give units of pressure (Pa). The area is 0.00019870574 m^2 and this gives 1 kgf = 49369.486 Pa = 49.37 kPa.

494 is the highest possible average value obtainable with the penetrometer so when the results show "C is a min avg" this means that the real result could have been higher if the range of the instrument allowed it. There is substantial variation in the values and no pattern is apparent between soil types or groups. When the average readings were plotted against the worst case readings (in Appendix III) for all horizons combined this gave: y = -1.54 + 0.69x R= 0.62. This shows a moderate correlation despite seven values being used that were minimum averages. Ignoring the values that have standard errors of zero, the two Tpd sites show that they are more variable than others, which supports observations in the field.

The sites had all horizons plotted against each other for the initial values (y axis) versus the final values (figure 4.2).

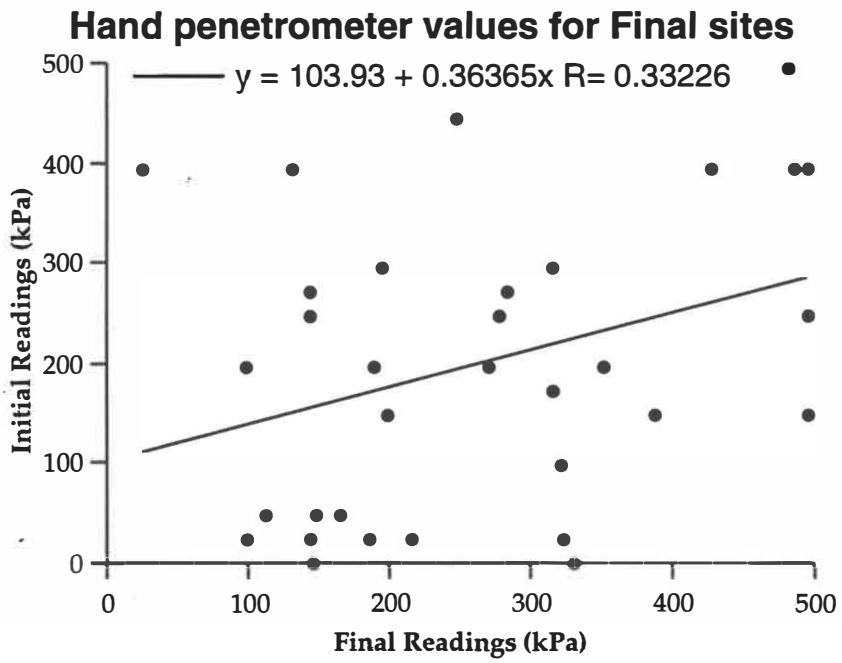

Figure 4.2 Correlation of hand penetrometer values from initial and final readings

The relationship is moderately weak, and it is unlikely that the slope of the line represents any significant increase in final values over initial values. The final readings are considered accurate as the standard errors are not large.

4.5.1 Other Parameters from the Hand penetrometer

As in 4.3, proxies for other geotechnical parameters may be derived from the original data. In table 4.8 below, they are summarised for the hand penetrometer.

Table 4.8 Summary of proxies for attenuation, amplitude enhancement, and seismic rigidity calculated from bulk density and penetrometer strength

Site / Soil	**Amplitude Enhancement**	**Attenuation**	**Seismic Rigidity**
	Average values		
5 (Wh)	0.00516	0.01227	461
6 (Wn)	0.00313	0.00551	563
8 (Hn+Wng)	0.00208	0.00278	644
11 (Tpd)	0.00382	0.00731	500
12 (31)	0.00698	0.01924	394
23 (Hn)	0.00235	0.00367	665
30 (Yp)	0.00203	0.00308	750
38 (Tpd)	0.00285	0.00499	614
43 (Oi)	0.04051	0.22990	140
44 (Yp)	0.00403	0.00925	569
45 (33)	0.01013	0.03303	322
Site / Soil	**Amplitude Enhancement**	**Attenuation**	**Seismic Rigidity**
	Worst case values		
5 (Wh)	0.02026	0.09539	233
6 (Wn)	0.00810	0.02297	350
8 (Hn+Wng)	0.00253	0.00374	583
11 (Tpd)	0.00675	0.01715	376
12 (31)	0.02026	0.09500	232
23 (Hn)	0.00675	0.01788	392
30 (Yp)	0.00203	0.00308	750
38 (Tpd)	0.01013	0.03340	326
43 (Oi)	0.04051	0.22990	140
44 (Yp)	0.00675	0.02004	440
45 (33)	0.01013	0.03303	322

From these calculations, peat is weaker than other materials; once again site 43 has the lowest readings for seismic rigidity and the highest for amplitude enhancement and attenuation. Also the materials at site 12 and 5 are reasonably weak. Overall, though the values are reasonably spread and do not lend themselves to grouping particular soils together.

4.6 Bush penetrometer

Readings for the penetrometer were taken at all the sites, for both initial and final surveys. In the Bush penetrometer manual a conversion factor of 0.762 is used for the small cone, to convert the on-screen readings into pressure readings of bars; from there they can be converted to kPa. For other cone sizes, the calibration is different. In Table 4.9 average values for the final sites are shown, in Appendix II are the initial results, and Appendix III the 'worst-case' results. With the Bush penetrometer the readings lie vertically down the profile and can be grouped together, but like the shear vane or hand penetrometer the worst case values are derived from the lowest reading at any one depth.

Table 4.9 Average Bush Penetrometer values (kPa)

Depth/Site No.	5 (Wh)	6 (Wn)	8 (Hn+ Wng)	11 (Tpd)	12 (31)	23 (Hn)
3 cm	6±1	0±0	5±1	1±0	2±1	0±0
6 cm	29±6	17±5	25±4	7±2	7±2	6±2
9	156±8	131±8	144±10	110±7	79±7	208±12
12	242±8	202±9	231±11	212±10	144±8	325±16
15	263±9	259±9	298±13	251±9	177±5	346±14
18	291±13	291±10	311±11	287±14	180±4	388±16
21	308±14	356±8	332±15	305±11	189±7	432±23
24	328±15	410±11	333±14	322±11	204±9	433±29
27	359±13	448±12	339±12	348±17	269±17	428±31
30	393±17	457±10	348±11	341±17	285±22	404±22
33	425±17	449±13	364±15	335±18	317±26	415±21
36	429±16	461±15	393±14	323±18	346±28	454±27
39	421±15	470±13	368±12	269±12	378±21	487±29
42	383±17	494±16	387±16	251±10	423±39	486±29
45	361±19	464±10	386±16	236±11	418±39	491±35

	30 (Yp)	38 (Tpd)	43 (Oi)	44 (Yp)	45 (33)
3 cm	0±0	2±1	1±0	9±1	4±1
6 cm	19±9	9±2	20±7	22±2	12±2
9	244±13	259±11	162±5	178±7	76±6
12	353±15	414±9	194±7	247±9	134±6
15	392±13	399±9	227±7	326±12	168±5
18	435±15	381±11	251±10	402±14	177±5
21	458±17	402±15	275±10	411±16	177±4
24	445±17	387±12	324±16	460±18	173±4
27	466±18	407±18	339±16	474±27	171±4
30	466±19	406±18	364±19	439±45	174±4
33	467±22	396±15	384±19	455±35	183±4
36	450±24	420±23	383±20	451±29	194±5
39	434±31	445±21	377±23	478±29	211±6
42	466±39	433±21	383±28	436±32	226±6
45	472±108	443±21	356±27	406±51	238±8

From the values down the profile sites 12, 23, 30, 43 are reasonably variable, from the size of the standard errors. Peat has little variability, and along with site 11, has low penetration values. Sites such as 23, 30, 38, and 44 have high readings at shallow depths, although site 6 and perhaps 12 are reasonably strong at a greater depth. Results from the Yp sites are similar, but those from the Tpd sites differ markedly, once again demonstrating how variable the Tp group of soils are.

Reproducibility of the results was tested for in the following way, for the bush penetrometer. The initial results (x axis) were plotted against the final results with each site individually analysed (for all depths combined) which gave:

5 (Wh)	y = -0.05 + 0.97x R= 0.95
6 (Wn)	y = -3.07 + 1.38x R= 0.95
8 (Hn+Wng)	y = -30.47 + 0.78x R= 0.95
11 (Tpd)	y = 60.05 + 0.69x R= 0.91
12 (31)	y = -40.24 + 1.34x R= 0.76
23 (Hn)	y = 6.02 + 0.67x R= 0.88
30 (Yp)	y = 80.55 + 0.81x R= 0.94
38 (Tpd)	y = -20.03 + 1.07x R= 0.94
43 (Oi)	y = 60.19 + 0.79x R= 0.94
44 (Yp)	y = 10.24 + 1.34x R= 0.95
45 (33)	y = 3.39 + 0.63x R= 0.83

Most of the sites show a strong relationship between initial and final readings but there is some variation in the strength (as seen from the slopes of the lines). This variation could be attributed to seasonal variation in moisture conditions.

Some sites in drier conditions had rather limited penetration, so correlation is not always possible for a complete range of values down the soil profile. Perhaps the most significant finding from this analysis is that site 43 (Oi) has a strong correlation between initial and final values, which confirms that it has low soil strength. Hand and shear values also show that site 43 is weak.

The relationship between initial values (y axis) versus final values was examined and all results from all depths were combined (figure 4.3).

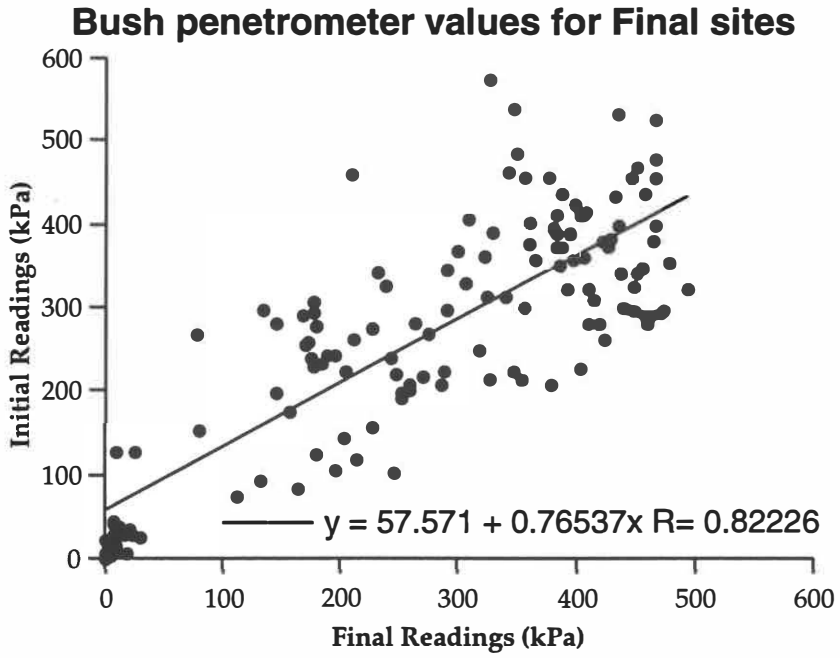

Figure 4.3 Correlation of Bush penetrometer values from initial and final readings

This shows that there is a strong correlation, and from the slope of the line it can be seen that the initial values are slightly lower than final values: this is thought to be from drier ground conditions for the initial values. Later in this chapter, correlations are made between the bush and hand penetrometer, and shear vane values.

4.6.1 Other Parameters from the Bush Penetrometer

As stated in 4.4.1, other parameters may be derived from the original data, and for the Bush penetrometer these are summarised in table 4.10.

The peat soil is distinctive once again, by being the weakest soil followed closely by site 11. The two Yp sites, along with site 23, are again reasonably strong, however the strength of the sites in the middle differ somewhat from that determined by shear vane and hand penetrometer values. From parameters calculated from dry density (Appendix IV) the peat is obviously the weakest, and sites 8, 11, and 43 form a group of relatively weak soils. Some grouping of soils is evident, but with the Bush penetrometer the rigidities are higher and the amplitude enhancement and attenuation are lower than for the hand penetrometer and the shear vane.

Dry density was used to calculate parameters such as attenuation and seismic rigidity so that the results would be comparable and not subject to variations in site conditions over time. The end members of the soils in terms of strength remain the same but those in between vary when calculated from dry or bulk densities. This gives some sort of basis on which to group soils. Cyclic loading and standard compression tests were carried out on samples that were saturated, to simulate the worst possible field conditions. Final readings themselves for hand penetrometer, bush penetrometer and shear vane tests were taken under varying conditions of soil moisture. However, no correlation was found to relate the change in soil moisture with the change of strength values.

Table 4.10 Summary of proxies of attenuation, amplitude enhancement, and seismic rigidity, calculated from bulk density and Bush penetrometer

Site / Soil	**Amplitude Enhancement**	**Attenuation**	**Seismic Rigidity**
	Average values		
5 (Wh)	0.00238	0.00384	679
6 (Wn)	0.00213	0.00310	682
8 (Hn+Wng)	0.00272	0.00415	563
11 (Tpd)	0.00371	0.00700	507
12 (31)	0.00265	0.00448	641
23 (Hn)	0.00205	0.00300	711
30 (Yp)	0.00230	0.00373	703
38 (Tpd)	0.00225	0.00349	691
43 (Oi)	0.00266	0.00386	547
44 (Yp)	0.00209	0.00346	790
45 (33)	0.00475	0.01061	470
Site / Soil	**Amplitude Enhancement**	**Attenuation**	**Seismic Rigidity**
	Worst case values		
5 (Wh)	0.00398	0.00830	525
6 (Wn)	0.00268	0.00437	609
8 (Hn+Wng)	0.00505	0.01052	413
11 (Tpd)	0.00625	0.01527	391
12 (31)	0.00423	0.00908	506
23 (Hn)	0.00268	0.00447	623
30 (Yp)	0.00320	0.00611	596
38 (Tpd)	0.00336	0.00640	565
43 (Oi)	0.00597	0.01299	365
44 (Yp)	0.00268	0.00501	698
45 (33)	0.00772	0.02198	369

4.7 Particle Size Analysis and photographs of cores

Particle Size Analysis (PSA) was done only on those cores which were spare from GDS testing. Two final sites were not texturally classified as a consequence; however, one of these was peat (site 45) and the other was site 11 (Tpd) which is the same soil type as in site 38. From the combined sieving and pipette analysis, the soils are plotted on figure 4.4 below to determine the soil texture.

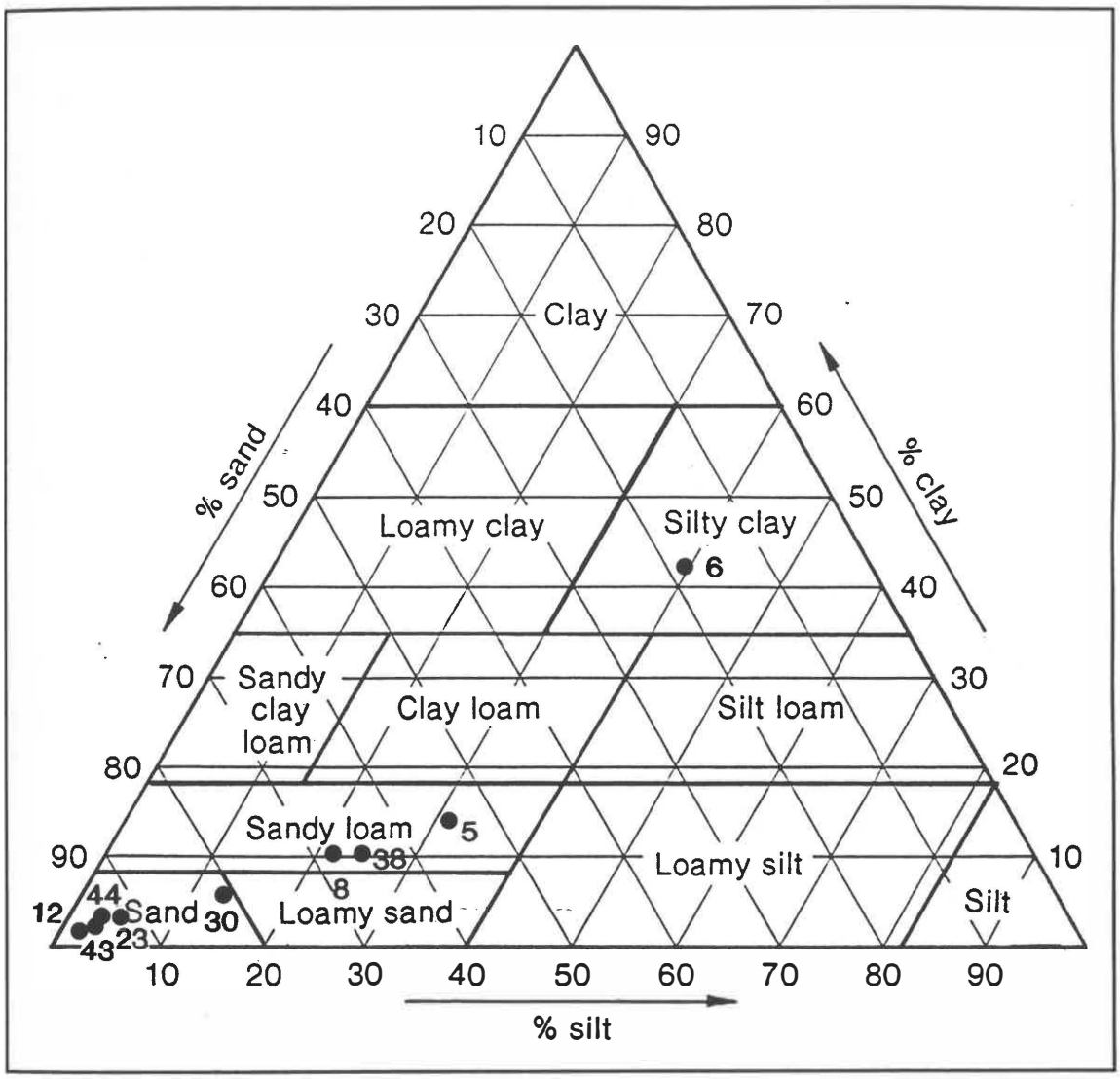

Figure 4.4 Soil texture classes (Milne *et al.*, 1991)

4.7.1 Uniformity Coefficient

This is the ratio of the 60% particle size to the 10% particle size:

$$U = \frac{D_{60}}{D_{10}}$$

which is measured as the slope of the line joining those two points. In table 4.11 are the coefficients for the final sites.

Table 4.11 Uniformity coefficient values for samples from C horizon

Sites	D_{10} (Effective Size)	D_{60}	Uniformity Coefficient	Textural Class
5	0.003	0.1	33	sandy loam
6	0.0013	0.023	18	silty clay
8	0.005	0.16	32	sandy loam
12	0.2	0.5	3	sand
23	0.1	0.8	8	sand
30	0.03	0.33	11	sand
38	0.01	0.17	17	sandy loam
43	0.19	0.9	5	sand
44	0.14	0.6	4	sand

Photographs of cores from ten sites are shown in figures 4.5 to 4.9 which help to illustrate the variation in composition of the parent material. Note: Site 23 and 30 had no cores left.

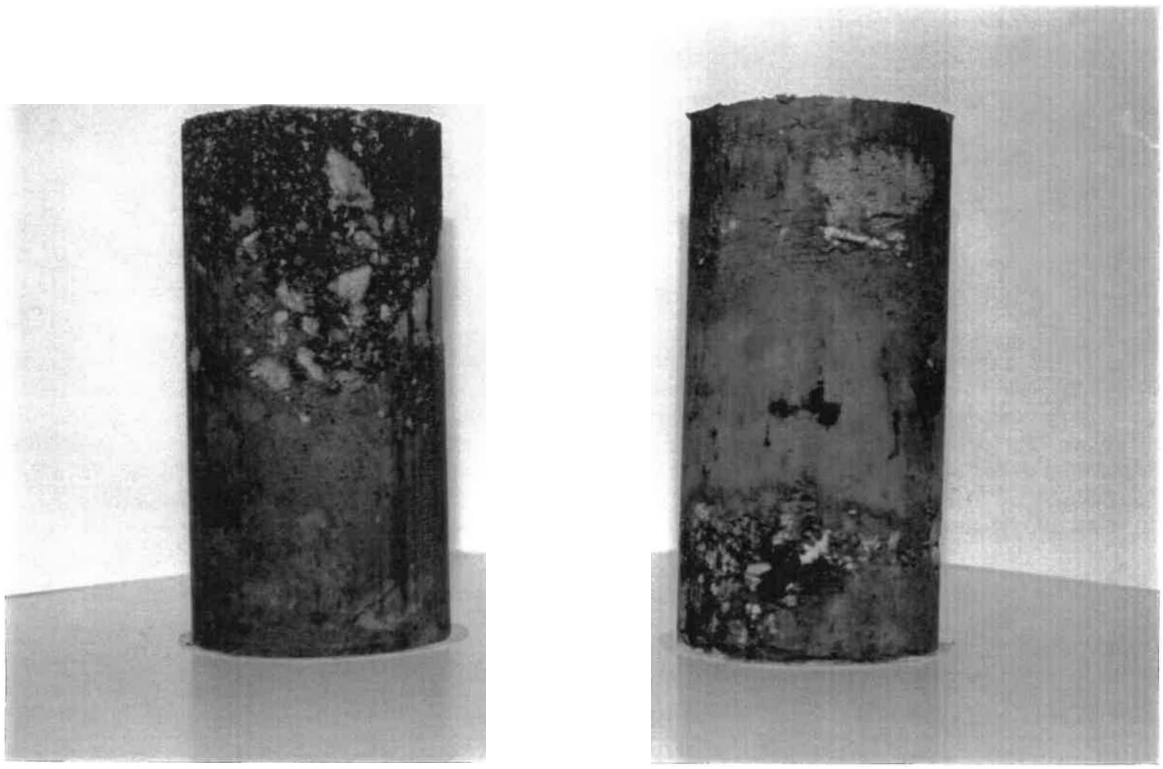

Figure 4.5

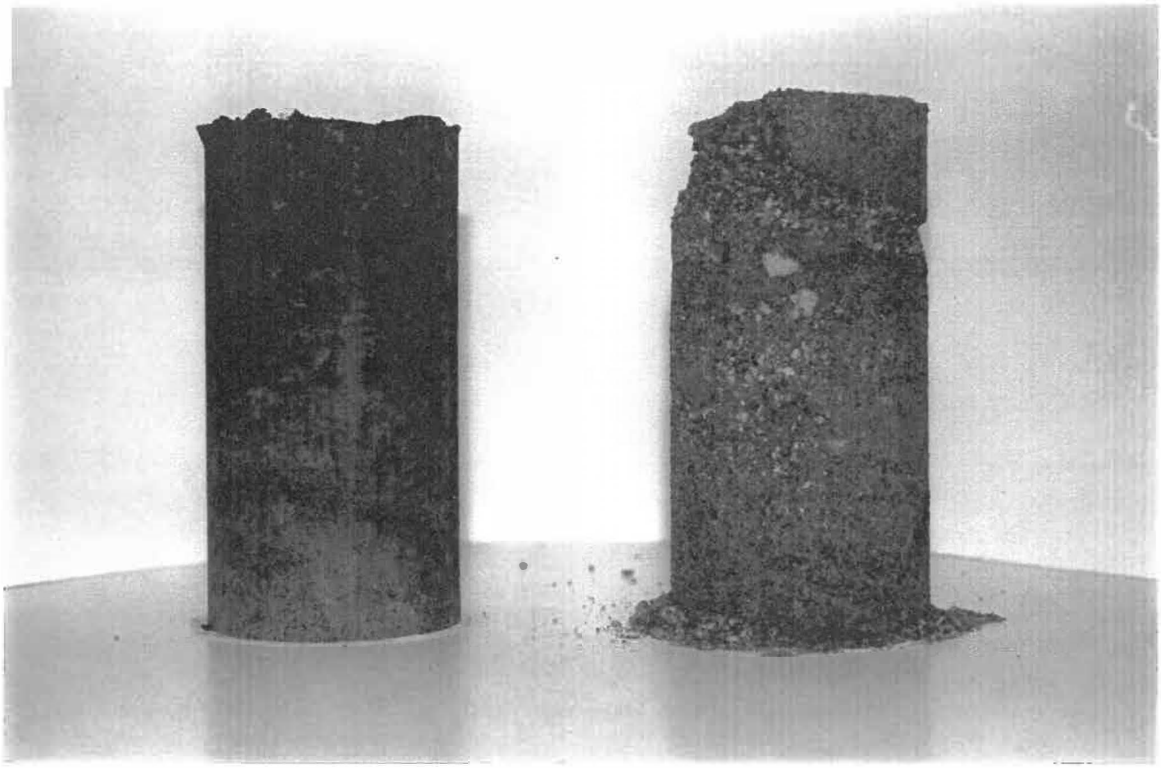

Figure 4.6

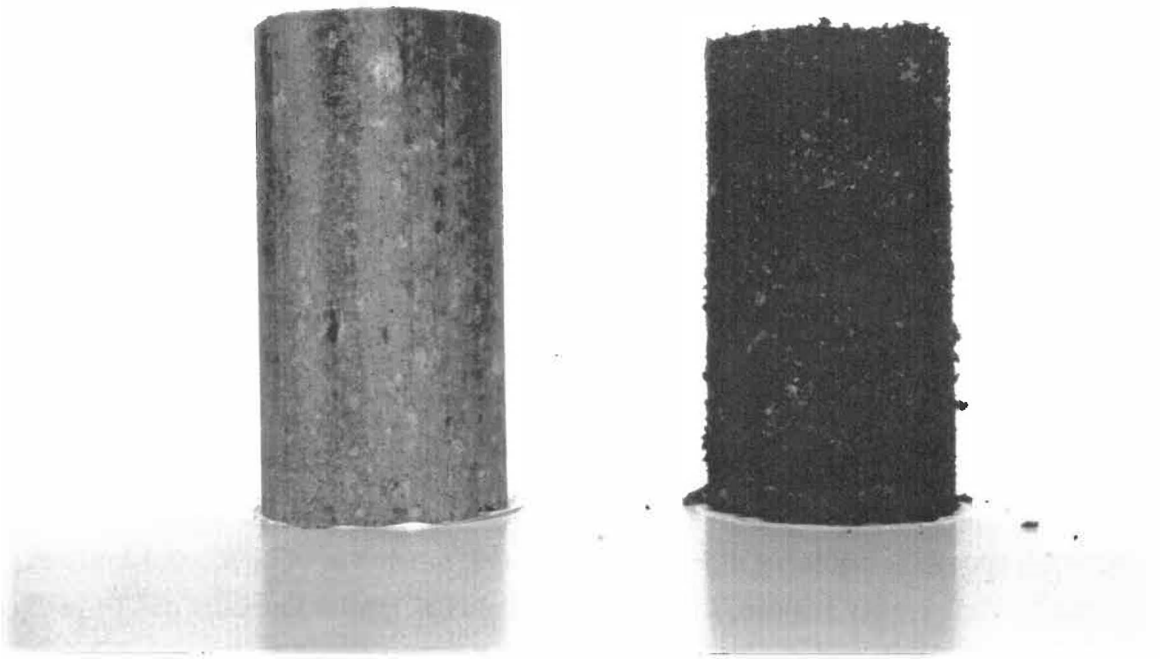

Figure 4.7

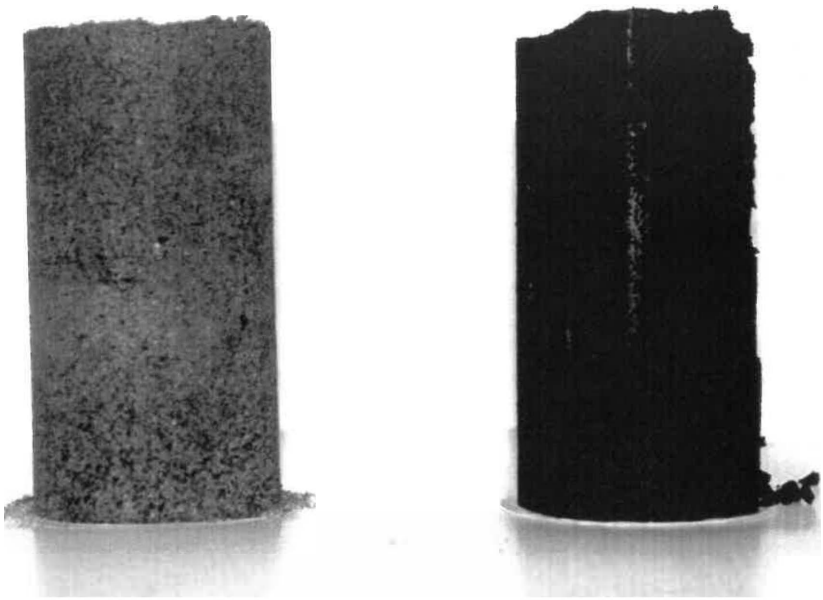

Figure 4.8

Figure 4.5 (left to right) Site 5 & Site 6
Figure 4.6 Site 8 (jagged on top due to pumice) & Site 12
Figure 4.7 Site 38 (extremely firm) & Site 43 (very weak)
Figure 4.8 Site 44 & Site 45 (pumice 1-3 mm ø at base - c0.8 m, von Host rating (Head, vol 2, 1985) of **H5**)

4.8 Triaxial Testing

4.8.1 Consolidated Undrained Test

The test was carried out for all final sites where possible over a range of confining pressures (10 - 50 kPa) in order to plot the Mohr strength envelope. The soils displayed either of two modes of failure, but all samples tested in each site always showed the same failure type.

For tests which showed barrel failure, the slope of the line of deviator stress versus axial strain decreases to zero in some cases at between 15 - 20% axial strain, beyond the range of the controllers on the GDS system. To overcome this, the test had to be re-run after the controllers were re-filled and the sample was kept under existing constant

pressure. The crossover to the follow-on tests were good enough so there was only minimal variation between the 'end' point of one and the 'start' point of the other.

For samples which showed brittle failure, the failure point was usually quite definite compared to those samples which had barrel failure (barrel failure generally indicates that the sample is a loose unconsolidated material). By examining the cores in figures 4.5 - 4.8 with the mode of failure (which is reported later) it can be seen it was not possible to predict the mode of failure from the texture of the soil. A comparison of failure types is given in figure 4.9.

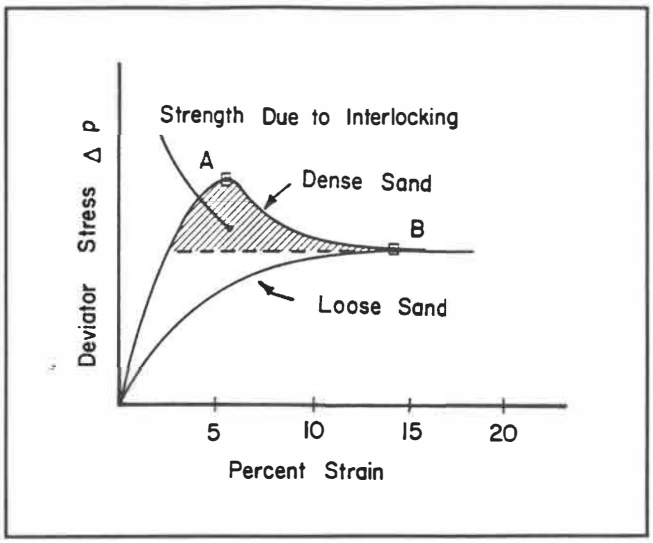

Figure 4.9 Stress versus strain for samples of dense and loose sand (from Dunn *et al.* 1980, p 165)

The peak shear strength can be determined from a plot of deviator stress versus percent axial strain (Dunn *et al.*, 1980). For dense samples, the failure point is referred to as the peak point stress condition (as seen in figure 4.10) and for weak samples (figure 4.10a) the ultimate stress conditions, are used. Dunn *et al.* (1980) notes 'The failure condition is generally defined by the stress condition at the maximum deviator stress or by the stress condition at a specific strain of value, such as 10 or 20%.'

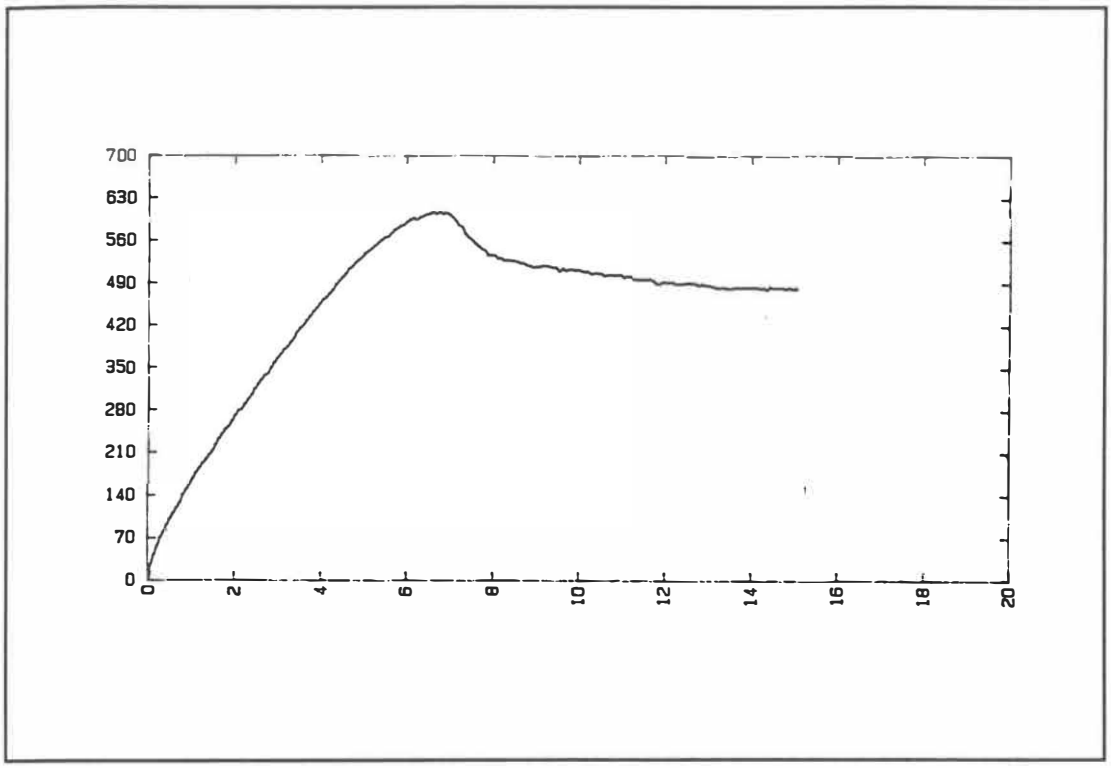

Figure 4.10 Brittle (shear) failure, deviator stress in kPa (y-axis), % axial strain (x-axis)

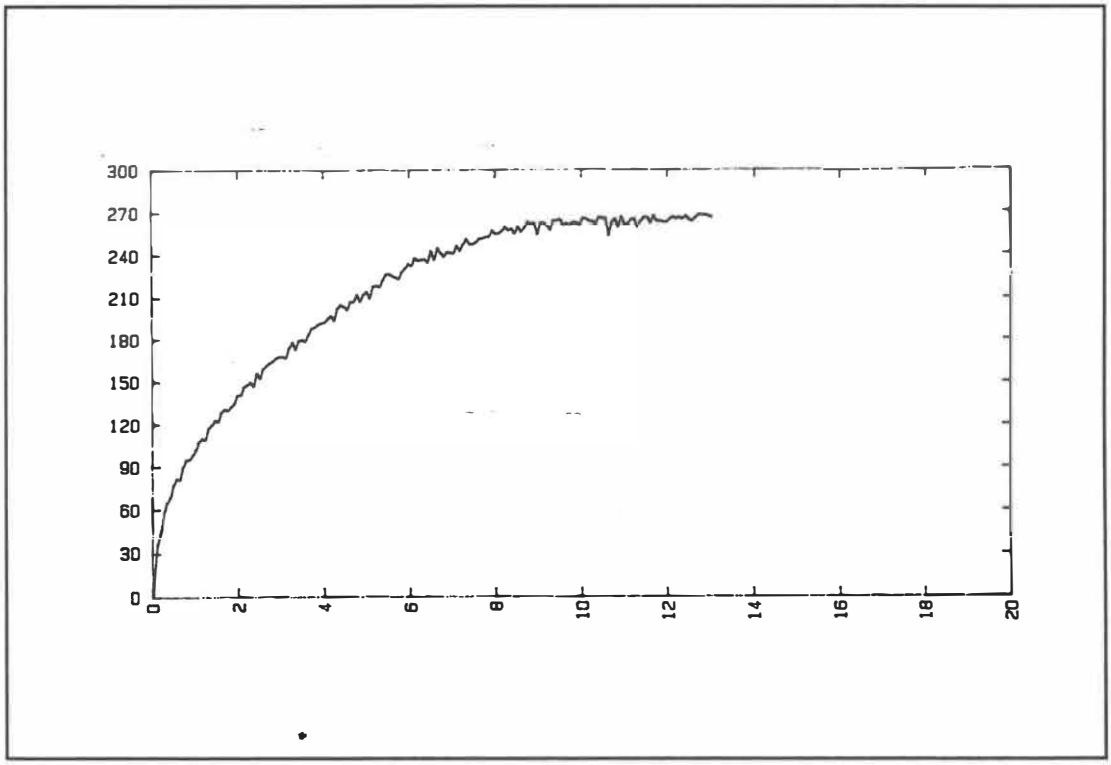

Fig. 4.10a Barrel failure, deviator stress in kPa (y-axis), % axial strain (x-axis)

The results of the test are summarised in table 4.12 below. Because of equipment limitations it was not possible to run the tests at the *in situ* confining pressures.

Table 4.12 Standard Compression Test Results

Site	Equation of Mohr strength envelope
Site 23 (Hn) barrel failure	$\tau_f = 20 + 5.09 \tan 36^o$
Site 43 (Oi) shear failure	$\tau_f = 10 + 3.90 \tan 45^o$
Site 44 (Yp) barrel	$\tau_f = 4 + 6.40 \tan 41^o$
Site 6 (Wn) shear	$\tau_f = 17 + 4.86 \tan 51^o$
Site 45 (33) peat	No result possible.
Site 30 (Yp) shear	$\tau_f = 10 + 5.58 \tan 42^o$
Site 38 (Tpd) shear	$\tau_f = 42 + 5.27 \tan 39^o$
Site 5 (Wh) barrel	$\tau_f = 20 + 5.37 \tan 40^o$
Site 8 (Hn+Wng) shear	$\tau_f = 12 + 4.22 \tan 43^o$

When the percentage sand was plotted against cohesion only a moderately weak correlation was found. Correlations are discussed in more detail later in the chapter.

From Terzaghi and Peck (1967) values for the friction angle are quoted as follows: Sandy gravels, loose - 35, dense - 50; Silty sand, loose - 27 - 33, dense - 30 -34; Inorganic silt, loose - 27 -30, dense - 30 -35.

From Particle Size Analysis, photos where applicable, mode of failure and friction angle, the soils could be classified in the following way. From Selby (1993) the descriptions are taken: Site 23 (Hn) loose sand, mixed grain size; Site 43 (Oi) dense sand, mixed grain size (although the uniformity coefficient doesn't show this); Site 44 (Yp) dense sand, uniform grain size; Site 6 (Wn) has an unusually high friction angle (possibly from allophane which has a high friction angle for a clay 30 - 40°); Site 45

(33) obviously peat; Site 30 (Yp) dense sand, mixed grain size; the remaining three sites were all sandy loams and might be expected to have lower friction angles as a result of the larger proportion of smaller particles. When comparing with friction angles for silty sand from Terzaghi and Peck (1967) there is also no correlation. The friction coefficient for sites 5, 6, 8, and 38 are similar to those for soft clay.

Type and material	Unit weight (Saturated/dry) kN/m^3	Friction angle (1) degrees	Cohesion kPa
COHESIONLESS			
Sand			
Loose sand, uniform grain size	19/14	28–34	
Dense sand, uniform grain size	21/17	32–40	
Loose sand, mixed grain size	20/16	34–40	
Dense sand, mixed grain size	21/18	38–46	
Gravel			
Gravel, uniform grain size	22/20	34–37	
Sand and gravel, mixed grain size	19/17	48–45	
Compacted broken rock			
Basalt	22/17	40–50	
Chalk	13/10	30–40	
Granite	20/17	45–50	
Limestone	19/16	35–40	
Sandstone	17/13	35–45	
Shale	20/16	30–35	
COHESIVE			
Clay			
Soft bentonite	13/6	7–13	10–20
Very soft organic clay	14/6	12–16	10–30
Soft, slightly organic clay	16/10	22–27	20–50
Soft glacial clay	17/12	27–32	30–70
Stiff glacial clay	20/17	30–32	70–150
Glacial till, mixed grain size	23/20	32–35	150–250
Rock			
Hard igneous rocks:	(2)		
granite, basalt, porphyry	25 to 30	35–45	35 000–55 000
Metamorphic rocks:			
quartzite, gneiss, slate	25 to 28	30–40	20 000–40 000
Hard sedimentary rocks:			
limestone, dolomite, sandstone	23 to 28	35–45	10 000–30 000
Soft sedimentary rock:			
sandstone, coal, chalk, shale	17 to 23	25–35	1 000–20 000

Fig. 4.10b Typical Soil and Rock Properties for sand, gravel, clay, and rock. (from Selby, 1993)

(Note: higher friction angles in cohesionless materials occur at low confining or normal stresses)

4.8.2 Cyclic Loading Test

From each cyclic loading test, a hysteresis loop was drawn (figure 4.11). As the end points of each cycle did not always match, they were averaged in order to form a complete loop. The loop was drawn by overlaying two graphs, one of the first half of the cycle and one of the second half. The cycle starting point was taken when the sample was under full extension ie. when % axial strain and pressure are at their lowest values. The area contained within the loop was calculated by subtracting the area (found by integrating) under the lower curve from the area under the upper curve.

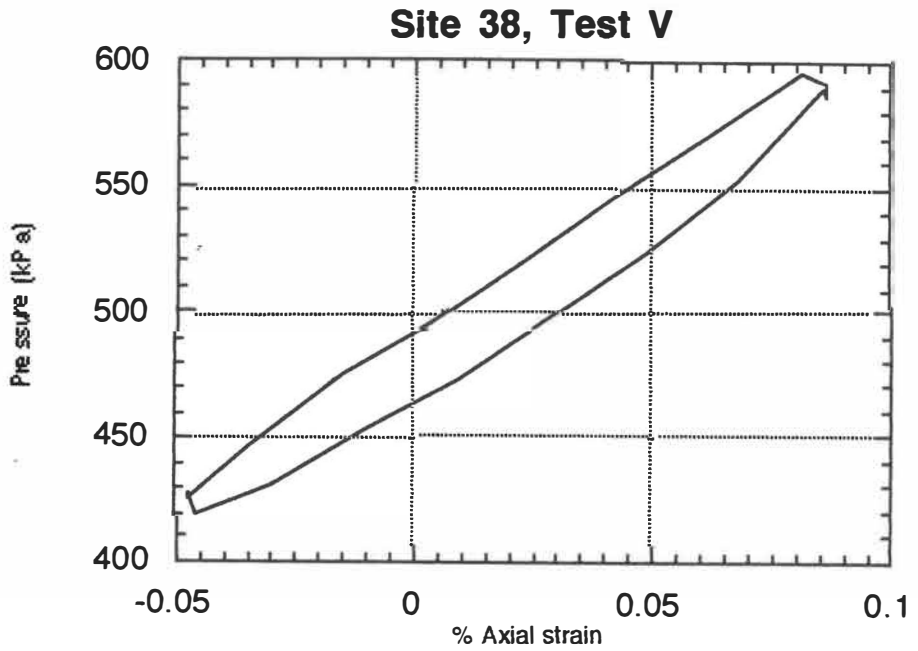

Figure 4.11 A sample hysteresis loop drawn from the 10th cycle of a cyclic loading test.

Poisson's Ratio was calculated for a random selection of five tests to determine how close it was to the theoretical value of 0.5 for saturated undrained conditions. The average ratio for these tests was **0.490371 ± 0.000157** (st. error). The error of the value is sufficiently low to be confident that there is very little variation in the result. This is very close to the theoretical value and should be, as the samples were always saturated and undrained in the tests. To check on whether these conditions held true, it was also possible to determine that there had been no change in volume from the GDS analysis program (GDSFBP). All results checked showed no volume change.

Parameters were derived from the cyclic loading test that give a direct indication of the likely behaviour of soils during earthquakes. They are summarised in table 4.13 below. The shear wave velocity has been calculated with the bulk density from the C horizon from each site.

Table 4.13 Average site values for parameters calculated from cyclic loading tests

	Viscous Damping Factor (D)	Quality Factor (Q)	Dynamic Modulus of Elasticity (Ed) (kN/m^2)	Dynamic Shear Modulus (Gd) (kN/m^2)	Shear Wave Velocity (m/s)
23 (Hn)	0.10074 ±0.00887	62	131959 ±7535	44281 ±2528	206 ±6
43 (Oi)	0.12045 ±0.00482	52	126000 ±10110	42282 ±3393	230 ±9
44 (Yp)	0.05762 ±0.00991	109	140067 ±3685	47002 ±1236	190 ±2
6 (Wn)	0.09536 ±0.01008	66	144828 ±5042	48600 ±1692	221 ±4
45 (33)	0.00737 ±0.00329	853	134688 ±3150	45197 ±1057	207 ±2
30 (Yp)	0.08444 ±0.01064	74	197609 ±48571	66312 ±16299	238 ±27
38 (Tpd)	0.11047 ±0.00513	57	127124 ±7506	42659 ±2519	199 ±6
5 (Wh)	0.07208 ±0.01434	87	150362 ±27515	50457 ±9233	212 ±19
8 (Hn+Wng)	0.03103 ±0.01399	202	135767 ±7508	45559 ±2519	230 ±6

Hodder *et al.* (1993) state "Shear modulus and shear wave velocity are measures of the ease with which energy is transmitted through the medium; by comparison viscous damping is a measure of the extent to which energy is absorbed....If energy is absorbed, particles in the soil might be expected to undergo re-ordering, with consequent settlement and subsidence of the soil."

From the results, shear wave velocity shows only a small variation. Results show that site 43 has a larger than expected velocity, and site 23 a smaller one. The quality factor is an indicator of weakness in the soil. The low damping ratio of the ground in Mexico

City (4% or 0.04 which equivalent to a Q-value of 157) contributed to the long lasting reverberations of surface waves in the valley floor (Lomnitz, 1994). One strong motion record on soft ground in 1985 in Mexico City had a total duration of more than 5 minutes. Clearly sites 8 and 45 show that they have significantly high enough values to be of some concern.

From the bulk density and the shear wave velocity, parameters were calculated, shown in table 4.14.

Table 4.14 Summary of proxies of amplitude enhancement, attenuation, and seismic rigidity, from bulk density and shear wave velocity

Site / Soil	**Amplitude Enhancement**	**Attenuation**	**Seismic Rigidity**
	Average values		
5 (Wh)	0.00472	0.01072	482
6 (Wn)	0.00452	0.00959	468
8 (Hn+Wng)	0.00435	0.00841	445
23 (Hn)	0.00485	0.01090	463
30 (Yp)	0.00420	0.00919	520
38 (Tpd)	0.00503	0.01167	462
43 (Oi)	0.00435	0.00808	428
44 (Yp)	0.00526	0.01379	498
45 (33)	0.00483	0.01088	466
Site / Soil	**Amplitude Enhancement**	**Attenuation**	**Seismic Rigidity**
	Worst values		
5 (Wh)	0.00562	0.01393	441
6 (Wn)	0.00476	0.01035	456
8 (Hn+Wng)	0.00444	0.00869	440
23 (Hn)	0.00515	0.01193	449
30 (Yp)	0.00474	0.01101	490
38 (Tpd)	0.00552	0.01346	441
43 (Oi)	0.00478	0.00933	408
44 (Yp)	0.00546	0.01459	489
45 (33)	0.00490	0.01112	463

The two Yp sites again are stronger, and site 43 again gives a weaker reading. Due to the small spread of values for the shear wave velocity the values for attenuation and seismic rigidity are clustered together for the rest of the sites. When worst case values are examined there is even less variation amongst the sites.

'Real' seismic rigidity values (table 4.15) are calculated from:

$J = \rho \times V_s$

Where V_s is the shear wave velocity.

Table 4.15 Seismic rigidity from shear wave velocity

Sites	from bulk density	from dry density
5 (Wh)	235	178
6 (Wn)	220	141
8 (Hn+Wng)	198	109
23 (Hn)	214	151
30 (Yp)	275	230
38 (Tpd)	214	177
43 (Oi)	183	141
44 (Yp)	248	211
45 (33)	218	37

4.8.3 Correlations between Methods

Table 4.16 Linear Correlation of methods from **Initial** Results from all horizons combined

	Hand	Shear	Bush
Hand	1	0.80	0.06
Shear	0.80	1	0.16
Bush	0.06	0.16	1

Both the initial (table 4.16) and final results (table 4.17) show a strong correlation between the hand penetrometer and the shear vane. The correlation from the final values show that there is a moderately weak correlation between the bush and hand penetrometers, and a moderate correlation between shear vane and the bush penetrometer. This contrasts with the correlations for initial values, which overall aren't as good: this implies increasing the number of readings has clarified their relationship.

Table 4.16 Linear Correlation of methods from **Final** Results from all horizons combined

	Hand	Shear	Bush
Hand	1	0.75203	0.44035
Shear	0.75203	1	0.52721
Bush	0..44035	0..52721	1

The relationship between soil moisture(x axis) versus bulk density was examined (peat excluded) and for all horizons results combined this gave as the equation of a best fit:

$$y = 995.42 + 0.36x \quad R = 0.04$$

This shows that there can be no overall trend drawn from soil moisture and bulk density in this study. However, when horizons were examined individually, this gave:

Horizon	Equation of best fit line
A	$y = 711.73 + 5.58x$ R= 0.80
B	$y = 974.86 + 1.15x$ R= 0.13
C	$y = 1200 + -3.97x$ R= 0.46

This shows a strong relationship for the A horizon where increasing soil moisture matched increasing bulk density. For the B horizon, result is insignificant, and for the C horizon a moderately weak relationship exists where decreasing soil moisture matched increasing bulk density. No relationship could be found between texture of the soil and bulk densities.

Bulk density, dry density, and soil moisture were plotted against the final readings for shear vane, Bush penetrometer, and hand penetrometer, but only a moderately weak correlation exists between the hand penetrometer and the soil moisture, and a moderately weak correlation between the bush penetrometer and the dry and bulk densities, for other tests there are none. The correlations that do exist are too weak to form any conclusions from the slope of the line.

For the analysis below, all comparisons are made in the C horizon.

The change in strength from initial to final readings overall showed that sites were almost as likely to show an increased average for the C horizon, as a decreased averaged value. In this study the soil moisture may have had some effect on the strength readings, but determined from bush penetrometer as it was the only method of the three which showed a strong correlation between initial and final readings, the final readings were only 1.10 times stronger than the initial readings. The shear vane and the hand penetrometer's correlations are too small to safely draw any conclusion about change in strength.

In the final sites when using the Bush penetrometer, the readings often went to a greater depth than in the initial sites, but this is because when high readings were encountered, the penetration was continued rather than stopped. The variability between the initial and final readings may also be a function of the variability of the soil texture.

Comparison between the average of ten readings versus the average of forty readings will also have a small effect, but the size of the standard error gives an indication on the reliability of the results.

A moderate correlation was found between the friction angle and the percentage of sand in a sample, which gave:

$$y = 49.51 + -10.36x \quad R = 0.61$$

This showed that as the amount of sand increased in a sample the friction decreased.

In figure 4.12, the viscous damping factor as determined by the cyclic loading tests showed some correlation with a similar parameter - proxy for attenuation, for the bush penetrometer, hand penetrometer and shear vane (from dry density):

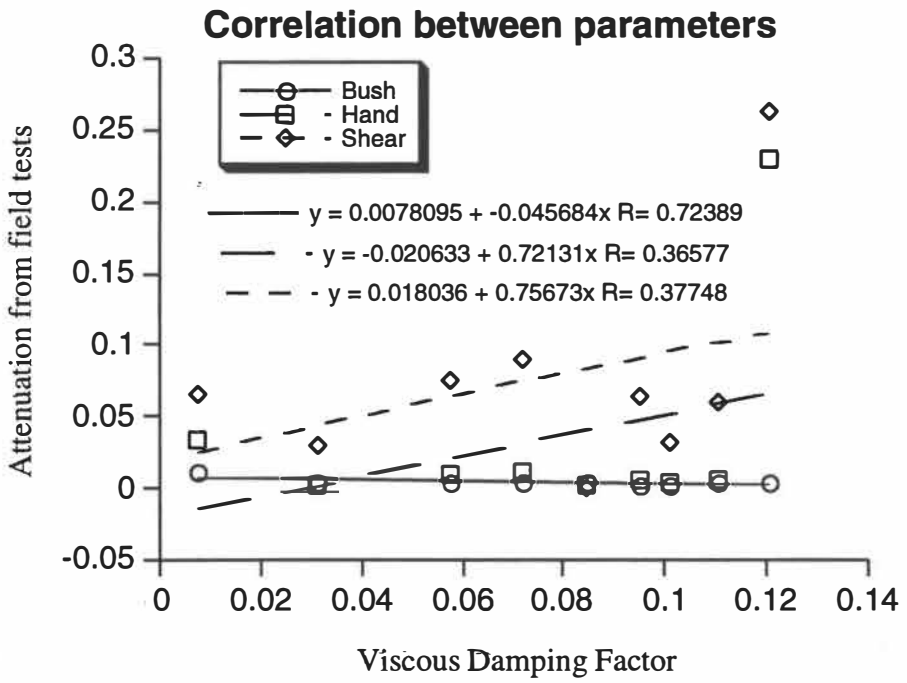

Figure 4.12 Proxies for attenuation, calculated from dry density and shear, hand and bush versus viscous damping factor

Please note: for all graphs where the line equation appears to start with '- y =', the 'negative sign' is actually part of the line symbol.

The proxy for attenuation (calculated from the cyclic loading test from both dry and bulk densities) versus the viscous damping factor was plotted. Both these parameters are measures of attenuation, however the correlation was non-existent when calculated from bulk densities, and only moderately weak when calculated from dry densities. The

proxies for attenuation from cyclic loading were plotted versus the proxies for attenuation from field tests but again the results were poor.

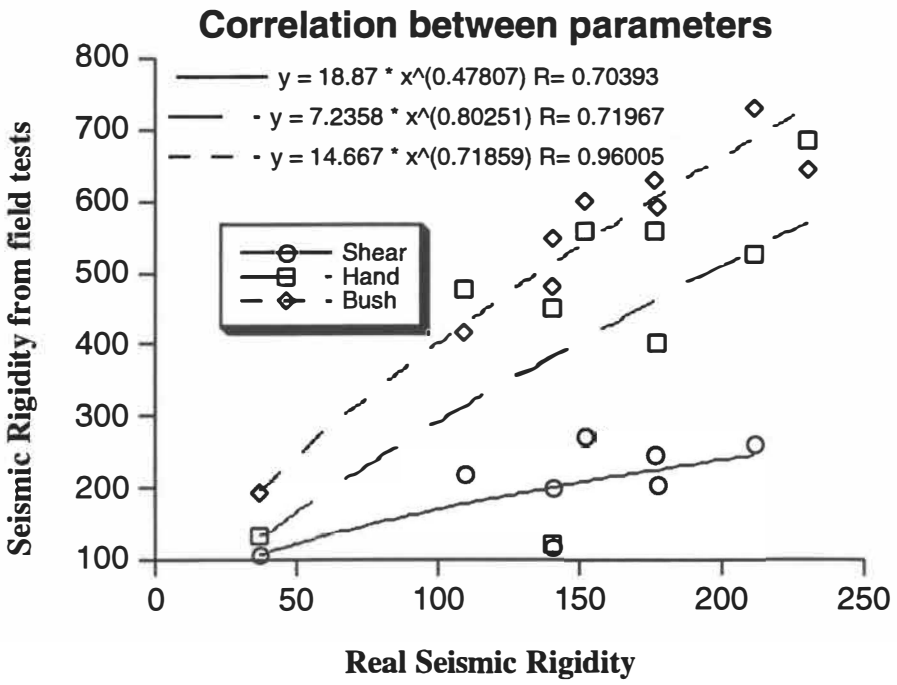

Figure 4.13 'Real' seismic rigidity from cyclic loading versus proxy for seismic rigidity from field tests (both calculated with dry density)

The proxies for seismic rigidity (from dry density and field tests) were plotted (figure 4.13) against each other and this gave moderate to strong correlations, proxies using bulk density gave poor results.

Selby (1993) states that cohesion is caused by the interactions between clay - sized particles or clay - sized particles and water. Particles with a large surface area per unit weight, such as clay, have a greater attraction towards each other, so it would be expected that cohesion would increase in soils with more clay. Tests however, showed no relationship between soil texture and apparent cohesion, so no conclusions could be drawn from this.

As expected there is a strong linear correlation overall (excluding peat), between bulk and dry density (figure 4.14), which shows that soil moisture on average accounts for the 24% difference in density between the two. The regression is reasonably strong so calculating parameters from the bulk or dry density will produce similar results, although weaker correlations can be produced with dry density due to the larger variation in values.

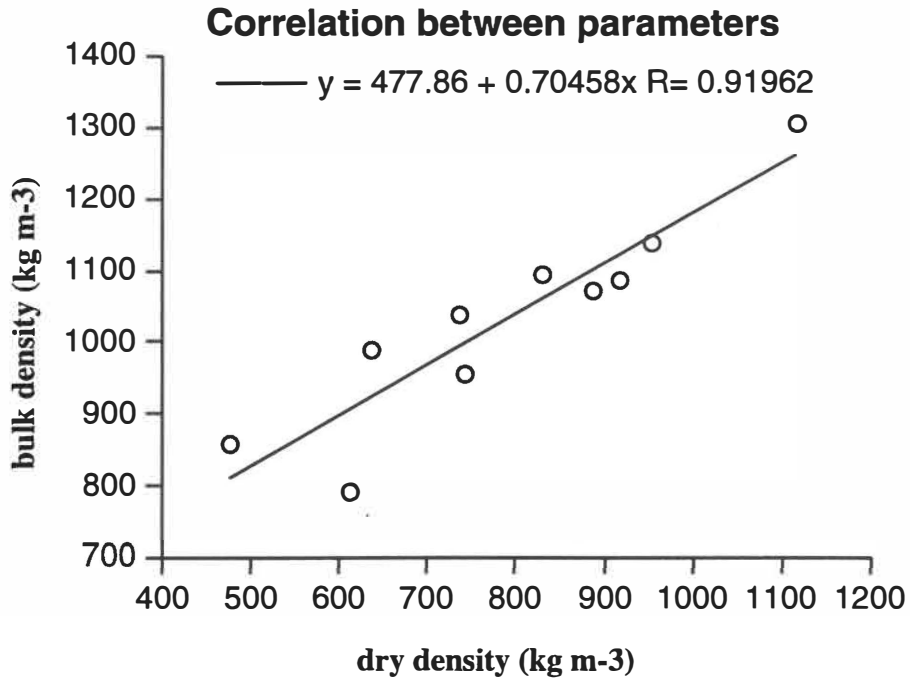

Figure 4.14 Dry density versus bulk density

As seen in figure 4.15 there is a moderate correlation between real seismic rigidity from the cyclic loading (from **bulk** density) and damping, showing that as the soil through which waves are passing becomes stiffer, the greater the ability of the soil to damp any shaking (as opposed to amplifying it). Correlation between seismic rigidity calculated from dry density and damping gives no correlation.

Attenuation versus seismic rigidity is plotted, as determined from the shear vane, hand penetrometer and bush penetrometer using dry density values. They use the same values of dry density and strength and show strong correlations for all parameters. They effectively demonstrate that soil that is more rigid, but the bush penetrometer tends to under-estimate the increase in attenuation as the seismic rigidity decreases.

Seismic rigidity (from cyclic loading, bulk density) versus the shear wave velocity gave no correlation (R= 0.06), but when seismic rigidity (from shear, hand bush values, bulk density) was plotted versus shear wave velocity slightly better results were obtained: bush- R= 0.35, hand- R= 0.01, and shear- R= 0.50, and the seismic rigidity slightly decreased when shear wave velocity increased, however R is too low to draw any conclusions from this.

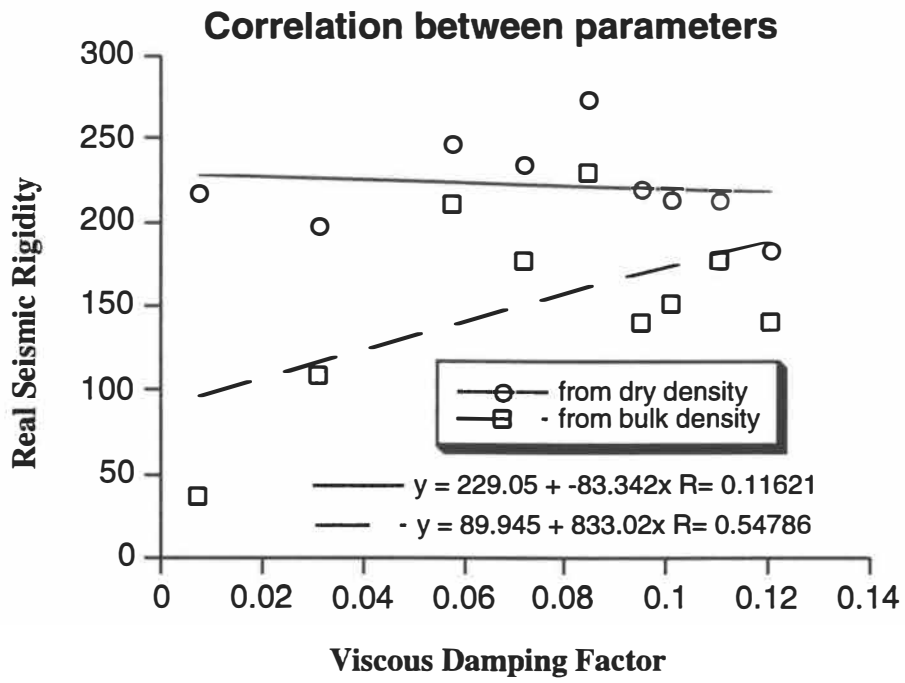

Figure 4.15 Seismic rigidity and viscous damping factor from cyclic loading.

Attenuation (cyclic loading, bulk density) was plotted against the viscous damping factor but this gave no correlation: R= 0.15, however when attenuation (cyclic loading, **dry** density) was used a moderately weak correlation was obtained: y = 0.01 + 0.03x R= 0.42 which shows an increase in attenuation with an increase in viscous damping, this is expected as they measure both measure the ability of the soil to absorb energy and reduce transmission to neighbouring soils.

Seismic rigidity (cyclic loading, bulk density) versus % sand was plotted, which showed no correlation: R= 0.03, but when seismic rigidity (cyclic loading, **dry** density) was used it gave a moderate correlation as in figure 4.16.

Again when 'real' seismic rigidity (**hand, shear, bush,** bulk density) were plotted versus % sand this gave poor results: shear- R= 0.14, hand- R= 0.09, and bush- R= 0.45. However when seismic rigidities were derived with dry densities this gave moderately poor to moderately strong correlations as shown in figure 4.17. The trend appears to show that those sites with a larger sand fraction show greater rigidity which supports the correlation from above.

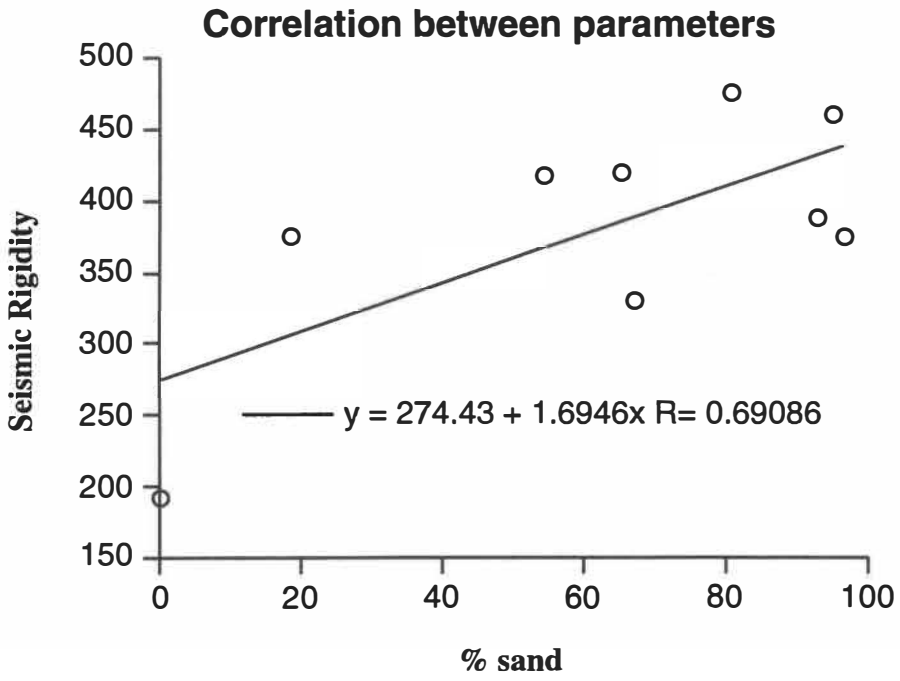

Figure 4.16 'Real' seismic rigidity as calculated from cyclic loading and dry density, versus % sand

Attenuation (cyclic loading, bulk density) was plotted against % sand and this gave no correlation: R= 0.05, but when attenuation (cyclic loading, **dry** density) was plotted the correlation was moderate: y = 0.01 + 4.09e-05x R= 0.58, which showed slight increasing attenuation with increasing sand fraction. Attenuation from hand, shear and bush values with dry and bulk density was plotted against % sand but overall correlations gave poor results.

Seismic rigidity (cyclic loading, bulk and dry density) was plotted versus apparent cohesion from the standard compression test but no correlation was found.

The rest of the parameters for the standard compression test were plotted against both bush, shear, and hand derived parameters as well as those derived from cyclic loading, where the parameters were measuring similar properties, but it was found that in all cases there was none or only a poor correlation.

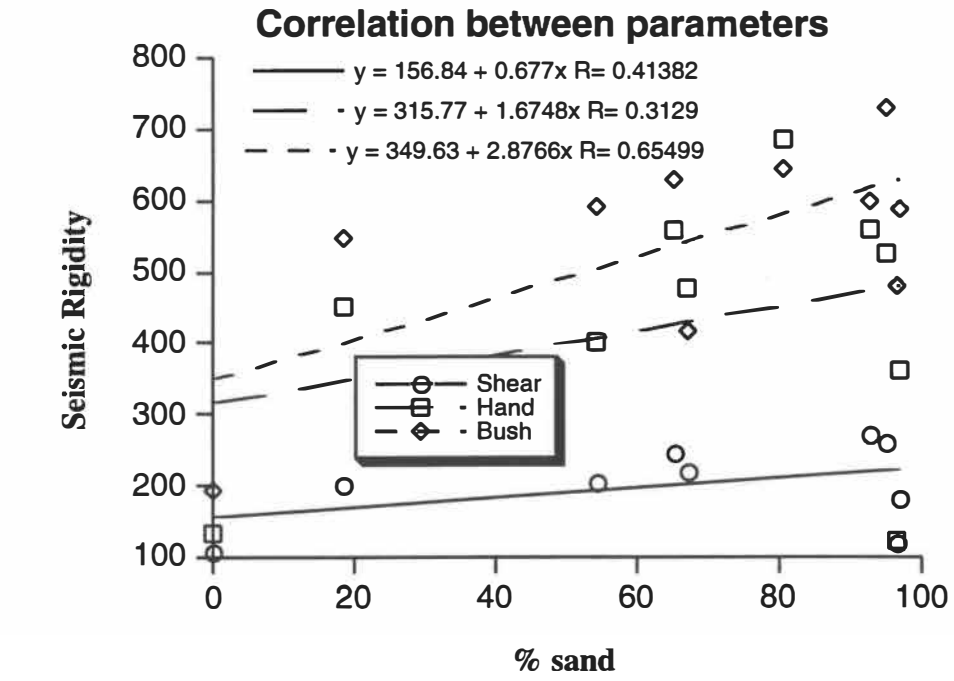

Figure 4.17 Proxies for seismic rigidity from the field test versus % sand.

4.9 Summary

Soil moisture, bulk and dry densities were not useful as parameters on their own, as no trends could be found from them. When compared with the values obtained from the field tests there was no real correlation.

Particle Size Analysis was useful in determining the textural analysis of the soil, which is difficult to do when observing the photographs. The texture of the soil expressed as percentage sand, showed some correlation with proxies and 'real' values for attenuation and seismic rigidity, although the higher clay content in some sites appeared to have no effect on the value for cohesion (derived from the standard compression test). The photographs however, do show at a glance that the soils represent a reasonable range of textural compositions.

Overall, the standard compression test provides mixed results for the sites in terms of assessing the strength of the soil. When compared with the results from Particle Size Analysis, typical friction angles and cohesion values, and results from the geotechnical field tests, there is little correlation.

The parameters (which are proxies) obtained from the shear vane, Bush penetrometer, and hand penetrometer give moderate to good correlations with those obtained from the cyclic loading, and with each other. The hand penetrometer and the shear vane showed a strong correlation.

Chapter Five

Chapter Five

Liquefaction, wave propagation, depth to basement, and resonance

5.1 Liquefaction Potential

5.1.1 Susceptibility of Soils

The liquefaction potential of final sites in the study were examined. The study of course only examines the likelihood of it occurring in the topmost metre, but the samples for analysis are taken from parent material. McMahon *et al.* (1993) states that "Liquefaction usually occurs in water saturated, cohesionless, granular sediment, in a relatively loose state and at depths of less than 10 to 15 metres. The potential susceptibility varies according to its depositional history and age." The Taupo Pumice Formation which makes up much of the material being tested for is relatively young- 1852 B.P. (Wilson, 1993), the effect of this being the younger the deposit, the less compacted it is likely to be, (possibly due to earthquake events that have already occurred), the greater the chance is of liquefaction.

While there are a number of methods that can be used in order to assess the liquefaction potential of sites, the approach taken here takes advantage of the tests that have already been carried out. Firstly, the soils are assessed to ascertain whether they are likely to liquefy from their physical characteristics, then secondly the shaking conditions that are needed to cause the liquefaction are considered.

According to the National Research Centre in the USA, there are a number of criteria that a soil should meet in order to liquefy. Liquefaction usually only occurs in deposits of uniform fine sands, with the following typical characteristics:

- The percentage of silt and clay sized particles is less than 10%, ie. sand > 90%
- The uniformity coefficient $U = D_{60} / D_{10}$ is less than 6
- The 20% passing size D_{20} satisfies $0.04 < D_{20} < 0.5$ mm

Table 5.1 shows those soils which pass this set of criteria.

Table 5.1 Soils that meet criteria

Criterion	**Soil**		
	12 (31)	43 (Oi)	44 (Yp)
% clay <10%	97	97	95
$U = D_{60} / D_{10} < 6$	3	5	4
$0.04 < D_{20} < 0.5$	0.27	0.3	0.2

The three soils were then further examined to see if their peak shear strains exceed those required for liquefaction. From laboratory testing NRC have found that there is a threshold strain γ_c of 0.01% (where τ is a percentage of G). Under this value no excess pore water pressures build up. The peak shear strain (γ) in an earthquake can be estimated from the equation:

$$\gamma = \tau / G$$

where τ is the peak shear stress,
and G is the shear modulus.

From the standard compression test values for τ can be found, and from the dynamic cyclical testing values for G are found, for the three sites. Table 5.2 shows the values for γ:

Table 5.2 Peak shear strain

Site	γ (%)
43 (Oi)	0.033
44 (Yp)	0.020

Site 12 (31) could not be calculated as there were insufficient data from the triaxial tests. In terms of areal extent of the soil, it covers only a small area of 105 hectares of farmland just north of Reporoa (for a further description refer to Appendix I). 31 is described as poorly drained (Vucetich *et al.,* 1978), so liquefaction could occur, but when the soil moisture profile is examined, the C horizon is only 18%. Similar soils (31a and 31b) are silty loams and do not contain sufficient sand for liquefaction. Sites 43 and 44 have sufficiently high values for excess pore pressures to develop.

Typical peak accelerations for moderately damaging earthquakes range from 0.1 to 0.2g on hard rock, which corresponds to a predicted 0.3g acceleration on 'soft to medium stiff clay and sand', (Finn, 1991) although near faults accelerations of up to 1.5g have been recorded (Lomnitz, 1994) so from:

$$V_S = 100 \sqrt{(1.2\ a\ D)}$$

where D is the depth (m)
and a is the peak acceleration at the ground surface. (NRC, 1985)

The expected shear wave velocity may be calculated and compared with those values obtained from sites 43 and 44 from the cyclic loading. Where the shear wave velocity of the earthquake exceeds that of the soil, damage may be expected to occur as the soil retards the transmission of the energy and liquefaction may occur. For a depth of 1 m and an acceleration of 0.3g this gives a shear wave velocity of 60 m/s. The samples were tested under saturated conditions, and according to Biot's theory (Richart *et al.,* 1970) measurement of shear waves in saturated soils does determine the shear wave velocity in the soil structure.

In general terms, Oi is found in areas of smooth rolling topography and its related soil types are found on undulating surfaces as well as moderately steep to steep slopes. Yp fills a number of small valleys and gullies, so unless an earthquake is preceded by sufficient rainfall, any liquefaction that may occur would be expected to be localised and quite limited.

Hodder (1994) notes that liquefaction requires saturated soils was well as the material being examined to be below or near the water table, citing a range of 5 -10 m. Water level readings taken in Taupo town (Dawson *et al.,* 1981) show readings where the water table is less than 10 metres from the ground's surface such as 15 Pataka Rd, 215 Rifle Range Rd, 40 Brice St, 18 Napier Rd, amongst others. More commonly the water

table ranges from 20 to 70 m depth. Unfortunately the water level surveys do not cover the area where soils may liquefy, however Dawson *et al.* (1981) states that for the area "Rain falling on the ground surface rapidly percolates through the porous and permeable upper pumice lapilli beds, causing, except in times of heavy rain storms, little surface runoff", so as Oi and Yp are well drained, the soils are not generally saturated.

5.1.2 Opportunity for Liquefaction

The other criteria in this study for soils to meet is found in Kuribayashi *et al.* (1975), who plotted in the relationship in figure 5.1 from actual observations in the field. The line defining the distance from the epicentre to the farthest site of liquefaction is given by:

$$\log_{10} R_{max} = 0.77M - 3.6$$

where R is the distance,
and M is the Magnitude.

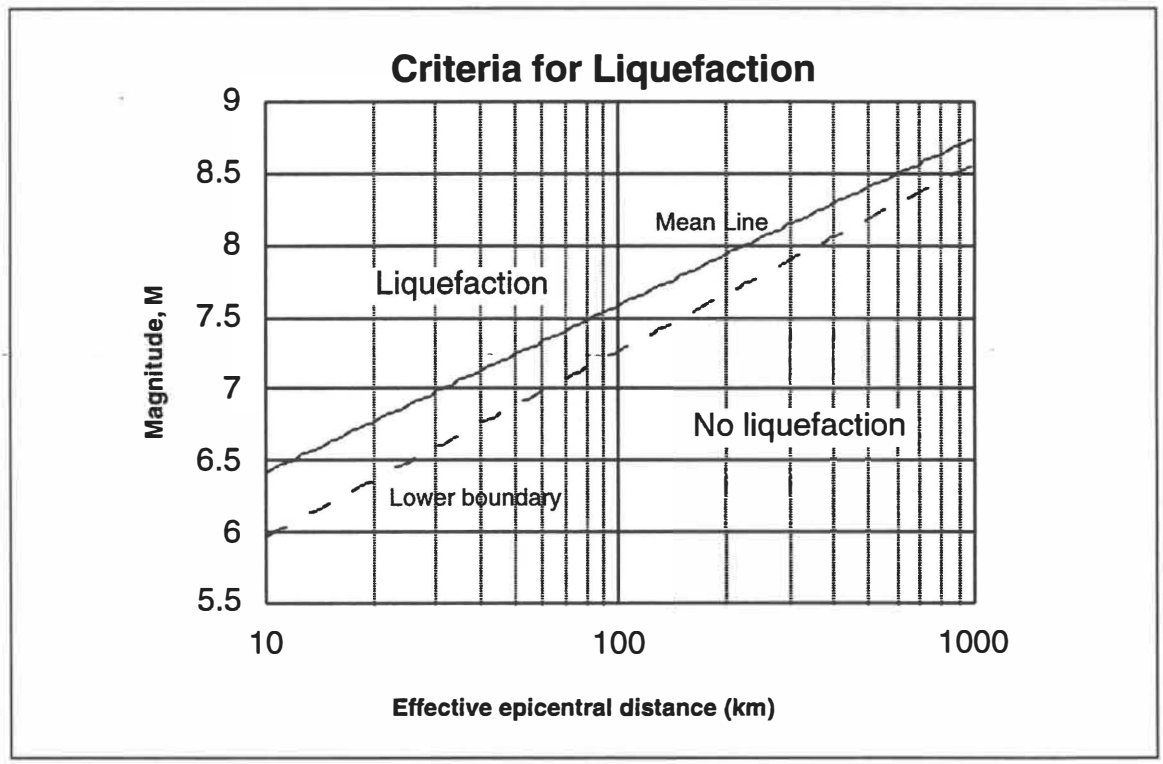

Figure 5.1 Relationship between maximum epicentral distance of liquefied sites and earthquake magnitude (adapted from Kuribayashi *et al.*, 1975)

Earthquakes of less than magnitude six were apparently not plotted. Work in New Zealand (Fairless *et al.,* 1984) supports the relationship, and so gives assurance that this relationship be used in this study.

From this relationship it can be seen that the above soils, that have passed the previous criteria, are found (Oi and Yp) predominantly in the southwest corner of the study area. The distance of these soils from the epicentre of the 1895 (M6.5) earthquake ranges from 33 to 53 km, which for liquefaction to occur would correlate to a magnitude of 6.6 - 6.9. However, from the 'lower boundary', which defines the lowest possible distance and magnitude at which liquefaction is possible, liquefaction may have occurred for the 1895 quake. The epicentre was c15 km east of Turangi. Certainly there were landslides and subsidence (from fault activity) in this area, from the quake, but no reports of near surface liquefaction.

From the figure 5.1, the 1922 (M6.0) earthquake, where the epicentral area of the swarm was located over the southwest corner of the study area and Taupo town, would predict liquefaction (from lower boundary). The main features of this quake were landslips at Whakaipo Bay, fissuring at Oruanui and subsidence, but there were localised manifestations of liquefaction, such as dozens of 1 m high waterspouts on the Kaiapo flats and sand blows on the western side of the Kaiapo Fault (Grindley *et al.,* 1986). The largest events in 1963 / 64 and 1983 are clearly not large enough to cause liquefaction (in Chapter two).

Should liquefaction occur again, the most likely scenario would be from an earthquake or swarm of, in the northwest corner of the Lake Taupo, which in distance from the liquefiable soils ranges from 10 to 30 km. For liquefaction to occur, the quake would need to be approximately M 6.6 for those soils furthest away from the epicentre, which is quite large given the history of quakes in the area. A large earthquake outside the region may induce liquefaction in the area, such as one at Napier of at least M 7.4 (from lower boundary) but more likely a magnitude of 7.7 would be required (mean line).

Landslide hazard was not considered due to most buildings being located on relatively flat areas, and the bulk of the population in this region is located in Taupo township.

5.2 Wave propagation, Depth to Basement, and Resonance

Attempts have been made to predict how the direction of wave motion may affect the amount of damage caused. However, soils are highly non-linear in their transfer of wave motion. So it is still not known what role non-linearity plays in wave propagation and how this is expressed in the behaviour of systems of soils (Lomnitz, 1994).

Ground shaking may also be enhanced by resonance effects within a layer of soft material overlying a more competent rock (Borcherdt, 1985). This effect is dependent of the relative seismic rigidity of the two. Resonance occurs when wavelength of the seismic vibration is comparable to the thickness of the soft material above solid rock (Hodder *et al.,* 1994). From Houghton *et al.* (1986) the inferred depth to basement material is in the order of 2 - 3 km, but the structure has only been modelled to 1 - 2 km depth. Hodder *et al.* (1994) states that "Typical seismic velocities in such materials of about 0.6 km s^{-1} and typical variation in the period of seismic waves of 0.1 to 100 seconds, gives a wavelength for seismic vibration of 6 - 600 m". As the depth of the volcanogenic material is substantially greater than the likely wavelength of an earthquake, resonance is unlikely to occur. Lomnitz (1994) examines resonance in tall buildings. This is an effect that will be limited in the study area as most buildings are two stories or less.

5.3 Summary

Soils Oi and Yp have been shown that they may be susceptible to liquefaction in the event of a sufficiently large earthquake. Earthquake swarms, unless their epicentral area is located in the same area as the soils (and there are shock(s) of greater than M6.0), are unlikely to be a mechanism for this to occur, however a large earthquake at some distance outside the region may cause liquefaction in these soils in the southwest corner of the study area. Based on historical observations, and the undulating relief, any liquefaction that may occur would be localised.

The effects of direction of wave propagation are unknown, and resonance is not expected to occur as the depth of unconsolidated materials is too great. Resonance is also unlikely to occur in any buildings.

Chapter Six

Chapter Six

Implications, Conclusions & Seismic Hazard map

6.1 Historical Damage from Earthquakes

Research was carried out on old records of earthquake claims from the Earthquake and War Damage Commission. While the records are incomplete, only 74 claims were found in the records since 1947. Some of them were not accepted, but most may be treated as legitimate claims. The claims were plotted as in figures 6.1 and 6.2.

As can be seen there are very few claims in Taupo, certainly insufficient to enable any firm conclusions to be drawn. Unfortunately, claims from events this year (1995) have not yet been processed. Sixteen claims were not plotted either because there were no street addresses available for them, or because they were designated 'not prosecuted' (ie. it was a doubtful claim). Claim sites with numbers next to them represent the year of the earthquake in which the claim was made. Un-numbered sites are all from the 1983 earthquake swarm.

In Reporoa and surrounding areas, as well as rural areas near Taupo township, claims had no street number, so positioning of the claims accurately was not possible. As can be seen in figure 6.2, Reporoa has had a greater number of claims per thousand buildings, and a greater number of claims in total than Taupo (37 in total for Reporoa although five claims could not be plotted, versus just one in Taupo and three in rural areas nearby). The claims come mostly from the 1983 earthquake swarm, even though most street addresses are not known, the roads on which most of the claims are situated are fairly short and are contained mainly within this group of soils ie. Wh, Wn, Wng, 31, 31a, 33, 34, Mok.

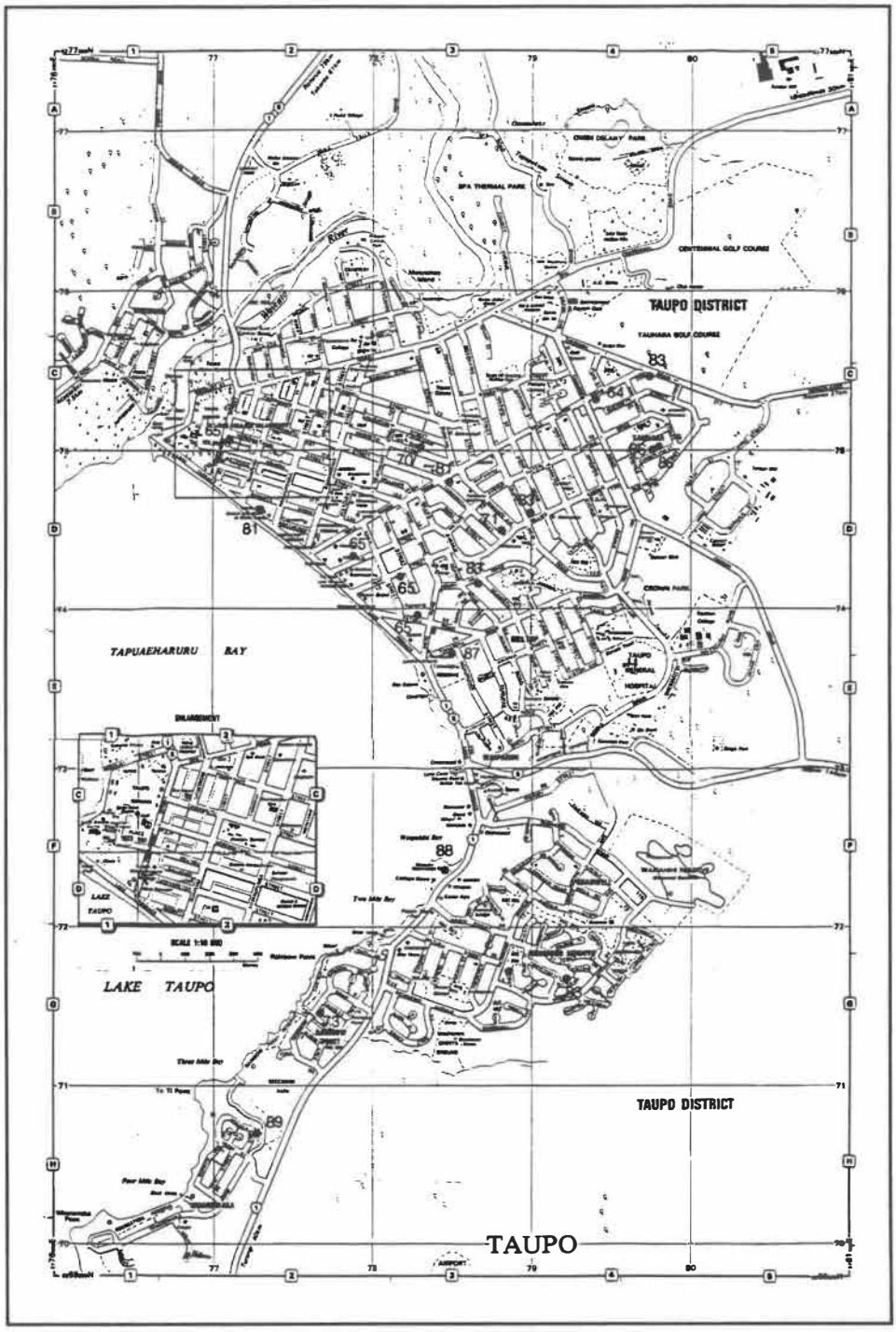

Figure 6.1 Claim map of Taupo

In Taupo there were no claims for this particular event, even though Taupo was closer to the epicentre. Most of the claims made in Taupo have been for earthquakes sourced well outside the region, such as the 1987 Edgecumbe earthquake. None of the soils that lie under Reporoa township are the same as those under Taupo, and results from Chapter four show that those underlying Taupo are generally stronger.

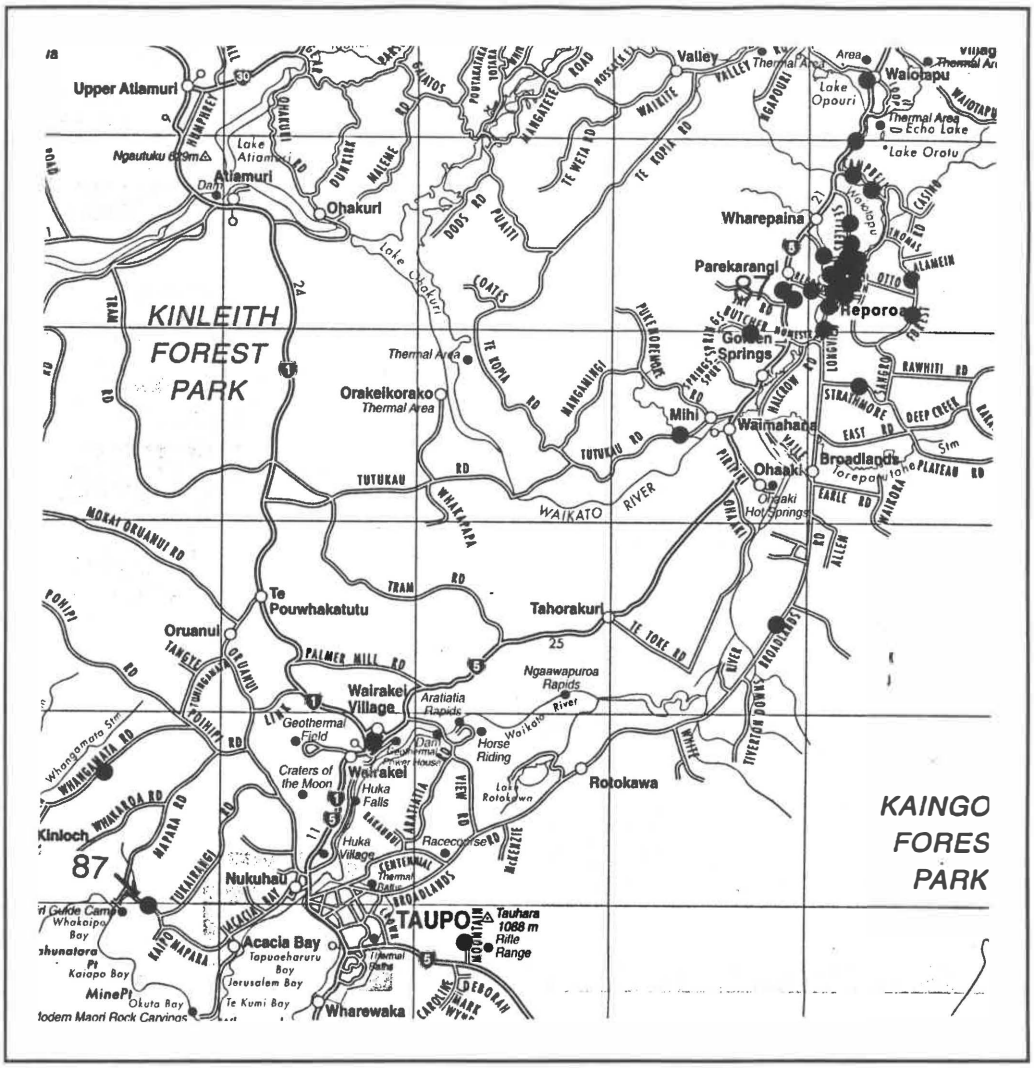

Figure 6.2 Claim map of Reporoa and surrounding areas.

Data from the EQC goes back only as far as the 1945, when Taupo was a small town. Records show that little damage has occurred from earthquakes close to the study area. The earthquake that has produced the most damage was in 1983 and the peak magnitudes of this swarm were relatively low (M2.5 - 4.3). The greater number of claims from 1983 as compared to earlier events is likely to be at least in part a function of a greater number of dwellings in the area.

However, when considering the 1895 and 1922 events alone, the Taupo - Reporoa region is likely to be disturbed again by a sizeable quake, but more likely a swarm of quakes, because of it's volcanic association. as Eiby, 1989) points out "Regions in which there are active or recently extinct volcanoes, like parts of Japan and the North Island of New Zealand, often experience earthquake swarms".

It is of course difficult to predict when and how large an earthquake may be, but by using a statistical analysis based on earthquakes for the whole of New Zealand, the return period (figure 6.3) (which is a misleading term as earthquakes are best considered as random events), and the likely intensities (figure 6.4) may be indicated.

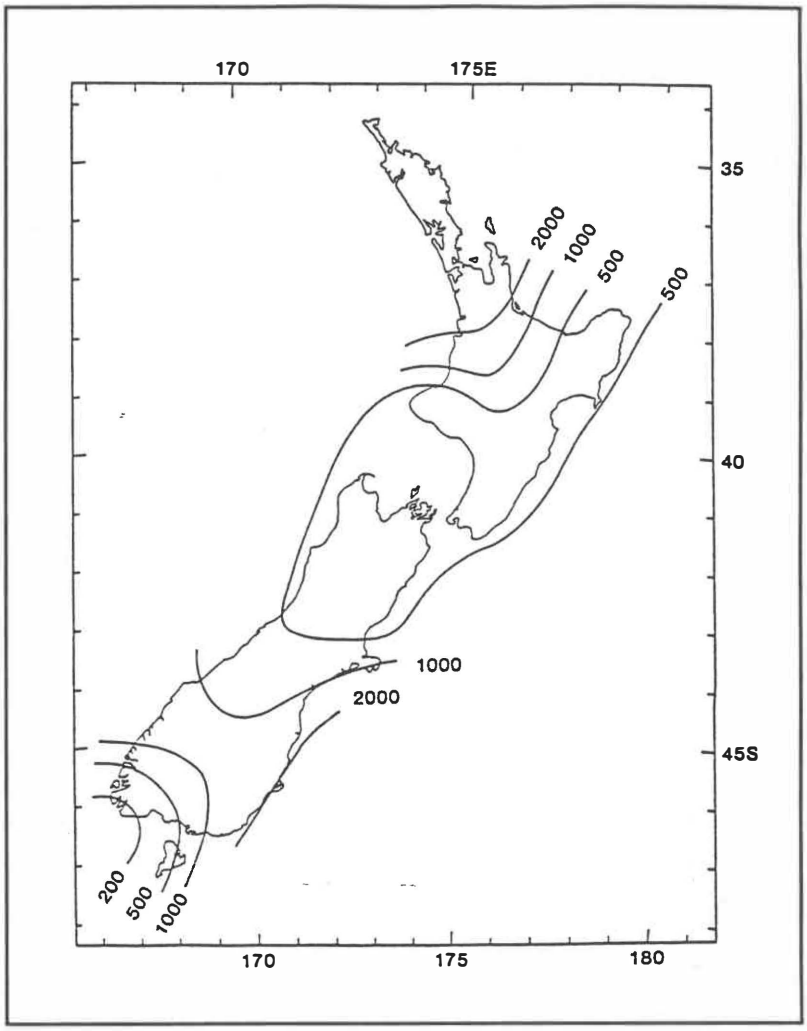

Figure 6.3 Return periods of New Zealand earthquakes. The contours express the average return period (in years) of shaking that reaches MM IX or above. (Eiby, 1989)

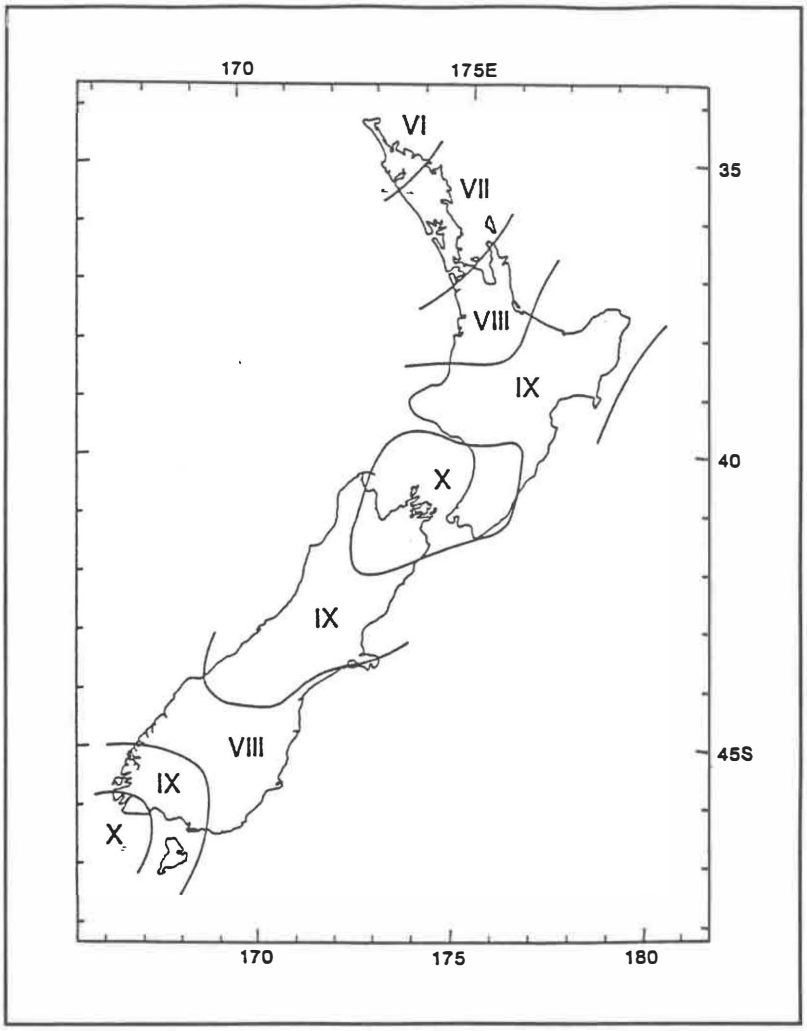

Figure 6.4 Likelihood of severe shaking. The map shows regions in which there is a probability of five percent that shaking of the indicated intensity will occur within 50 years. (Eiby, 1989)

There is a return period of 30 ± 10 yrs for swarms of felt (any intensity) earthquakes in the Taupo region this century, when the 1895 earthquake is included (Grindley *et al.*, 1986). Mean returns periods for Taupo for various intensities (table 6.1) are given by Smith *et al.* (1986).

Table 6.1 Return periods

Intensity (MM)	Years
VI	5
VII	41
VII	180
IX	900

It is important to realise that this is the 'baseline' intensity that would be expected and "These averages take account of previous records of earthquake magnitude and distance, and thus account statistically for seismic wave generation opportunities, and also for the effect of regional geological features." (Hodder, 1994) They do not take account of the small scale variations in the near surface geology ie. in the soils, which is the basis of the whole approach of study. The conclusions are, that descriptions of damage from earthquakes in the past (Chapter two), correlate with larger intensities (MM) than the baseline intensity, owing to the local variations in soil strength. This is illustrated in liquefaction in the Oi group of soils in the 1922 swarm, and from damage claims in Reporoa from the 1983 swarm.

6.2 Summary of methods

• Hand penetrometer and shear vane showed a reasonable correlation despite the fact that they measure strength differently, but they did not correlate particularly well with the bush penetrometer. Of the field methods, bush penetrometer has by far the best reproducibility of results. By comparing initial results with final results, by the size of the standard error, the correlation coefficient (R), and the depth at which values of strength become stronger, it is possible to more accurately characterise the soil in terms of penetrative strength.

• There was a good correlation between bulk density and dry density as expected, which basically shows that each soil had approximately the same quantity of water per unit mass.

• Moderately poor to moderate correlations were shown between the viscous damping factor and the attenuation (from field readings using dry density, and cyclic loading) which is expected as the damping factor and the attenuation are considered to be the same soil property (Lomnitz, 1994), but are just measured differently.

• The standard compression test was not very useful in the final analysis. It is best used for analysis in investigations such as slope stability.

6.3 Relative strength of soils and relation to building damage

Seismic rigidity proved to be the most useful parameter in terms of classifying soils' strength. It could be proxied from the hand penetrometer, shear vane, and bush

penetrometer, by substituting (Hodder, 1994) the readings (in kPa) into the equation for rigidity. As the shear wave velocity could be calculated from the cyclic loading tests, the seismic rigidity could be calculated this way as well. The sites in Table 6.2 have been ranked for the calculated value of seismic rigidity for each parameter. '1' represents the highest value of seismic rigidity, and then all the seismic rigidity rankings are averaged together for each site, to give a semi-quantitative overall ranking of strength. These average rankings are shown for both average and worst case values derived with bulk density (using the dry density gives a similar overall result).

Table 6.2 Overall ranking of soils based on soils' Seismic Rigidity (**bulk** density)

Sites	Overall ranking from average values from final sites (bulk density)	Overall ranking from worst case values from final sites (bulk density)
5 (Wh)	7	8=
6 (Wn)	6	5
8 (Hn+Wng)	5	4
11 (Tpd)	8	6=
12 (31)	10	10
23 (Hn)	2	2=
30 (Yp)	1	1
38 (Tpd)	4	6=
43 (Oi)	11	11
44 (Yp)	3	2=
45 (33)	9	8=

This does not show the relative difference in seismic rigidity from each of the methods, but is the simplest way of showing the soils' expected response to earthquake based on all the methods for which seismic rigidities may be obtained. In Table 6.3, the resulting values are derived with the dry density, (although correlating strongly with bulk density) which tends to differentiate more strongly between soils.

As would be expected, site 45 (33 - peat) has the lowest ranking for both average and worst case results, and is followed closely by site 43 (Oi) and 12 (31). Sites 23 (Hn), 30 (Yp), 38 (Tpd), and 44 (Yp) are clearly the strongest when using both tables. When examining the tables of seismic rigidity in Appendix IV it can be seen that the rest of the sites showed mixed results in terms of magnitude of rigidity relative to each other.

The lowest ranked sites are substantially lower in their seismic rigidity than the middle-ranked sites.

Table 6.3 Overall ranking of soils based on soils' Seismic Rigidity (**dry** density)

Sites	Overall ranking from average values from final sites (dry density)	Overall ranking from worst case values from final sites (dry density)
5 (Wh)	5	9
6 (Wn)	6	7
8 (Hn+Wng)	8	5=
11 (Tpd)	7	5=
12 (31)	9	8
23 (Hn)	3=	3
30 (Yp)	1	1
38 (Tpd)	3=	4
43 (Oi)	10	10
44 (Yp)	2	2
45 (33)	11	11

When attenuation, which again is able to be measured from four different methods, is compared (from Appendix IV), sites 43 (Oi), 12 (31), and 45 (33) show that overall they would expected to produce the greatest attenuation. Sites 23 (Hn), 30 (Yp) and 44 (Yp) clearly will produce the least attenuation. This parameter also proved useful, along with amplitude enhancement for confirming the results of seismic rigidity.

Viscous damping factor, as calculated from the cyclic loading tests, showed some moderately poor to moderate correlations with the attenuation for both lab and field methods when calculated from the dry rigidity. The viscous damping factor (or Q) indicates that two sites 45 (33) and 8 (Hn+Wng) would cause more damage in buildings; EQC claims in the Reporoa area tend to support this.

Earlier in the chapter, the relationship between damage claims and soil types was briefly mentioned and it was obvious that despite the overall small number of claims, almost no claims had been made in Taupo township from the 1983 earthquake, whereas quite a number of claims had been made in Reporoa. This earthquake swarm is the only event for which a significant number of claims has been made. Of the few other claims made in the Taupo region, they are from earthquakes sourced outside the study area.

6.4 How the soils were grouped

The soils under Reporoa area are different from those under Taupo with the exception of a few small areas of Hn. In general, when looking at the textural composition of these soils (Appendix I) they are finer than those found in Taupo. Some of the soils are alluvial or peat. Eiby (1989) notes "one of the most unsatisfactory foundations appears to be alluvium... Japanese results indicate that a foundation of alluvium has the effect of absorbing small earthquakes, but it amplifies the vibrations of larger ones" Peat is well known to behave poorly in earthquakes.

Soils on Map One are grouped together under subheadings on the basis of origin of the parent material (eg. Taupo Pumice, Re-sorted Taupo Pumice, Organic Soils). Those groups do not equate with groups of soils based on strength, with the exception of alluvial and organic soils. From the initial survey as these latter soil groups were weaker than the rest (and distinctively different in origin of deposition) they were placed together.

The Strongest Soils

Overall, two soils stand out as being stronger than the rest: **Yp** and **Hn**. For both Yp sites the results for strength are remarkably consistent with each other despite a distance of some 8 km between them. However, Yp may be susceptible to liquefaction in a sufficiently large enough earthquake (see Chapter five), along with the Oi soils in the southwest corner of the region.

The Weakest Soils

Two soils are noted for their lack of strength: **33** and **Oi**. Oi and OiH are essentially the same soil on different topography. From initial results they are geotechnically similar and the soil descriptions for them tend to agree. Additional evidence that supports the inference that the Oi group of soils is weak, from landslides and fissures in the southwest area from the 1895 earthquake and 1922 earthquake swarm. The Bush penetrometer showed the best correlation between initial and final sites for Oi. Analysing the initial data, all the alluvial and peaty soils produced similar results and so are grouped together, which includes these soils: **31**, **31a, 31b**, **Mok**, **33**, and **34**. These alluvial and peaty soils are also known to behave poorly in earthquakes.

The Intermediate Soils

Soils of overall intermediate strength are grouped together (excluding Tp soils and peat / alluvial soils), these are sites 5 (**Wh**), 6 (**Wn**) and 8 (**Hn+Wng**). From initial data it can be observed that some variation in strength occurs (and average of initial strength readings across sites do concur with final site results). To more accurately assess the seismic hazard to structures, the soils should be investigated on a site by site basis. From the claim map of Reporoa (although claim locations are quite approximate) a reasonable portion of the claims are located on these soils. From the soil descriptions of their textures (Appendix I) it was expected that they might show intermediate strength values compared with the other soils in the region.

The Variable Soils

The difference in the Tpd sites in terms of all the measured parameters confirms what was found from the initial data. The **Tp** group of soils exhibit a wide range of strength, although all the Tpe sites tended to be consistently strong. This is significant as roughly 40% of Taupo is located on this particular soil (Tpe). To more accurately assess the hazard from the Tp group of soils it is recommended that this be done on a site by site basis.

Ai was not assessed fully in the final sites. However, no towns or townships are located on it so any potential for damage is minimised mainly to a stretch of Broadlands Rd and a very short stretch of S.H.5 near Wairakei. The initial values to tend to indicate that it is of moderate strength relative to other soils.

On the basis of these groupings, a seismic microzoning map can be drawn showing how susceptible soils are expected to be to ground shaking from a large earthquake. This is in Map Two in the pocket. Some soils have not been assessed as they cover only a small area. The soils are grouped for seismic hazard on the basis of their strength measured from the geotechnical tests, and in the case of the peaty and alluvial soils, also from the origin of formation.

Although records for damage are limited in the Taupo - Reporoa region, it can be seen from these, and from observations of earthquake events, that there is a correlation

between the strength of the soil and damage that occurs, though the link is semi-quantitative. On this basis, the approach provides a reconnaissance tool for pinpointing potential problem areas (specific sites or soil types) which can then be investigated in more detail.

Bibliography

Bibliography

Baver, L.D., Gardener, W.H. and W.R. Gardener, 1972, *Soil Physics,* Wiley, New York, USA.

Bell, F.G., 1980, *Engineering Geology and Geotechnics.* Butterworths, London, UK.

Berryman, K.R., 1993, *Earthquake Hazards in the Waikato Region,* Client report of the Institute of Geological and Nuclear Sciences Limited, NZ.

Bishop, A.W., and D.J. Henkel, 1962, *The Measurement of Soil Properties in the Triaxial test,* Edward Arnold Ltd, 25 Hill St, London, UK.

Borcherdt, R.D., 1985, *Predicting Earthquake Ground Motion: an introduction,* In Ziony, J.I. (ed.): *Evaluating Earthquake Hazards in the Los Angeles Region - An Earth Science perspective,* United States Goverment Printing Office, Washington, USA.

Dunn, I.S., Anderson, L.R., Kiefer, F.W., 1980, *Fundamentals of Geotechnical Analysis,* Dept. of Civil Engineering, Utah State University, John Wiley and Sons, New York, USA.

Eiby, G.A., 1968, *An annotated list of New Zealand earthquakes 1460 - 1965,* New Zealand Journal of Geology and Geophysics, 11 (3), p630-647.

Elder, D.McG., McCahon, I.F, Yetton, M.D., 1991, *The earthquake hazard in Christchurch: a detailed evaluation,* Research Report to EQC, Soils and Foundations, Christchurch, NZ.

Fairless, G.J., and J.B. Berrill, 1984, *Liquefaction during Historic Earthquakes in New Zealand,* Bulletin of the New Zealand National Society for Earthquake Engineering, Vol 17, No 4, December.

Finn, W.D.L., 1991, *Site conditions and seismic response,* Proceedings of International Symposium on Effects of Surface Geology on Seismic Motion, Odawara, Japan, Vol 1., 3-31.

Fredrickson, D., 1988, *Triaxial Testing with the GDS Triaxial Testing System,* Department of Earth Sciences, Unpublished Internal Report series in Geomechanics, University of Waikato, Hamilton, NZ.

Froggatt, P.C., 1981, *Stratigraphy and nature of Taupo Pumice Formation,* New Zealand Journal of Geology and Geophysics, Vol. 24, p231 - 248

GDS Instruments Ltd., 1988, *The GDS Users Handbook Part II: Introducing the GDS Triaxial Testing System, GDSTTS (version 5),* Prestige Data Files Ltd, Gateshead, Tyne & Wear, England.

Graham, M.Z., 1993, *Use of Geotechnical measurements for earthquake microzoning of areas of unconsolidated sediments and deep soils,* Unpublished thesis, Dept. of Earth Sciences, University of Waikato, NZ.

Grange, L.I.,1937, *The Geology of the Rotorua-Taupo Subdivision, Rotorua and Kaimanawa Divisions,* New Zealand Department of Scientific Research Bulletin, 37 (new ser.).

Grant-Taylor, T.L., Northey, R.D., Adams, R.A., 1970, *Microzoning for earthquake effects in the Pauatahanui area,* New Zealand Department of Scientific Research.

Grant-Taylor, T.L., Adams, R.D., Hatherton, T., Milne, J.D.G., Northey, R.D., Stephenson, W.R., 1974, *Microzoning for earthquake effects in Wellington, New Zealand,* New Zealand Department of Scientific Research Bulletin, 213.

Grindley, G.W., 1960: *Sheeet 8 - Taupo. Geological map of New Zealand 1:250 000,* New Zealand Department of Scientific Research Bulletin, Wellington, New Zealand.

Grindley, G.W., and A.G. Hull, 1986, *Historic Taupo earthquakes and earth deformation, 1922, 1964, 1983,* Proceedings of the Conference on Recent Crustal Movements, 1984, Royal Society of New Zealand Bulletin.

Hardin, B.O., and V.P. Drnevich, 1972, *Shear modulus and damping in soils: design equations and curves,* Journal of Soil Mech. Found. Div., Proc. m. Soc. Civil Eng., SM7, 98.

Head, K.H., 1984, *Manual of Soil Laboratory Testing, Volume 1: Soil Classification and Compaction Tests,* ELE International Limited, Pentech Press, London: Plymouth, UK.

Head, K.H., 1984, *Manual of Soil Laboratory Testing, Volume 2: Permeability, Shear Strength and Compressibility Tests,* ELE International Limited, Pentech Press, London: Plymouth, UK.

Healy, J., Vucetich, C.G., Pullar, W.A., 1964, *Stratigraphy and Chronology of Late Quaternary Volcanic Ash in Taupo, Rotorua, and Gisborne Districts,* N.Z. Geological Survey Bulletin, new ser., Vol 73.

Hodder, A.P.W., and M.Z. Graham, 1993, *Earthquake Microzoning from Soil Properties,* Earthquake Spectra, Vol 9, No 2, NZ.

Hodder, A.P.W., and V.G. Moon, *Seismic Risk to underground services, Hamilton City,* Department of Earth Sciences, University of Waikato, Hamilton, NZ.

Houghton, B.F., and S.D. Weaver (editors), 1986, *Taupo Volcanic Zone, Tour guides C1, C4, C5, and A2,* New Zealand Geological Survey Record 11, Department of Scientific and Industrial Research, Lower Hutt, NZ.

Hvorslev, M.J., 1962, *Subsurface exploration and sampling of soils for Civil Engineering purposes,* Report on a research project of the Committee on Sampling and Testing, Soil Mechanics and Foundations Division, American Society of Civil Engineers, Engineering Foundation, United Engineering Center, 345 East 47 St, New York City, New York, USA.

Idriss, I.M., 1990, *Response of soft soil sites during earthquakes,* Proceedings of H.B. Seed Memorial Symposium, (U.C. Berkeley, CA, USA), II.

Kuribayashi, E., and F. Tatsuoka, 1975, *Brief review of Liquefaction during earthquakes in Japan,* Soils and Foundations, 15, p81-92.

Lewis, D.W. and D. McConchie, 1994, *Analytical Sedimentology,* Chapman & Hall, One Penn Plaza, New York, New York 10119, USA.

Lomnitz, C., 1994, *Fundamentals of Earthquake Prediction,* John Wiley & Sons, Inc., New York, USA.

McCahon, I.F., Yetton, M.D., Cook, D.R.L., *The Earthquake Hazard in Dunedin, Soils and Foundations,* EQC Research Project, Wellington, NZ.

Menzies, B., 1987, *A computer controlled hydraulic triaxial testing system,* A.S.T.M symposium on advanced triaxial testing of soil and rock, Philadelphia, USA.

Milne, J.D.G., Clayden, B., Singleton, P.L., Wilson, A.D., *Soil Description Handbook,* DSIR Land Resources, New Zealand Department of Scientific and Industrial Research, Lower Hutt.

Moon, V., 1990, *Geomechanics Manual Number 12: 72.351 Engineering Geology Laboratory Manual,* Dept. of Earth Sciences, University of Waikato, NZ.

Nairn, I.A., and C.P. Wood, 1987, *Active volcanoes of the Taupo Volcanic Zone,* In: Active Volcanoes and Geothermal systems, Taupo Volcanic Zone, New Zealand Geological Survey Record 22, Department of Scientific and Industrial Research, Lower Hutt, NZ.

N.R.C., 1985, *Liquefaction of soils during earthquakes,* National Research Council, Washington DC, USA.

Ogawa Seiki Company Ltd., 1992, *Geological Equipment,* Tokyo, Japan.

Parton, I.M. and R.W. Melville Smith, 1971, *Effects of Soil Properties on Earthquake Response,* Bulletin of New Zealand National Society for Earthquake Engineering, Vol. 4, No. 1, p73 - 93.

Pullar, W.A. and K.S. Birrell, 1973, *Age and distribution of late Quaternary pyroclastic and associated cover deposits of the Rotorua and Taupo area, North Island, New Zealand,* N.Z. Soil Survey Report 1 (Part 1 of 2), New Zealand Soil Bureau.

Richart, F.E.(Jr.), Hall, J.R.(Jr.), Woods, R.D., *Vibrations of Soils and Foundations,* Prentice-Hall International, Inc., London, UK.

Rijkse, W.C., 1974a, *Definftion: Boundaries between yellow-brown pumice soils and related or associated soils in Soil Groups of New Zealand, Part 1: Yellow Brown Pumice Soils.* N.Z. Society of Soil Science (N.E. Read, editor)

Rijkse, W.C., 1974b, *Diagnostic criteria and classification of mapping unit in Soil Groups of New Zealand, Part 1: Yellow-brown Pumice Soils,* N.Z. Society of Soil Science (N.E. Read, editor)

Rijkse, W.C., 1986, *Soils of the Taupo region: interim soil maps and legend,* N.Z. Soil Bureau District Office, Rotorua.

Sanglerat, G.,1972, *The Penetrometer and Soil Exploration* , Developments in Geotechnical Engineering, 1, Elselvier Publishing Company, Amsterdam, Netherlands.

Seed, H.B., 1960, *Soil Strength during Earthquakes,* Proc. 2nd World Conference on Earthquake Engineering, vol. 1, p183 - 197.

Selby, M.J., 1993, *Hillslope Materials and Processes,* 2nd Edition, Oxford University Press, Oxford, UK.

Smith, K.A. and C.E. Mullins, (editors), 1991, *Soil Analysis - Physical Methods,* Marcel Dekker Inc., 270 Madison Ave, New York, USA.

Smith, W.D., and K.R. Berryman, 1986, *Earthquake hazard in New Zealand: inferences from seismology and geology,* Royal Society of New Zealand Bulletin 24, p223-243

Terzaghi, K. and R.B. Peck, 1967, *Soil Mechanics in Engineering Practice,* 2nd Ed., Jonh Wiley & Sons, New York, USA.

Vickers, B., 1978, *Laboratory Work in Civil Engineering - Soil Mechanics,* Granada Publishing Limited, Crosby Lockwood Staples, UK.

Vucetich, C.G., Leamy, M.L., Stokes,E., 1978, *Soils of Reporoa District, Central North Island, New Zealand,* N.Z. Soil Survey Report 14, New Zealand Soil Bureau.

Walker, G.P.L., Heming, R.F., Wilson, C.J.N., 1980, *Ignimbrite veneer deposits or pyroclastic surge deposits? Reply,* Nature 286.

Walker, G.P.L., Wilson, C.J.N., Froggatt, P.C., 1981, *An ignimbrite veneer deposit: the trail marker of a pyroclastic flow,* Geology 8, p245-249.

Wan Tianfeng, and J.W. Hendenquist, 1981, *a reassessment of the structural control of the Broadlands geothermal field, New Zealand,* Proceedings of the New Zealand Geothermal Workshop, 1981: p195-202, University of Auckland, NZ.

Wilson, C.J.N., 1993, *Stratigraphy, chronology, styles and dynamics of late Quaternary eruptions from Taupo volcano, New Zealand,* Phil. Trans. Royal Society, London, A (1993) 343, p205-306

Wilson, C.J.N., Ambraseys, N.N., Bradley, J., Walker, G.P.L., 1981, *Did Taupo's eruption enhance European sunsets, Reply,* Nature 293, p491-492.

Appendices

Appendix I

Soil Profile descriptions

Soils of the Reporoa and Taupo Districts

Acknowledgments and Background

These descriptions are compiled from Vucetich *et al.* (1978) and Rijkse (1986). The original soil maps had different names for same soils and so both names / numbers are given where possible in case the reader wishes to examine the original maps. The descriptions also contain information on topography and location, tephra beds comprising the profile, the natural drainage, and a brief profile description. The area covered by a soil is found only on the Reporoa soil map and not the Taupo interim map, so only those soils found only in the Reporoa basin will have their area shown. To show the areas of other soils would be misleading as the values would be minimum values only and some soils are by far more prevalent near Lake Taupo than in the Reporoa basin. All soils are allophanic to varying degrees.

TP : 2

Taupo sandy silt is found on rolling surfaces, some moderately steep slopes, smooth ridges: widely distributed along terraces of Reporoa basin and just north east of Taupo town, and has tephra beds of 40 - 150 cm Taupo Pumice on Holocene ash. It's profile is 15 cm - very dark greyish brown silty sand; friable; granular / nut structure, 13 cm - very dark greyish brown silty sand; very friable; crumb structure, 25 cm - yellowish brown sand with pumice stones; loose, on brown silty sand to gravelly sand.

Tp belongs to the group of Yellow-brown pumice soils, which have all or most of the following characteristics (Rijkse, 1974):
- have at least 50 centimetres of the soil developed in young coarse textured tephra,
- have A - Bw - BC - CB - or C horizons developed in the young tephra,
- have a predominant texture coarser than fine sandy loam or silt loam,
- have predominantly friable to loose consistency and a weakly developed structure or at least one horizon with these properties,
- have a low bulk density,
- are weakly weathered,
- have a low clay fraction consisting predominantly of allophane.

Tp and associated soil types (eg. Tpe) are part of the yellow-brown pumice soils which are the most extensive and the most frequently occurring soil group in the Taupo region. These are formed from very thick to thin Taupo Pumice. In southern parts of the Taupo region very shallow (less than 20 centimetres) Ngauruhoe Ash overlies Taupo Pumice and in north-western parts of the region very shallow to very thick Kaharoa Ash overlies Taupo Pumice.

Yellow-brown pumice soils have been subdivided in series according to differences in kind and mode of deposition of the parent material (eg. airfall tephra, flow-tephra, water-sorted pumice), the climate under which they occur, often associated with the influence of indigenous vegetation or previous indigenous vegetation, and topography where erosion may have altered any of the above named factors. Further subdivisions have been made according to the thickness of individual tephras.

TpH : 2H

Taupo hill soil, silty sand, is found on moderately steep slopes, smooth and widely distributed, especially along eastern margin of map, and has tephra beds of 50 - 130 cm Taupo Pumice on brown silty sand to gravelly sand (pumice and rhyolite). It is well to somewhat excessively drained, and it's profile is: 13 cm - black silty sand; very friable; granular structure, 10 cm - very dark greyish brown silty sand with pumice stones; nut/crumb structure, 15 cm - dark brown sand with pumice stones; compact, 20 cm - brown gravel; loose, on brown silty sand to gravelly sand.

This is also a yellow-brown pumice soil, and the description is the same as Tp.

Tpd : 2a

Taupo silty sand, undulating phase, is found on undulating terraces and fans: extensive on terraces bordering Reporoa Basin and just north east of Taupo town, and has tephra beds of 50 - 150 cm Taupo Pumice on Holocene ash. It is well drained, and it's profile is: similar to 2, but on undulating slopes.

This is also a yellow-brown pumice soil, and the description is the same as Tp.

Tpe : 2b

Taupo silty sand, upland phase, is found on undulating to rolling surfaces: small areas along north-eastern margin of map and around Taupo town, and has tephra beds of 46 cm Taupo Pumice, 46 cm Taupo Lapilli, on brown silty sand to gravelly sand (pumice and rhyolite). It is well drained, and it's profile is: 13 cm - black silty sand; very friable; granular/crumb structure, 33 cm - silty sand to sand; very friable; massive, on pale yellow pumice gravel; loose.

This is also a yellow-brown pumice soil, and the description is the same as Tp.

Tpls : 2c

Taupo sandy silt is found on rolling surfaces, generally smooth, with some irregular shallow channels: few small areas along northern margin of map and large areas along the Western Boundary Road, and has tephra beds of 0 -25 cm Ngautuku block and lapilli, and 25 - 76 cm Taupo Pumice below. It is well drained, and it's profile is: 15 cm - very dark brown sandy silt; very friable; granular/crumb structure, 8 cm - very dark greyish brown sandy silt with pumice stones; nut structure, 23 - cm pale olive brown silty sand; friable; compact structure, on dark brown sandy loam; friable; crumb structure.

This is also a yellow-brown pumice soil, and the description is the same as Tp.

Aig : 1

Atiamuri silty sand and stony sand is found on undulating to flat surfaces: moderate areas north west of Mihi along Pukemoremore Road, also Torepatutahi Stream, and has tephra beds of +6 cm Taupo Pumice breccia. It is well drained, and it's profile is: 13 cm- dark greyish brown silty sand; crumb/nut structure, 13 cm olive brown stony silty sand; friable to firm; crumb structure, on pale yellow silty sand; massive.

This is also a yellow-brown pumice soil, and the description is the same as Tp.

Ai : 1

Atiamuri sandy silt is found on undulating to flat surfaces (broken by narrow steeply walled gullies): several areas, most extensive near Te Kopia and just East-North-East of Taupo town, and has tephra beds of 13 - 50 cm Ngautuku block and lapilli, and minor alluvium, on +3 m of Taupo Pumice breccia. It is well drained, and it's profile is: 10 cm - black sandy silt with pumice stones; very friable; nut / crumb structure, 10 cm - dark brown sandy silt with pumice stones; very friable; crumb structure, on yellowish brown to pale yellow silty sand; massive.

This is also a yellow-brown pumice soil, and the description is the same as Tp.

Oi : 3

Oruanui silty sand and sand is found on rolling smooth surfaces broken by infrequent gullies: few small areas west near Mangakaka Stream and some other areas in the south west corner of the map, and has tephra beds of 30 - 130 cm Taupo Pumice on Holocene ash. It is well drained, and it's profile is: 13 cm - black silty sand; few gravels; very friable and spongy; crumb granular structure, 13 cm - dark brown gravelly sand; soft; crumb structure, 30 cm - olive brown gravelly sand; much rhyolite, on dark brown sandy loam; friable; crumb structure.

This is also a yellow-brown pumice soil, and the description is the same as Tp.

OiH : 3H

Oruanui hill soil, silty sand, is found on moderately steep to steep slopes: extensive on lower slopes of the Paeroa Ranges as well as in the south west corner of the map, and has tephra beds of 25-250 cm Taupo Pumice on Holocene ash. It is well drained, and it's profile varies considerably in (a) depth of Taupo Pumice, and (b) subsoil textures.

This is also a yellow-brown pumice soil, and the description is the same as Tp.

Oi : 3a

Oruanui silty sand, undulating phase is found on undulating surfaces: small areas on lower slopes of the Paeroa Ranges and some other areas in the southwest corner of the map, and has tephra beds of 76 - 150 cm Taupo Pumice on Holocene ash. It is well drained, and it's profile is: similar to 3 but on undulating slopes.

This is also a yellow-brown pumice soil, and the description is the same as Tp.

OiH : 3bH

Oruanui hill soil, sandy silt, is found on moderately steep to steep slopes: several areas in northwest part as well as in the southwest corner of the map, and has tephra beds of 25 - 100 cm Taupo Pumice on Holocene ash. It is well drained, and it's profile is: 18 cm - black sandy silt ; some gravel; very friable; nut / crumb structure, 25 cm - brown sandy silt; slightly firm; crumb structure, on dark greyish brown gravelly sand.

This is also a yellow-brown pumice soil, and the description is the same as Tp.

Oi : 3c

Oruanui sandy silt, undulating phase, is found on undulating surfaces: in a small area in Waiharuru valley and some other areas in the southwest corner of the map, and has tephra beds of 13 - 50 cm Ngautuku block and lapilli, 50 - 100 cm Taupo Pumice on Holocene ash. It is well drained, and it's profile is: 15 cm - black sandy silt; very friable; crumb/granular structure, 13 cm - dark greyish brown sandy silt; some gravel; friable to firm; crumb structure, 38 cm - olive brown sand; massive; structureless.

This is also a yellow-brown pumice soil, and the description is the same as Tp.

Wnm : 10

Whenuaroa sand is found on flat low terraces: many small areas in Reporoa Basin, but mainly along Vaile Rd with a few small areas further south, and has tephra beds of +76 cm - alluvium from Taupo Pumice. It is excessively drained, and it's profile is: 13 cm - very dark brown; very friable; weak crumb structure, 5 cm - dark brown gravelly sand; loose; structureless, on- yellow pumice gravel and sand; loose.

This is also a yellow-brown pumice soil, and the description is the same as Tp.

Wng : 10a

Whenuaroa stony silty sand is found on flat to undulating surfaces: a large area south of Strathmore Rd, many small areas in Reporoa Basin and also found along stretches of Broadlands Rd and the Waikato River, and has tephra beds of 46 - 60 cm - coarse rubbly alluvium, weakly bedded, from Taupo Pumice. It is well to excessively drained, and it's profile is: 13 cm - black stony silty sand; very friable: weak crumb structure, 25 cm - brown silty sand; many rounded pumice stones; massive, on- yellow stony sand.

This is also a yellow-brown pumice soil, and the description is the same as Tp.

Wn : 10b

Whenuaroa silty sand is found on flat surfaces: many small areas in Reporoa and some further south, and has tephra beds of +76 cm - alluvium from Taupo Pumice. It is excessively drained, and it's profile is: 13 cm - black silty sand; friable; crumb / granular structure, 13 cm - brown silty sand; slightly firm; massive, on- yellow gravelly sand.

This is also a yellow-brown pumice soil, and the description is the same as Tp.

Wnls

Whenuaroa loamy sand is also a yellow-brown pumice soil, and the description is the same as Tp.

Yp, Ypg

Waipahihi sand and Waipahihi gravelly sand are also yellow-brown pumice soils, and the description is the same as Tp.

Wa

Wairakei sand is also a yellow-brown pumice soil, and the description is the same as Tp.

Rt

Rautawiri sand is also a yellow-brown pumice soil, and the description is the same as Tp.

TaS : 9

Tauhara steepland soil is found on steep to very steep slopes, some precipitous (55–), including some rolling surfaces: extensive on Paeroa Ranges, and in gullies in north-eastern part of map (Kaingaroa State Forest) and of course on Mt Tauhara, and has tephra beds of 0 - 50 cm Ngautuku block and lapilli, and 0 - 76 cm Taupo Pumice. It is well drained, and it's profile is 15 cm - black sand loam; very friable; crumb / granular structure, 8 cm - very dark brown sandy loam; friable; crumb structure, on yellowish brown sandy loam to sand; friable; crumb structure.

TaS belongs to the group of Steepland soils related to yellow-brown pumice soils, composite soils, yellow - brown loams and podsolised soils. This is a large group of steepland soils covering some 240, 220 hectares in the Taupo region, contains all the steepland soils on slopes on and over 30 degrees.

The steepland soils have the characteristics of the group they are related to and the variability of soil profiles within the mapping units is considerable.

Note: TaS along with a number of other soils described, is not actually considered in terms of soil strength in the thesis, but is added in to give a complete soil legend and description.

MotS

This is also a steepland soil, and the description is the same as the TaS soil.

Hn : 11

Hinemaiaia sand and stony sand is found on undulating to easy rolling surfaces: extensive in Reporoa Basin mainly along Forest Rd and in some areas further south as well as in and around Taupo town, and has tephra beds of 10 - 30 cm - coarse rubble drift, on Taupo breccia. It is imperfectly drained, and it's profile is: 10 cm - very dark brown sand with few pumice stones; very friable; weak crumb structure, 10 cm - dark brown sand; friable; compact, on- pale grey sand; massive (pumice pan).

This is also a yellow-brown pumice soil, and the description is the same as Tp.

31

Reporoa sandy loam is found on flat surfaces: small areas along Campbell Rd and north of Birch Rd, and has tephra beds of +76 cm - very mineralised alluvium from hydrothermal deposits. It is poorly drained, and it's profile is: not described from this area. It covers 105 hectares.

31a

Reporoa silt loam is found on the undulating surface of levee of Waiotapu River: extensive north of Reporoa, and has tephra beds of +46 - 150 cm - alluvium from hydrothermal deposits of Waiotapu explosion. It is poorly drained, and it's profile is: 20 cm - dark brown silty loam; firm to friable; weak nut structure, 8 cm - dark reddish

brown silt loam; few iron concretions; weak nut structure, 20 cm - brown silt loam; firm, on - pale brown clay; very firm. It covers 345 hectares.

31b

Reporoa heavy silt loam is found on flat surfaces: many small areas in Reporoa Basin, north of Mihi, on floodplain of Waiotapu River, and has tephra beds of variable thickness of alluvium from hydrothermal deposits. It is poorly drained, and it's profile is: similar to 31a but with heavier textures and stronger mottling.

Mok : 32

Mokai peaty loam is found in shallow depressions: many areas widely distributed in Reporoa Basin and also near the Waikato River, and has beds of up to 76 cm - peat. It is very poorly drained, and it's profile is: 10 cm - dark brown peaty loam; spongy; granular structure, 66 cm - dark brown to very dark brown peat loam with thin layers of coherent plant material, on- pale grey pumice sand.

Mok belongs to the group of Organic soils that occur in basins, depressions and in valley floors throughout the Taupo region. They are formed from 40 - 50 centimetres or more organic material overlying water-sorted Taupo Pumice.

In southern parts of the Taupo region amounts of Ngauruhoe Ash have been accumulated in the upper part of the soils.

Mok : 32a

Mokai shallow peaty loam is found in very shallow depressions: many areas widely distributed in Reporoa Basin and also near the Waikato River, and has beds of up to 46 cm - peat. It is poorly drained, and it's profile is: similar to 32, but shallower and more decomposed.

33

Tokiaminga peaty loam and peaty silt loam are found on peat swamps: extensive areas flanking Waiotapu River, north of Reporoa, and has beds of 50 - 120 cm - peat deposits inter-layered with pale brown silt (from hydrothermal deposits), on hydrothermal deposits. It is very poorly drained, and it's profile is: 13 cm - very dark brown peat loam; friable; granular structure, 5 cm - pale brown silt, 50 cm - very dark brown peat loam, on - pinkish clay, massive. It covers 570 hectares.

34

Tokiaminga-Reporoa complex is found on irregular surfaces with marked swampy depressions: limited area bordering Wharepapa Rd, and has beds like 33 and 31a. It has variable drainage, and it's profile is: as for 33 and 31a. It covers 190 hectares.

Pt

Gley soils occur in small shallow depressions and in valley floors throughout the Taupo region and cover 5091 hectares.

Some features of gley soils are:
- a high ground water table for all or part of the year,
- occur in low-lying areas,
- are not accumulating fresh material,
- are undergoing reduction particularly in the subsoils which may be expressed by low-chroma colours,
- often have high organic matter levels.

The gley soils of the Taupo region are subdivided according to parent materials and altitude.

Wh : 12

Wharepaina silty sand is found on flat to undulating with slight depressions: many small areas, widely dispersed in Reporoa Basin and in a few small areas near Broadlands village, and has tephra beds of 30 - 50 cm - alluvium from Taupo Pumice,

on Taupo breccia. It is poorly drained, and it's profile is: 15 cm - very dark brown silty sand with few pumice stones; sandy light to firm; nut structure, 10 cm - pale yellow silty sand with few pumice stones; firm; nut structure, on - pale olive silty sand; flecked reddish yellow; massive.

This is also a gley soil, and the description is the same as the Pt soil.

Wh : 12a

Wharepaina silt loam is found on flat depressions: many small areas in Reporoa Basin, large area along Otto Rd and in a few small areas near Broadlands village, and has tephra beds of +30 cm - alluvium from Taupo Pumice, on Taupo breccia. It is poorly drained, and it's profile is: similar to 12 but more mottled in the subsoil.

This is also a gley soil, and the description is the same as the Pt soil.

Ha

(Recent soils and gleyed recent soils)

Recent soils occur on active flood plains of rivers and streams, along the shores of Lake Taupo and in the southern uplands of the Taupo region. The soils are subdivided firstly according to their parent materials into those derived from river alluvium, lacustrine deposits and recent volcanic ash. Further subdivisions are made according to natural drainage, alluvial parent material and climate.

Some of the recent soils have imperfect to poor natural drainage and they are classified as gleyed recent soils.

All recent soils have in common:
- an A - C profile,
- active accumulation of fresh material.

Yn, Yng

These are also recent soils, and their description is the same as the Ha soil.

Px

(Podsolised yellow-brown pumice soils and podsols)

Px belongs to the group of Podsolised yellow-brown pumice soils and podsols which are commonly related to areas with high annual rainfall and a strong leaching environment and acid litter-forming vegetation. These conditions tend to be present on the extensive uplands of the Taupo region.

Spodic and/or albic horizons are diagnostic of the series of podsolised yellow-brown pumice soils and they should perhaps be called pumice podsols.

Podsolised yellow-brown pumice soils and podsols cover most of the large areas of the Taupo region. They are subdivided according to the degree of podsolisation, differences in tephra formation, and the mode of deposition.

Appendix II

Initial Results

Table of Average Hand Penetrometer values (kPa)

Horizon	1 (34)	2 (33)	3 (31a)	5 (Wh)	6 (Wn)	7 (Hn+Wng)
A	99	148	247	25	25	25
B	444	444	444	247	173	197
C	346	148	346	296	99	494
						C is min avg.

8 (Hn+Wng)	9 (Wh+Mok)	10 (Mok)	11 (Tpd)	12 (31)	13 (Tpd)	14 (Wh)
49	148	25	25	25	247	247
272	296	148	148	148	494	444
494	247	99	49	272	395	197
C is min avg.					B is min avg.	

15 (Wnm)	16 (Tp)	17 (Wn+Wng)	18 (31b)	19 (Wn)	20 (Wng)	21 (Mok+Ma)
99	25	25	197	148	49	74
395	148	148	296	395	148	99
494	494	148	247	99	25	25
C is min avg.	C is min avg.					

22 (Wng)	23 (Hn)	25 (Wh)	26 (Tpls)	27 (Ai)	28 (Tpd)	29 (Tp)
74	197	49	25	148	99	148
296	395	346	296	296	247	148
444	395	494	494	494	loose pumice	148
		C is min avg.	C is min avg.	C is min avg.		

30 (Yp)	31 (Ai)	32 (Tpe)	33 (Tp)	34 (Hn)	36 (Tpe)	37 (OiH)
49	99	99	25	0	197	25
296	296	247	197	25	247	74
395	296	494	395	247	494	346

38 (Tpd)	39 (Ypg)	41 (Tpe)	42 (Ai)	43 (Oi)	44 (Yp)	45 (33)
0	99	25	49	25	0	247
148	197	296	247	197	247	395
197	197	494	296	395	444	197

46 (Wn)	47 (Wh)
0	99
49	395
25	494

Table of Average Shear Vane values (kPa)

Horizon	1 (34)	2 (33)	3 (31a)	5 (Wh)	6 (Wn)	7 (Hn+Wng)
A	20	20	50	25	5	5
B	75	85	95	50	45	60
C	85	90	110	80	50	140

8 (Hn+Wng)	9 (Wh+Mok)	10 (Mok)	11 (Tpd)	12 (31)	13 (Tpd)	14 (Wh)
20	20	10	15	5	50	55
60	70	50	50	30	60	80
140	60	35	15	75	100	70

15 (Wnm)	16 (Tp)	17 (Wn+Wng)	18 (31b)	19 (Wn)	20 (Wng)	21 (Mok+Ma)
25	30	20	30	30	20	5
100	60	30	60	100	35	15
140	60	35	60	50	60	30

22 (Wng)	23 (Hn)	25 (Wh)	26 (Tpls)	27 (Ai)	28 (Tpd)	29 (Tp)
50	55	25	10	30	20	30
60	70	110	15	55	50	30
80	80	100	too hard	140	loose pumice	30

30 (Yp)	31 (Ai)	32 (Tpe)	33 (Tp)	34 (Hn)	36 (Tpe)	37 (OiH)
25	25	30	5	20	35	5
50	60	60	50	20	50	50
70	70	too hard	120	35	180	70

38 (Tpd)	39 (Ypg)	41 (Tpe)	42 (Ai)	43 (Oi)	44 (Yp)	45 (33)
10	30	10	15	25	5	30
40	45	35	70	40	45	50
70	40	120	too hard	90	110	40

46 (Wn)	47 (Wh)
5	60
15	110
10	100

Table of Average Bush Penetrometer values (kPa)

Depth (cm)	1 (34)	St Error	2 (33)	St Error	3 (31a)	St Error
3	10	3	14	3	12	
6	26	8	70	15	48	8
9	158	11	208	21	250	12
12	270	30	252	15	336	10
15	264	27	342	28	316	8
18	330	40	350	22	312	15
21	344	31	294	24	280	13
24	326	22	264	16	264	16
27	328	27	240	21	248	23
30	314	23	214	22	246	14
33	290	12	232	29	260	15
36	278	14	224	17	238	16
39	276	16	264	14	224	8
42	306	19	413	50	224	7
45	318	21	440	66	256	10

5 (Wh)	St Error	6 (Wn)	St Error	7 (Hn+Wng)	St Error	8 (Hn+Wng)	St Error
8		4	2	13	2	4	2
26	5	28	7	68	11	128	36
176	16	92	7	275	31	280	28
240	17	144	14	365	28	342	46
282	24	206	17	437	39	367	39
344	34	296	13	438	80		
404	21	300	18				
390	25	322	28				
378	16	298	17				
388	16	290	17				
372	21	326	15				
382	32	290	18				
380	37	294	19				
372	32	322	17				
402	26	380	33				

9 (Wh+Mok)	St Error	10 (Mok)	St Error	11 (Tpd)	St Error	12 (31)	St Error
6	2	14	3	8	3	12	5
18	8	66	8	28	5	46	10
216	12	142	13	72	13	154	45
278	20	182	18	118	6	198	14
288	48	218	10	192	6	230	13
298	35	192	17	224	14	278	13
338	30	182	27	328	34	242	16
364	21	196	30	360	30	222	16
320	39	228	46	485	21	216	7
288	36	226	39	463	46	208	8
306	28	210	38			248	12
306	26	194	38			222	14
338	28	190	36			206	10
298	03	262	66			262	23
310	24	147	28			280	20

13 (Tpd)	St Error	14 (Wh)	St Error	15 (Wnm)	St Error	16 (Tp)	St Error
18	8	6	2	8		6	4
186	12	60	11	104	15	22	9
338	26	158	29	218	16	174	42
386	32	234	27	250	53	226	24
436	34	302	17	224	19	264	10
418	30	278	14	274	23	316	27
436	30	320	34	432	45	384	20
406	31	336	26	405	103	342	24
456	26	324	26			398	12
444	34	320	24			348	26
462	21	384	27			354	14
466	24	434	32			406	35
430	31	424	20			354	30
363	29	476	18			328	9
323	13	450	26			425	38

17 (Wn+Wng)	St Error	18 (31b)	St Error	19 (Wn)	St Error	20 (Wng)	St Error
0	0	4	3	24	11	24	4
14	5	92	33	211	45	61	10
144	17	350	19	408	36	163	39
310	43	350	15	460	36	202	41
338	33	344	23	511	38	223	45
332	24	340	22	567	46	281	61
364	26	396	36	565	10	290	65
490	23	386	36			342	49
480	37	318	32			393	56
476	25	338	32			415	59
490	37	318	30			401	67
520	41	330	32			450	70
494	18	308	48			455	74
588	27	334	42			395	66
480	80	306	17			337	70

21 (Mok+Ma)	St Error	22 (Wng)	St Error	23 (Hn)	St Error	25 (Wh)	St Error
10	8	4	2	0	0	0	0
85	26	60	27	43	20	39	15
209	24	254	36	461	67	249	25
276	34	308	17	573	30	318	24
341	37	365	16	538	49	342	30
453	24	412	20	438	32	365	27
471	39	427	17	433	67	431	15
459	38	509	24			505	21
515	39	562	27			501	31
506	27	557	30			512	47
532	41	574	29				
508	12	542	38				
533	23	508	58				
		484	47				
		422	42				

26 (Tpls)	St Error	27 (Ai)	St Error	28 (Tpd)	St Error	29 (Tp)	St Error
18	9	0	0	0	0	34	35
220	51	15	13	7	5	195	63
393	27	54	16	242	38	327	56
441	17	123	20	414	31	375	40
427	24	196	33	492	27	360	30
460	27	324	67	499	27	290	25
533	32	301	34	444	33	267	26
487	47	380	51	436	52	245	28
557	87	481	45	381	29	244	24
540	69	543	61	428	46	231	15
493	57	541	74	400	45	235	23
473	15	563	79	425	36	250	17
440	19			455	60	249	19
510	100			428	46	254	30
				384	71	268	30

30 (Yp)	St Error	31 (Ai)	St Error	32 (Tpe)	St Error	33 (Tp)	St Error
0	0	11	7	2		16	2
5	3	113	31	21	11	21	2
103	22	293	30	134	41	36	4
214	19	260	50	260	36	86	23
321	22	327	32	330	35	167	42
398	30	355	30	356	19	302	56
438	39	443	24	380	31	457	56
457	35	414	21	334	16	459	42
400	41	400	29	303	14	474	47
458	46	443	41	339	28	408	60
479	49	496	25	340	24		
468	40	490	33	383	41		
534	40		164	283	24		
528	66			312	22		
				310	32		

34 (Hn)	St Error	36 (Tpe)	St Error	37 (OiH)	St Error	38 (Tpd)	St Error
7	2	6	4	0	0	12	2
39	10	103	32	21	20	129	51
125	18	254	45	65	29	200	38
171	14	353	43	109	39	309	30
248	19	448	73	167	30	426	49
289	17			233	34	397	37
284	22			240	32	411	44
267	17			317	35	373	43
287	24			354	40	416	66
284	19			362	41	413	122
289	22			357	40	357	111
303	27			391	58		
303	31			384	41		
291	24			376	50		
371	41			392	39		

39 (Ypg)	St Error	41 (Tpe)	St Error	42 (Ai)	St Error	43 (Ol)	St Error
9	2	7	2	8	2	22	2
12	3	20	10	14	5	34	4
122	49	77	19	99	14	82	10
292	34	217	33	169	22	107	12
373	55	328	43	264	21	155	21
461	32	354	22	327	27	197	24
485	38	401	28	401	49	268	38
483	44	436	47	411	39	314	46
510	49	399	38	366	59	313	37
527	50	370	17	394	72	357	40
554	45	432	38	367	75	351	46
553	20	452	64	334	85	388	47
607	18	433	37	418	102	456	57
						413	32
						457	53

44 (Yp)	St Error	45 (33)	St Error	46 (Wn)	St Error	47 (Wh)	St Error
15	2	5	2	3	3	9	2
29	6	38	22	8	3	15	3
124	23	268	41	112	29	79	11
219	28	296	16	221	37	123	11
215	31	292	19	312	43	173	15
228	33	295	15	354	48	272	27
282	38	305	29	452	41	333	29
281	34	258	24	518	29	345	30
297	27	255	23	534	20	409	17
299	28	240	15	580	40	530	36
348	34	232	11	596	46	613	68
341	32	242	14	618	43	590	51
354	37	263	10	640	58		
341	42	274	13				
362	65	326	21				

Table of Worst Bush Penetrometer values (kPa)

1 (34)	2 (33)	3 (31a)	5 (Wh)	6 (Wn)	7 (Hn+Wng)	8 (Hn+Wng)
0	8	8	0	0	8	0
0	15	15	8	8	8	23
91	76	160	84	46	114	91
122	145	213	145	76	160	114
137	160	221	168	99	206	229
145	198	221	145	183	145	358
152	168	175	236	168	198	
183	152	145	236	168	343	
191	137	107	236	183	282	
191	107	130	244	175		
183	84	137	198	198		
175	122	137	191	168		
152	152	145	152	145		

183	206	152	152	198		
198	213	175	198	213		

9 (Wh+Mok)	10 (Mok)	11 (Tpd)	12 (31)	13 (Tpd)	14 (Wh)	15 (Wnm)
0	0	0	0	0	0	0
0	30	8	15	99	8	30
130	76	8	23	168	8	122
145	99	76	114	198	84	122
122	137	130	152	198	175	99
137	84	137	183	191	168	137
183	76	160	145	213	198	213
206	46	191	145	198	168	191
122	46	320	145	282	145	251
122	38	251	130	244	183	434
130	38	213	145	312	221	
137	30	213	122	282	244	
206	38	244	122	244	259	
221	46	343	137	191	320	
175	53	411	160	229	267	

16 (Tp)	17 (Wn+Wng)	18 (31b)	19 (Wn)	20 (Wng)	21 (Mok+Ma)	22 (Wng)
0	0	0	0	0	0	0
0	00	0	23	61	0	0
76	53	206	191	61	84	46
114	99	213	206	61	114	175
175	183	198	274	114	160	206
175	198	191	297	114	259	213
236	213	198	411	61	221	274
183	312	191	442	465	244	305
259	229	198		465	297	335
191	282	175		404	312	312
229	251	160		351	335	290
206	305	168		526	358	259
152	328	122		579	389	122
229	381	107		526	389	290
213	274	191		579	366	251

23 (Hn)	25 (Wh)	26 (Tpls)	27 (Ai)	28 (Tpd)	29 (Tp)	30 (Yp)
0	0	0	0	0	0	0
0	0	0	0	0	0	0
99	84	175	0	0	0	0
335	168	290	23	221	91	107
305	152	236	30	274	160	175
290	175	259	84	282	160	236
274	282	274	114	251	130	236
267	328	259	99	206	107	229
305	274	137	229	183	91	130
495	267	282	229	152	99	221
389	434	305	160	168	114	206
389		343	335	229	130	229
411		312	526	213	137	343

419		267	511	229	114	320
		251	465	152	130	396

31 (Al)	32 (Tpe)	33 (Tp)	34 (Hn)	36 (Tpe)	37 (OiH)	38 (Tpd)
0	0	8	0	0	0	0
0	0	8	8	0	0	8
137	0	15	46	61	0	0
8	91	15	91	145	0	107
152	130	23	114	191	76	99
168	221	76	152	191	99	198
282	175	99	130	503	53	213
236	213	236	145		152	198
191	175	229	168		137	229
160	183	191	160		191	183
320	183	335	160		130	137
297	198	381	152		122	
84	191	419	145		198	
152	206		137		145	
175	183		198		213	

39 (Ypg)	41 (Tpe)	42 (Ai)	43 (Oi)	44 (Yp)	45 (33)	46 (Wn)	47 (Wh)
0	00	0	8	0	0	0	0
0	00	0	8	8	0	0	0
23	00	23	15	23	0	8	30
137	53	84	46	61	191	61	61
30	107	114	46	69	152	99	84
168	198	145	69	84	183	15	130
183	236	114	107	114	160	221	130
236	229	229	122	130	130	312	152
274	198	175	137	130	107	351	259
267	229	183	168	122	114	297	290
305	259	114	137	122	130	373	267
389	251	130	160	114	152	411	404
442	259	160	152	137	168	389	411
	221	145	229	152	160	305	419
	213	160	244	145	191	297	495

Appendix III

Final Results

Table of Average Hand Penetrometer values (kPa)

Horizon	5 (Wh)	St Error	6 (Wn)	St Error
A	185	12	322	22
B	494	0	315	16
C	194	28	320	16
	B is min avg.			

8 (Hn+Wng)	St Error	11 (Tpd)	St Error	12 (31)	St Error
111	21	99	24	215	26
284	18	198	36	494	0
481	10	148	22	143	27
C is min avg.		B is min avg.		B is min avg.	

23 (Hn)	St Error	30 (Yp)	St Error	38 (Tpd)	St Error
269	23	165	23	330	18
485	9	315	19	386	20
426	19	494	0	351	29
B & C are min avg.		C is min avg.		B & C are min avg.	

43 (Oi)	St Error	44 (Yp)	St Error	45 (33)	St Error
143	9	146	13	143	12
188	15	278	14	130	8
25	0	248	13	99	0
C is max avg.					

Table of Worst Hand Penetrometer values (kPa)

Horizon	5 (Wh)	6 (Wn)	8 (Hn+Wng)	11 (Tpd)	12 (31)
A	74	148	0	99	74
B	493	173	173	197	494
C	49	123	395	148	49

23 (Hn)	30 (Yp)	38 (Tpd)	43 (Oi)	44 (Yp)	45 (33)
148	0	197	987	74	49
321	148	173	494	173	74
148	494	99	247	148	99

Table of Average Shear Vane values (kPa)

Depth / Horizon	5 (Wh)	St Error	6 (Wn)	St Error
A	41	2	48	3
B	67	5	54	3
C	51	5	62	3

8 (Hn+Wng)	St Error	11 (Tpd)	St Error	12 (31)	St Error
29	2	28	2	36	3
83	10	63	6	61	4
100	7	75	8	37	7

23 (Hn)	St Error	30 (Yp)	St Error	38 (Tpd)	St Error
62	3	50	3	66	3
91	5	71	3	59	3
102	6	C is too hard		67	6
				C is min avg.	

43 (Oi)	St Error	44 (Yp)	St Error	45 (33)	St Error
49	2	46	2	36	2
51	2	62	2	36	1
23	3	62	4	63	3

Table of Worst Shear Vane values (kPa)

Horizon	5 (Wh)	6 (Wn)	8 (Hn+Wng)	11 (Tpd)	12 (31)
A	24	30	20	18	22
B	26	33	54	33	45
C	16	25	60	46	14

23 (Hn)	30 (Yp)	38 (Tpd)	43 (Oi)	44 (Yp)	45 (33)
45	22	38	39	32	23
60	41	30	34	45	20
50	C is too hard	32	6	34	39

Table of Average Bush Penetrometer values (kPa)

Depth (cm)	5 (Wh)	St Error	6 (Wn)	St Error	8 (Hn+Wng)	St Error
3	6	1	0	0	5	1
6	29	6	17	5	25	4
9	156	8	131	8	144	10
12	242	8	202	9	231	11
15	263	9	259	9	298	13
18	291	13	291	10	311	11
21	308	14	356	8	332	15
24	328	15	410	11	333	14
27	359	13	448	12	339	12
30	393	17	457	10	348	11
33	425	17	449	13	364	15
36	429	16	461	15	393	14
39	421	15	470	13	368	12
42	383	17	494	16	387	16
45	361	19	464	10	386	16

11 (Tpd)	St Error	12 (31)	St Error	23 (Hn)	St Error	30 (Yp)	St Error
1	0	2	1	0	0	0	0
7	2	7	2	6	2	19	9
110	7	79	7	208	12	244	13
212	10	144	8	325	16	353	15
251	9	177	5	346	14	392	13
287	14	180	4	388	16	435	15
305	11	189	7	432	23	458	17
322	11	204	9	433	29	445	17
348	17	269	17	428	31	466	18
341	17	285	22	404	22	466	19
335	18	317	26	415	21	467	22
323	18	346	28	454	27	450	24
269	12	378	21	487	29	434	31
251	10	423	39	486	29	466	39
236	11	418	39	491	35	472	108

38 (Tpd)	St Error	43 (Oi)	St Error	44 (Yp)	St Error	45 (33)	St Error
2	1	1	0	9	1	4	1
9	2	20	7	22	2	12	2
259	11	162	5	178	7	76	6
414	9	194	7	247	9	134	6
399	9	227	7	326	12	168	5
381	11	251	10	402	14	177	5
402	15	275	10	411	16	177	4
387	12	324	16	460	18	173	4
407	18	339	16	474	27	171	4
406	18	364	19	439	45	174	4
396	15	384	19	455	35	183	4

Appendix IV

Amplitude Ehancement , Attenuation, and Seismic Rigidity.

Table of Amplitude Ehancement, for initial sites

	Bush Pen.	Hand Pen.	Shear Vane
1 (34)	0.00362	0.00289	0.01176
2 (33)	0.00379	0.00676	0.01111
3 (31a)	0.00446	0.00289	0.00909
5 (Wh)	0.00263	0.00338	0.01250
6 (Wn)	0.00340	0.01010	0.02000
7 (Hn+Wng)	too hard	0.00202	0.00714
8 (Hn+Wng)	too hard	0.00202	0.00714
9 (Wh+Mok)	0.00296	0.00405	0.01667
10 (Mok)	0.00526	0.01010	0.02857
11 (Tpd)	too hard	0.02041	0.06667
12 (31)	0.00485	0.00368	0.01333
13 (Tpd)	0.00233	0.00253	0.01000
14 (Wh)	0.00236	0.00508	0.01429
16 (Tp)	0.00282	0.00202	0.01667
17 (Wn+Wng)	0.00202	0.00676	0.02857
18 (31b)	0.00325	0.00405	0.01667
19 (Wn)	too hard	0.01010	0.02000
20 (Wng)	0.00220	0.04000	0.01667
15 (Wnm)	too hard	0.00202	0.00714
21 (Mok+Ma)	0.00188	0.04000	0.03333
25 (Wh)	too hard	0.00202	0.01000
22 (Wng)	0.00197	0.00225	0.01250
26 (Tpls)	0.00227	0.00202	too hard
23 (Hn)	too hard	0.00253	0.01250
30 (Yp)	0.00187	0.00253	0.01429
27 (Ai)	too hard	0.00202	0.00714
28 (Tpd)	0.00220	loose pumice	loose pumice
29 (Tp)	0.04016	0.00676	0.03333

37 (OiH)	0.00260	0.00289	0.01429
39 (Ypg)	0.00165	0.00508	0.02500
34 (Hn)	0.00330	0.00405	0.02857
33 (Tp)	too hard	0.00253	0.00833
32 (Tpe)	0.00353	0.00202	too hard
31 (Ai)	0.00278	0.00338	0.01429
36 (Tpe)	too hard	0.00202	0.00556
38 (Tpd)	too hard	0.00508	0.01429
41 (Tpe)	0.00231	0.00202	0.00833
42 (Ai)	0.00239	0.00338	too hard
43 (Oi)	0.00219	0.00253	0.01111
44 (Yp)	0.00282	0.00225	0.00909
45 (33)	0.00380	0.00508	0.02500
46 (Wn)	0.00156	0.04000	0.10000
47 (Wh)	too hard	0.00202	0.01000

Table of Amplitude Ehancement, for final sites

	Bush average	Bush worst	Hand average	Hand worst	Shear average	Shear worst
5 (Wh)	0.00238	0.00398	0.00516	0.02026	0.01949	0.06250
6 (Wn)	0.00213	0.00268	0.00313	0.00810	0.01610	0.04000
8 (Hn+Wng)	0.00272	0.00505	0.00208	0.00253	0.00998	0.01667
11 (Tpd)	0.00371	0.00625	0.00382	0.00675	0.01330	0.02174
12 (31)	0.00265	0.00423	0.00698	0.02026	0.02725	0.07143
23 (Hn)	0.00205	0.00268	0.00235	0.00675	0.00981	0.02000
30 (Yp)	0.00230	0.00320	0.00203	0.00203	too hard	too hard
38 (Tpd)	0.00225	0.00336	0.00285	0.01013	0.01487	0.03125
43 (Oi)	0.00266	0.00597	0.04051	0.04051	0.04425	0.16667
44 (Yp)	0.00209	0.00268	0.00403	0.00675	0.01621	0.02941
45 (33)	0.00475	0.00772	0.01013	0.01013	0.01594	0.02564

Table of Attenuation for final sites, calculated from dry density

	Bush average	Bush worst	Hand average	Hand worst	Shear average	Shear worst
5 (Wh)	0.00333	0.00721	0.01066	0.08290	0.07827	0.44934
6 (Wn)	0.00248	0.00350	0.00442	0.01841	0.05157	0.20191
8 (Hn+Wng)	0.00308	0.00781	0.00206	0.00277	0.02171	0.04684
11 (Tpd)	0.00616	0.01345	0.00643	0.01510	0.04174	0.08725
12 (31)	0.00412	0.00834	0.01768	0.08730	0.13620	0.57809
23 (Hn)	0.00252	0.00376	0.00308	0.01503	0.02634	0.07663
30 (Yp)	0.00341	0.00559	0.00281	0.00281	too hard	too hard
38 (Tpd)	0.00317	0.00581	0.00454	0.03035	0.05398	0.16453
43 (Oi)	0.00338	0.01139	0.20155	0.20155	0.23007	1.68188
44 (Yp)	0.00319	0.00463	0.00854	0.01852	0.06887	0.16835
45 (33)	0.00438	0.00907	0.01364	0.01364	0.02692	0.05493

Table of Attenuation for final sites, calculated from bulk density

	Bush average	Bush worst	Hand average	Hand worst	Shear average	Shear worst
5 (Wh)	0.00384	0.00830	0.01227	0.09539	0.09006	0.51704
6 (Wn)	0.00310	0.00437	0.00551	0.02297	0.06436	0.25197

8 (Hn+Wng)	0.00415	0.01052	0.00278	0.00374	0.02925	0.06314
11 (Tpd)	0.00700	0.01527	0.00731	0.01715	0.04741	0.09910
12 (31)	0.00448	0.00908	0.01924	0.09500	0.14822	0.62910
23 (Hn)	0.00300	0.00447	0.00367	0.01788	0.03134	0.09117
30 (Yp)	0.00373	0.00611	0.00308	0.00308	too hard	too hard
38 (Tpd)	0.00349	0.00640	0.00499	0.03340	0.05940	0.18104
43 (Oi)	0.00386	0.01299	0.22990	0.22990	0.26243	1.91848
44 (Yp)	0.00346	0.00501	0.00925	0.02004	0.07454	0.18222
45 (33)	0.01061	0.02198	0.03303	0.03303	0.06519	0.13304

Table of Seismic Rigidity for final sites, calculated from dry density

	Bush average	Bush worst	Hand average	Hand worst	Shear average	Shear worst
5 (Wh)	590	456	400	202	206	115
6 (Wn)	547	488	451	280	199	126
8 (Hn+Wng)	418	306	478	433	218	169
11 (Tpd)	447	344	440	331	236	185
12 (31)	589	465	362	213	183	113
23 (Hn)	598	524	559	330	273	192
30 (Yp)	643	546	686	686	too hard	too hard
38 (Tpd)	628	513	558	296	244	168
43 (Oi)	480	320	123	123	118	61
44 (Yp)	730	645	526	406	262	195
45 (33)	194	152	133	133	106	84

Table of Seismic Rigidity for final sites, calculated from bulk density

	Bush average	Bush worst	Hand average	Hand worst	Shear average	Shear worst
5 (Wh)	679	525	461	233	237	132
6 (Wn)	682	609	563	350	248	157
8 (Hn+Wng)	563	413	644	583	294	227
11 (Tpd)	507	391	500	376	268	210
12 (31)	641	506	394	232	200	123
23 (Hn)	711	623	665	392	325	228
30 (Yp)	703	596	750	750	too hard	too hard
38 (Tpd)	691	565	614	326	269	185
43 (Oi)	547	365	140	140	134	69
44 (Yp)	790	698	569	440	284	211
45 (33)	470	369	322	322	257	202

Appendix V

EQC Claims

Claim No.	Claimant	Address	Town
84 E 879	HA Mills & Son Co	?	Reporoa
85 E 87	Mrs JC Jenson	?	Taupo
87 E 137	BJ Wylie	Mapara Rd	Taupo
64 E 46	Mrs N Prince	211 Rifle Range Rd	Taupo
65 E 4	HE Kereopa	Huia St	Taupo
65 E 56	J and RC Dunbar	16 Tui St	Taupo
65 E 57	RE Bullivant	?	Taupo
66 E 74	H Sherwood	10 Cumberland St	Taupo
86 E 87	G Reed	12 Cumberland St	Taupo
87 E 75	M Bunney	23 Taherepa Rd	Taupo
88 EQ 5	NZ Dairy Co-op Co	S.H.5	Reporoa
88 EQ 165	Cascade Motor Lodge	Lake Terrace	Taupo
89 EQ 672	DL and PM Furminger	11 Pokaka Cr	Taupo
81 E 543	HW Edwards	?	Taupo
81 E 1141	B and C Clark	186 Tamamutu St	Taupo
81 E 2306	Ashley Court Motor Hotel	62-66 Lake Terrace	Taupo
70 E 113	Mr J Mishewski	34 Wheretia St	Taupo
71 E 216	Mrs GA Cammock	222 Tamamutu St	Taupo
72 E 119	Bray	?	Taupo
73 E 549	J and GA Lourie	44 Rainbow Dr	Taupo
73 E 1871	EP Piper	?	Taupo
73 E 2229	RW Bell	?	Reporoa
73 E 2926	Salvage and Recoveries	?	Taupo
73 E 3077	WE Tito	?	Taupo
73 E 3237	WH Davis	?	Taupo
83 E 23	GL Short	46B Taupo View Rd	Taupo
83 E 26	HW Edwards	137 Tauhara Rd	Taupo
83 E 72	Mrs ID Palmer	30 Henry Hill Rd	Taupo
83 E 380	Mrs JA Alderton	2 Battersea Pl	Taupo
84 E 39	JE Phillips	Whangamata Rd RD1	Taupo
84 E 47	GW Reid	6 Green Pl	Taupo
84 E 57	Peter R Bicknell	87 Mountain Rd	Taupo
84 E 489	NM and ? Wrightson	?	Reporoa
84 E 494	C and G Martelli	Main Rd	Reporoa
84 E 495	MW Webb	Main Rd	Reporoa

84 E 496	GJ Morrison	Main Rd	Reporoa
84 E 497	Waiotapu Hotel	SH5	Waiotapu
84 E 500	M Thomas	Forest Rd	Reporoa
84 E 541	GR and ME Turnbull	RD1	Reporoa
84 E 543	SM Stairmand	Reporoa Butchery	Reporoa
84 E 548	N Sinclair	Forest Rd RD2	Reporoa
84 E 586	D Jensen	House 30, NZ Dairy Co-op Co	Reporoa
84 E 598	WD Judson	Strathmore Rd RD1	Reporoa
84 E 599	RG Lloyd	Box 112	Reporoa
84 E 601	Mrs J Brennan	22 Woolvern Cr	Reporoa
84 E 618	Mrs R Young	Creighton Rd	Reporoa
84 E 656	P Belcher	?	Reporoa
84 E 711	MW Webb	Main Rd RD2	Reporoa
84 E 727	JP Norris	Tutukau Rd	Reporoa
84 E 770	KA Freundlich	?	Taupo
65 E 58	R and JH Pomeka	Waipahihi	Taupo
65 E 59	Davies Co Ltd	Tongariro St	Taupo
65 E 60	S Holland	House 20	Wairakei
65 E 63	C Aislabie	30 Pataka Rd	Taupo
84 E 521	H Allen Mills And Sons Ltd	?	Reporoa
84 E 522	TM Daly	RD2	Reporoa
84 E 523	DA Corney	RD2	Reporoa
84 E 524	SM Lee	3 Woolvern Cr	Reporoa
84 E 528	Waikato River Lodge	Vaile Rd	Reporoa
84 E 530	Mrs J Gilbertson	Butcher Rd RD2	Reporoa
84 E 535	ID and JM Silvester	?	Reporoa
84 E 537	Ms MD Bowler	Massey Road	Reporoa
84 E 539	CD Martelli	Settlers Rd	Reporoa
84 E 540	KA and JM Nixon	Wharepapa Rd	Reporoa
84 E 501	GD Lockley and BA Rodgers	Loop Rd	Reporoa
84 E 502	AL Stannett	Longview Rd RD2	Reporoa
84 E 509	J and M Dekker	Settlers Rd RD2	Reporoa
84 E 511	WL and LM Moore	Broadlands Rd	Reporoa
84 E 513	Mrs P Moore	Reporoa Rd RD	Reporoa
84 E 516	CR and WA Broomfield	Campbell Rd	Reporoa
84 E 517	RLS and E Smith (Smith Ltd)	Campbell Rd	Reporoa
84 E 518	RW Bell	Rotorua - Taupo Rd	Reporoa
84 E 519	M Bell	Main Rd RD2	Reporoa
84 E 520	Mrs M Parker	House 28 Woolvern Cr	Reporoa

Claim No.	Date of Loss	Property damaged	Payments
84 E 879	15/12/83	?	$344.00
85 E 87	5/3/84	?	$179.23
87 E 137	?	chimney	$1,214.10
64 E 46	24/4/63	chimney and fireplace	$5.00
65 E 4	12/4/63	dwelling	$0.00
65 E 56	12/12/64	chimney	$10.00
65 E 57	12/12/64	chminey	not pursued
66 E 74	11/64 - 2/65	chimney / dwelling	late
86 E 87	?	building	closed
87 E 75	?	?	?
88 EQ 5	2/3/87	?	late
88 EQ 165	2/3/87	?	late
89 EQ 672	23/10/88	?	$413.36
81 E 543	6/10/80	?	$360.00
81 E 1141	6/10/80	?	$60.46
81 E 2306	6/10/80	?	late
70 E 113	2/2/69	?	late
71 E 216	18/1/71	?	$430.00
72 E 119	14/8/71	?	$15.00
73 E 549	6/1/73	?	$100.00
73 E 1871	6/1/73	?	$95.00
73 E 2229	6/1/73	?	$23.00
73 E 2926	22/2/73	?	$254.63
73 E 3077	?	?	late
73 E 3237	6/1/73	?	late
83 E 23	6/5/82	?	not insured
83 E 26	?	?	late
83 E 72	?	?	water pipes excluded
83 E 380	3/9/82	?	water pipes excluded
84 E 39	?	?	$90.00
84 E 47	?	?	$190.00
84 E 57	5/6/83	?	$128.40
84 E 489	15/12/83	?	$405.53
84 E 494	15/12/83	?	not prosecuted
84 E 495	15/12/83	?	not prosecuted
84 E 496	15/12/83	?	$671.30
84 E 497	15/12/83	?	$1,016.59
84 E 500	15/12/83	?	$216.00
84 E 541	15/12/83	?	not prosecuted
84 E 543	15/12/83	?	$372.00
84 E 548	15/12/83	?	$16.13
84 E 586	15/12/83	?	$156.00
84 E 598	15/12/83	?	$80.00
84 E 599	15/12/83	?	$225.00
84 E 601	15/12/83	?	$332.25
84 E 618	15/12/83	?	$65.60
84 E 656	15/12/83	?	$84.75
84 E 711	15/12/83	?	$538.62
84 E 727	15/12/83	?	$246.33
84 E 770	?	?	not prosecuted
65 E 58	21/12/64	dwelling	$640.00

65 E 59	31/12/64 - 1/1/65	stock in trade	$11.57
65 E 60	12/12/64	movie projector	nil
65 E 63	?/12/64	chimney	nil
84 E 521	15/12/83	?	$790.00
84 E 522	15/12/83	?	$456.60
84 E 523	15/12/83	?	$1,013.27
84 E 524	15/12/83	?	$200.00
84 E 528	15/12/83	?	not prosecuted
84 E 530	15/12/83	?	$110.00
84 E 535	15/12/83	?	$322.00
84 E 537	15/12/83	?	$24.45
84 E 539	15/12/83	?	$196.98
84 E 540	15/12/83	?	$584.94
84 E 501	15/12/83	?	$408.30
84 E 502	15/12/83	?	$506.00
84 E 509	15/12/83	?	$74.99
84 E 511	15/12/83	?	$339.24
84 E 513	15/12/83	?	$285.50
84 E 516	15/12/83	?	$40.00
84 E 517	15/12/83	?	$390.00
84 E 518	15/12/83	?	$805.10
84 E 519	15/12/83	?	$254.90
84 E 520	15/12/83	?	$381.75